Chapter-3

Chapter-3a

Synthesis of Pyrazolone Derivatives of Coumarin as Anticancer Agents

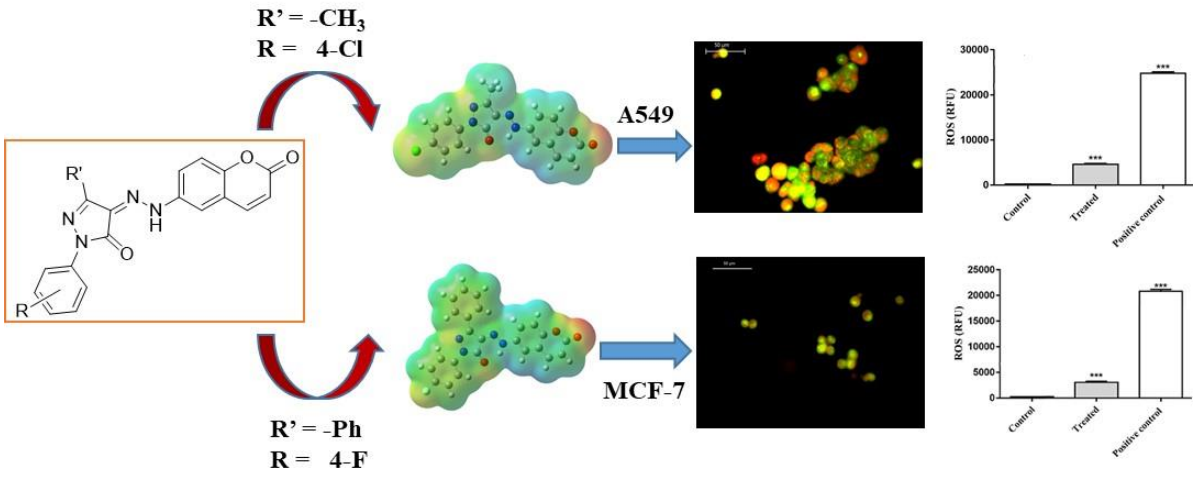

3a.1 Introduction

Pyrazolone is one of the important class of heterocyclic compounds and the primary structural component of numerous molecules with biological and pharmacological effects [1-4]. A wide range of biological effects, including anti-inflammatory [5], antibacterial [6], antidepressant, antitubercular [7] and anticancer [8] are displayed by them. The insertion of heterocyclic rings into prospective candidates is a crucial technique utilized to create more effective and selective pharmaceutical prospects. Coumarin scaffold is pervasive in nature and is a highly privileged motif for the development of novel drugs due to its biodiversity and versatility. Many substituted coumarin and their derivatives have been developed synthetically with wide range of biological activities [9-11]. In the recent years, coumarin-pyrazolone derivatives have been reported which contain potent biological activity with less side effects for medicinal applications leading to design and development of derivatives based on this class. [12-13]. Sivakumar *et al*. synthesized different pyrazolone derivatives of coumarin and out of all the screened compounds, compound **1** showed nearly equipotent anti-inflammatory and analgesic activity than the standard drug **(Fig-3.1)** [14]. Moreover, the synthetic and natural drugs containing coumarin scaffolds are well-known as anti-bacterial and antifungal agents. Parekh *et al.* synthesized coumarin pyrazolone derivatives **2** with very good antibacterial activity [15]. Hybrid compound is a combination of two or more heterocyclic pharmacophores into a single molecule to increase its therapeutic activity and affinity while lowering adverse effects and combating drug resistance. Thus, coumarin-containing hybrids occupy an important position in the recent research in anticancer agents. Kulkarni *et al*. synthesized series of novel coumarin-pyrazolones with excellent yield for their anticancer activities with different substituent like methoxy, methyl group on coumarin nucleus. Compounds **3** and **4 (Fig-3.1)** showed marked anticancer activity against A549-lungs cancer cell line and MCF-7 breast cancer cell line [16]. Therefore, coumarin moiety hybridized with additional anticancer pharmacophores may result in novel anticancer candidates with low toxicity, high specificity, and great efficacy against both drug-susceptible and drug-resistant cancers.

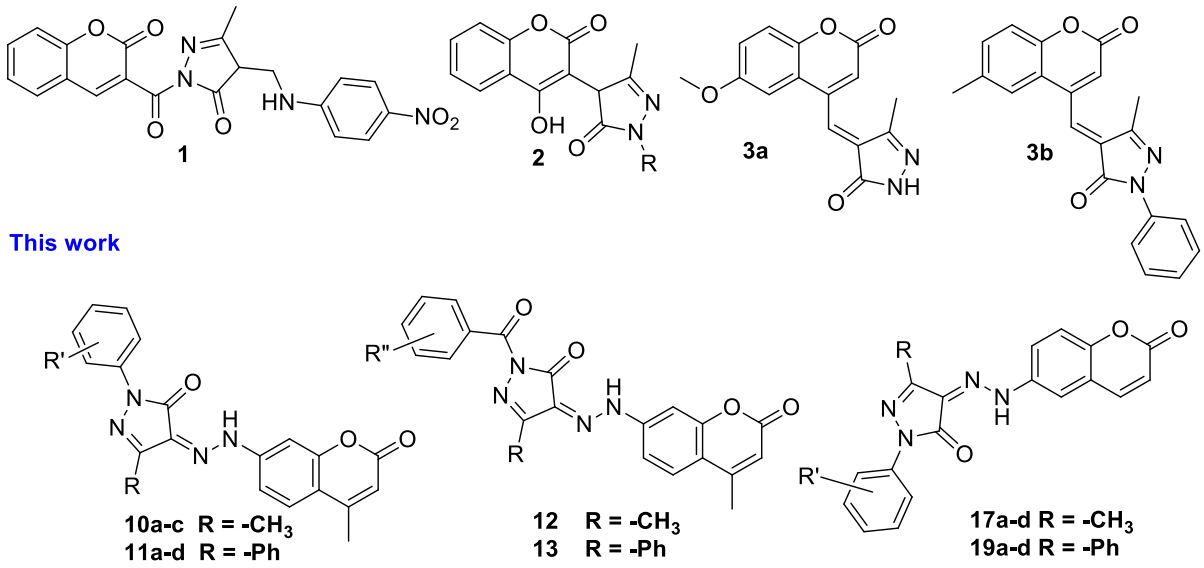

Figure- 3a.1 Coumarin-pyrazolone derivatives with different biological applications

On the basis of the above facts and our ongoing focus on developing novel candidates featuring potential anticancer activity of coumarin hybrids [17-19], we have synthesized a new series of pyrazolone derivatives of 7-amino 4-methylcoumarin and 6-aminocoumarin. These molecules were studied against Lungs cancer cell lines (A549) and Breast cancer cell lines (MCF-7) for their anticancer activities using MTT assay. Furthermore, the experimental findings were fine-tuned through the utilization of density functional theory (DFT) investigations.

3a.2 Results and discussion

3a.2.1 Chemistry

Compounds **10a-c, 11a-d, 12, 13** were synthesized from 7-amino-4-methylcoumarin **7 (Scheme 1)**. In the first step carbamate protection of 3-aminophenol was carried out followed by Pechmann reaction using ethylacetoacetate to give 7-carboethoxy amino-4-methyl coumarin **6**. Further, deprotection of carbamate group in compound **6** was carried out under acidic conditions (sulfuric acid: acetic acid (1:1)) to give desired 7-amino-4-methylcoumarin **7**. Compound **7** was dissolved in concentrated HCl and Acetic Acid (1:1) and stirred until amine completely dissolved then the mixture cooled to temperature (0-5^{o}C). Sodium nitrite solution in water was then added dropwise with vigorous stirring during 30 minutes then this solution was poured into the cold solution of sodium acetate, ethyl acetoacetate **(Scheme-1)** or ethyl benzoyl acetate in absolute ethanol, then stirred for completion of reaction at room temperature for 2 hours to give compound **8** (with Ethyl acetoacetate) and compound **9** (with Ethyl benzoylacetate).

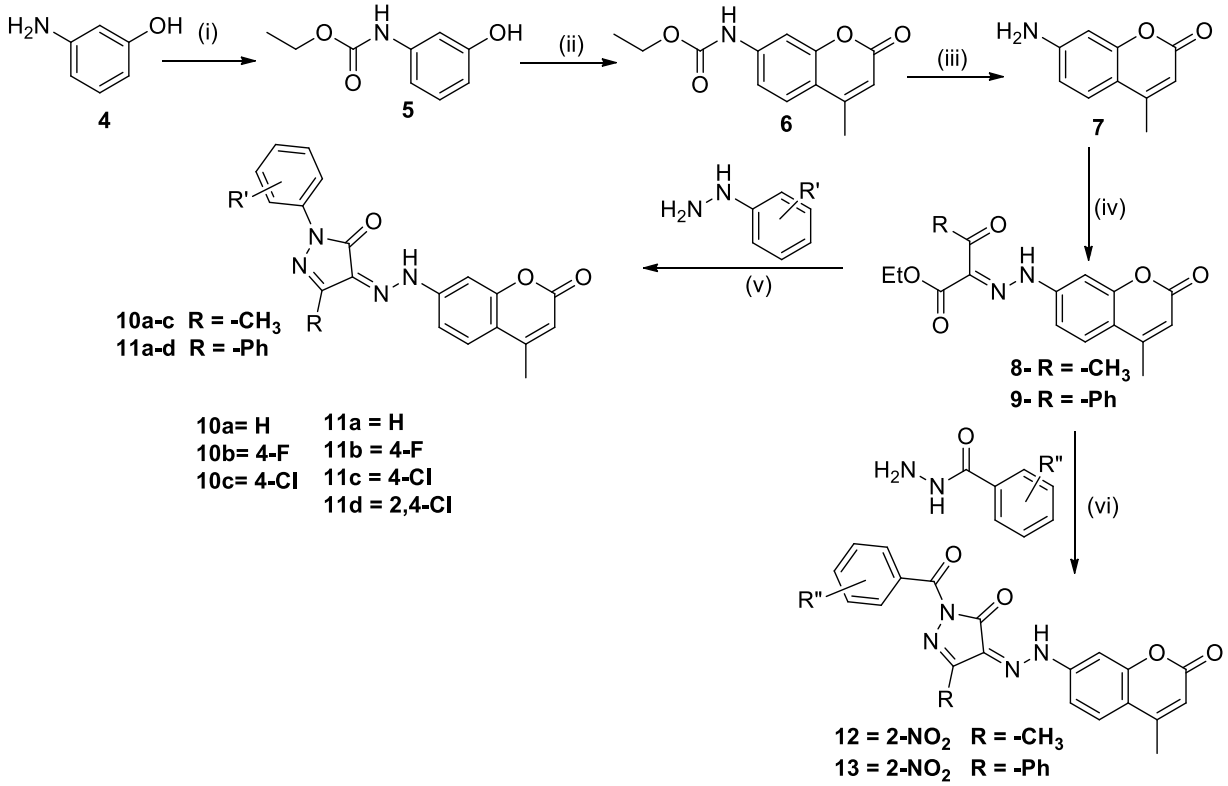

Reagents & Conditions: (i) CH_3CH_2OCOCl, ethyl acetate, rt; (ii) CH_3COCH_2COOEt, H_2SO_4:C_2H_5OH(3:7),rt;(iii) H_2SO_4:CH_3COOH(1:1),reflux; (iv) $NaNO_2$; HCl:AcOH(1:1),Sodium acetate,EAA/Ethyl benzoyl acetate Ethanol,0°Cto 5°C; (v)/(vi) absolute Ethanol,3-4 drops AcOH, reflux

Scheme 1: Pyrazolone derivatives **10a-c, 11a-d,12** and **13**

IR of compound **8** and **9** N-H stretching frequency appeared **(Fig.-3a.3.1)** at 3130 cm^{-1} and 3435cm^{-1}.C-H stretching frequency appeared from 3053-2924 cm^{-1}. 1733 cm^{-1} and 1740 cm^{-1} stretching frequency observed for lactone carbonyl carbon of **8** and **9** respectively. In ^{1}H-NMR spectra of compound **8 (Fig.-3a.3.2)** all aliphatic protons observed in the range of δ 1.41 to 4.81 and all aromatic carbons ranging from δ 6.23 -7.68, N-H protons observed at δ 14.59. In ^{13}C-NMR aliphatic carbons observed in the range of 14.31 to 61.39 ppm and all aromatic carbons observed from δ 103.74-160.80 ppm along with lactone carbonyl carbon and ester carbonyl carbon at δ 164.47 and 197.60 ppm respectively **(Fig.-3a.3.3)**. Similar patterns are observed in ^{1}H-NMR and ^{13}C-NMR of compound **9 (Fig.-3a.4.2 and Fig.-3a.4.3)** only extra protons and carbons are observed due to additional phenyl ring. Compounds **8** and **9** were refluxed with different substituted phenyl hydrazines in absolute ethanol by the addition of 3-4 drops of glacial acetic acid to gives pyrazolone derivatives **10a-c** and **11a-d** and substituted phenyl hydrazides gave pyrazolone derivatives **12** and **13**.

All the final compounds were characterized by using different analytical techniques such as ^{1}H-NMR, ^{13}C-NMR, IR, ESI-MS and CHN analysis.

When methyl group is attached to pyrazolone ring as in compound **10a-c**, the IR spectra of compounds **10a-c** showed one band for N-H stretching in the range of 3075-3450 cm^{-1}, while carbonyl stretching for lactone at 1729-1740 cm^{-1} and for amide carbonyl frequency at 1611-1672 cm^{-1}. The -C=N stretching frequency of pyrazolone ring observed from 1530-1560 cm^{-1}. In ^{1}H-NMR analysis **(Fig.-3a.5.2)**, compound **10a** exhibited two singlets one for methyl group of coumarin ring at δ 2.46 and other for methyl group of pyrazolone ring at δ 2.41. Compound **10a** showed all aromatic protons in region of δ 6.27-7.97 and N-H proton at δ 13.58. ^{13}C-NMR of compound **10a (Fig.-3a.5.3)** showed two -CH_3 carbons at δ 11.85 and 18.72 ppm, aromatic carbons in the range of δ 103.15-157.44 ppm along with amide carbonyl carbon observed at δ 155.00, while lactone carbonyl carbon was observed at 157.44 ppm. In ESI-MS analysis of compound **10a**, it showed $[M+H]^+$ peak at 361.13 **(Fig.-3a.5.4)**.

In compounds **11a-d** when phenyl ring is attached to the pyrazolone ring in place of methyl group**,** the IR spectra of compound **11a-d**, N-H stretching band was observed in the range of 3075-3450 cm^{-1}, stretching frequency for carbonyl of lactone was observed at 1720-1730 cm^{-1} and for amide carbonyl frequency at 1614-1652 cm^{-1}. -C=N stretching frequency of pyrazolone ring observed from 1526-1558 cm^{-1}. In ^{1}H-NMR spectrum of compound **11c**, –CH_3 protons for only one methyl was observed as singlet at δ 2.44 which is attached to 4th carbon of coumarin ring. Aromatic protons of compound **11c** observed in the range of 6.25-8.16 **(Fig.-3a.10.2)**. One N-H proton appears at δ 13.89 as a singlet. In ^{13}C-NMR of compound **11c**, one -CH_3 carbons was observed at δ 18.73, aromatic carbons in the range of δ 103.34-160.57 ppm along with amide carbonyl carbon and lactone carbonyl carbon **(Fig.-3a.10.3)**.

We have also synthesized pyrazolone derivatives of 6-amino coumarin. First we have synthesized 6-aminocoumarin from simple coumarin. Nitration of coumarin carried out by using nitrating mixture of H_2SO_4 and HNO_3 which gave 6-nitrocoumarin **14** which on reduction by using Fe powder and ammonium chloride in water gave 6-aminocoumarin **15** (**Scheme-2).** Diazotization of 6-aminocoumarin was carried out by using ethyl acetoacetate and ethyl benzoylacetate **(Scheme-2)** to give compounds **16** and **18.** Compounds **16** and **18** were refluxed with different substituted phenyl hydrazines in absolute ethanol with addition of catalytic amount (3-4 drops) of glacial acetic acid to give pyrazolone derivatives **17a-d** and **19a-d**

respectively. All the compounds were characterized using ^{1}H-NMR, ^{13}C-NMR, IR, ESI-MS and CHN analysis.

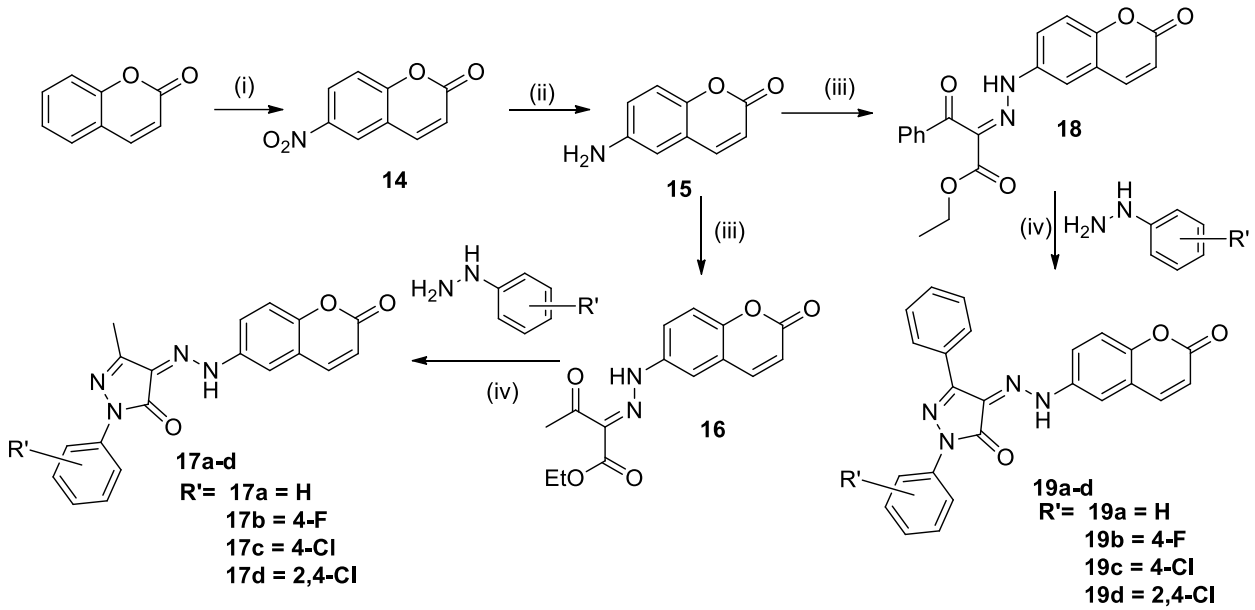

Reagents & Conditions: (i)HNO_3:H_2SO_4 (1:3) Conc. H_2SO_4 RT, 2hr (ii)Fe (powder), NH_4Cl,H_2O, 80^{o}C (iii) $NaNO_2$; HCl:AcOH(1:2),Sodium acetate,EAA/Ethyl benzoyl acetate Ethanol,0^{o}Cto 5^{o}C; (iv)Ethanol,3-4 drops AcOH, reflux

Scheme 2: Pyrazolone derivatives **17a-d and 19a-d**

The IR spectra of compounds **17a-d** showed one band for N-H stretching in the range of 3416-3438 cm^{-1}, lactone carbonyl at 1712-1725 cm^{-1} and amide carbonyl at 1654-1687 cm^{-1}. The -C=N stretching of pyrazolone ring observed at 1530-1565 cm^{-1}. In ^{1}H-NMR spectrum of compound **17c**, methyl protons attached to pyrazolone ring appeared at δ 2.41 and all aromatic protons appeared the range of δ 6.54-7.96, while N-H proton appeared at δ 13.65 as a singlet. In ^{13}C-NMR of **17c** one peak at 11.56 ppm was observed for one methyl group attached to pyrazolone ring. All aromatic carbons observed in the range of δ 114.71 to 159.57 including amide carbonyl carbon and lactone carbonyl carbon **(Fig.-3a.17.3)**. In IR spectra of compounds **19a-d**, phenyl ring attached to pyrazolone in place of methyl, the N-H stretching observed in the range of 3425-3445cm^{-1}, lactone carbonyl stretching at 1713-1721cm^{-1} and amide carbonyl observed at 1657-1670cm^{-1}. In ^{1}H-NMR of compounds **19a-d** similar pattern was observed as previous one, Absence of methyl protons and additional aromatic protons were observed in aromatic region due to attachment of phenyl ring on pyrazolone ring, Aromatic protons observed from δ 6.44-8.23, while N-H proton observed in the range δ12.80-14.00. In ^{13}C-NMR of compound **19a-d**, all the aromatic carbons as well as amide and lactone carbonyl carbon observed between δ 113.91-160.05 ppm.

Figure- 3a.3.1 IR of (Z)-ethyl 2-(2-(4-methyl-2-oxo-2H-chromen-7-yl)hydrazono)-3-oxobutanoate **(8)**

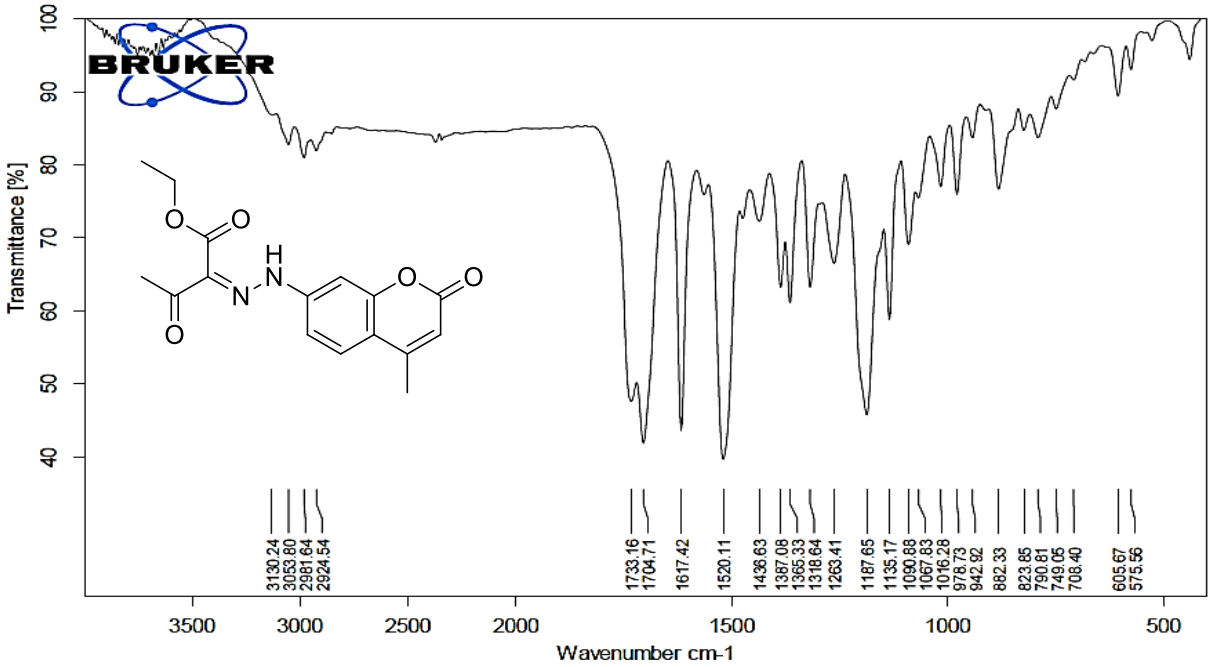

Figure-3a.3.2 ^{1}H-NMR of (Z)-ethyl 2-(2-(4-methyl-2-oxo-2H-chromen-7-yl)hydrazono)-3-oxobutanoate **(8)**

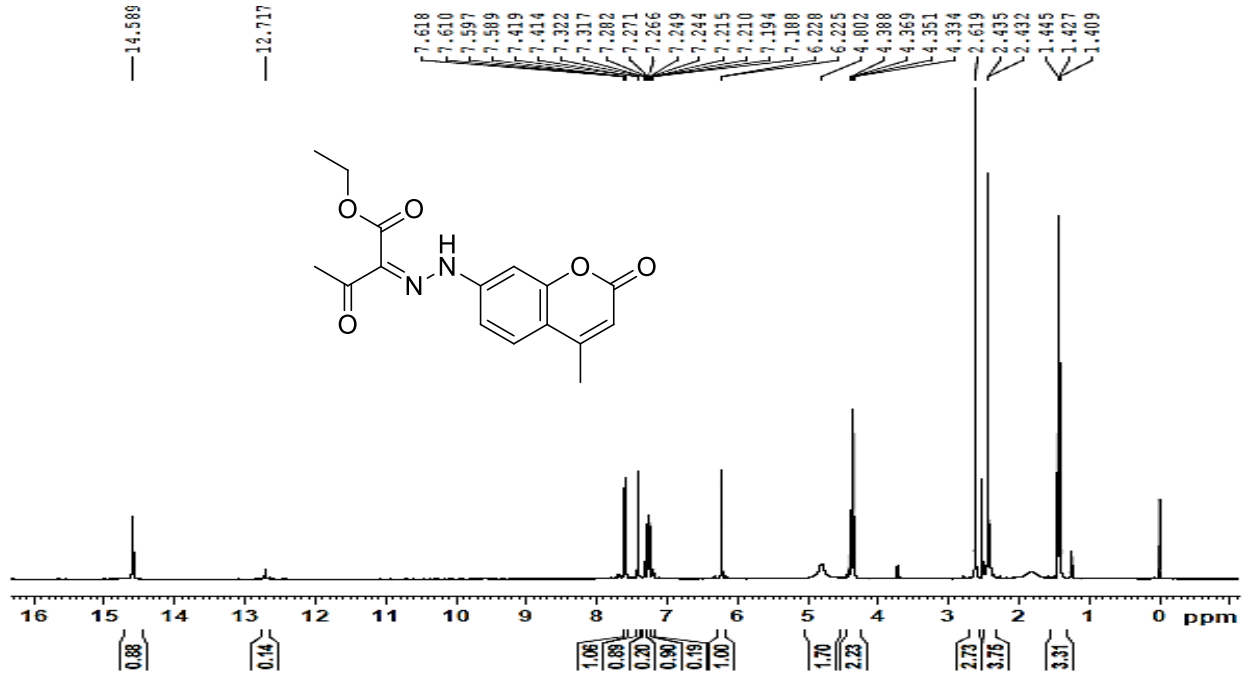

Figure- 3a.3.3 ^{13}C-NMR of (Z)-ethyl 2-(2-(4-methyl-2-oxo-2H-chromen-7-yl)hydrazono)-3-oxobutanoate **(8)**

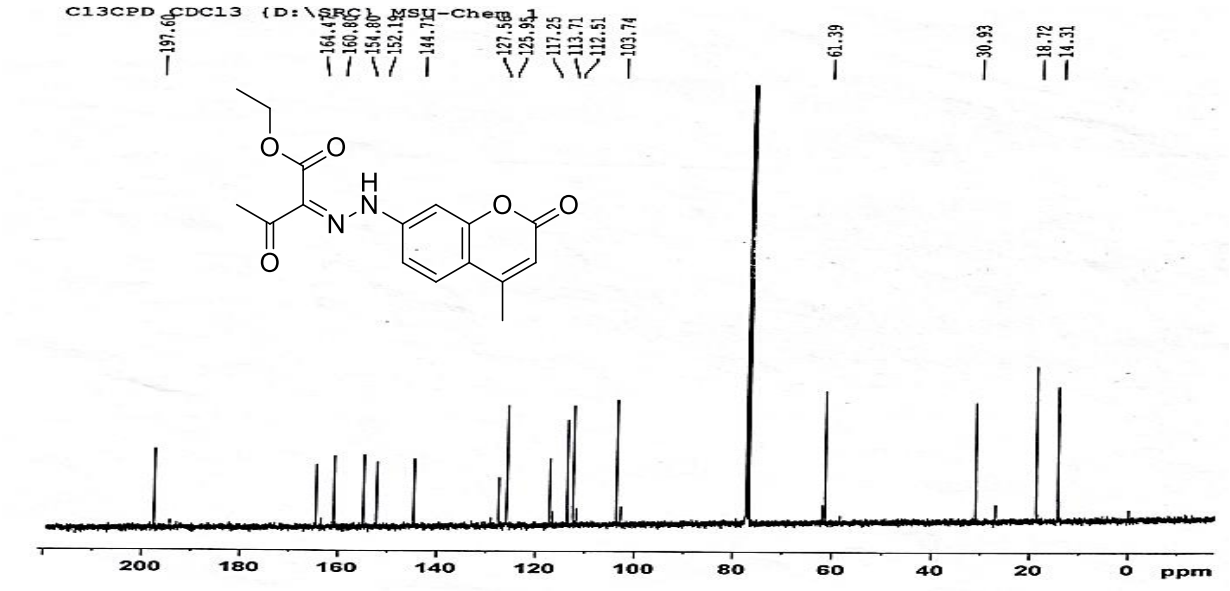

Figure- 3a.4.1 IR of (Z)-ethyl 2-(2-(4-methyl-2-oxo-2H-chromen-7-yl)hydrazono)-3-oxo-3-phenylpropanoate **(9)**

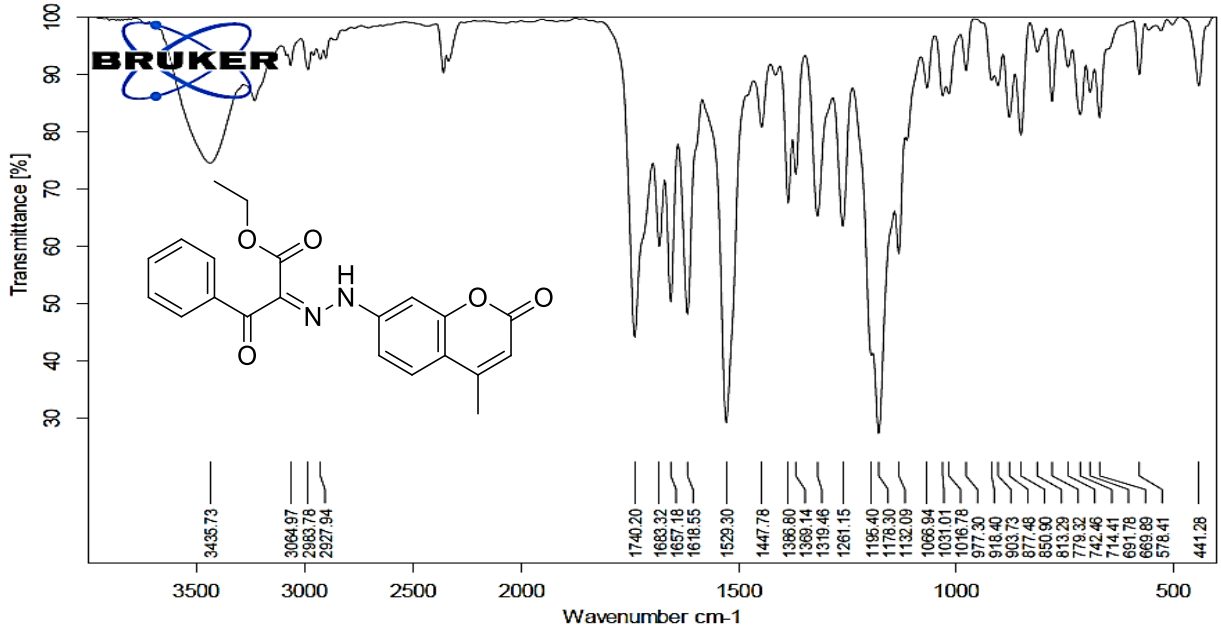

Figure- 3a.4.2 ^{1}H-NMR of (Z)-ethyl 2-(2-(4-methyl-2-oxo-2H-chromen-7-yl)hydrazono)-3-oxo-3-phenylpropanoate **(9)**

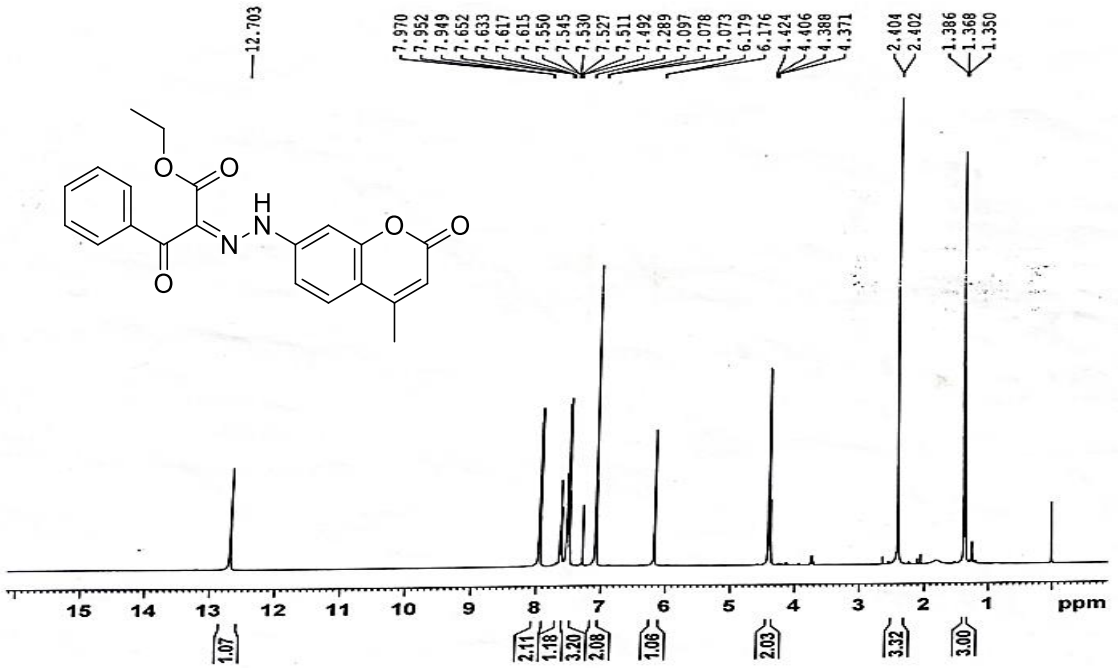

Figure- 3a.4.3 ^{13}C-NMR of (Z)-ethyl 2-(2-(4-methyl-2-oxo-2H-chromen-7-yl)hydrazono)-3-oxo-3-phenylpropanoate **(9)**

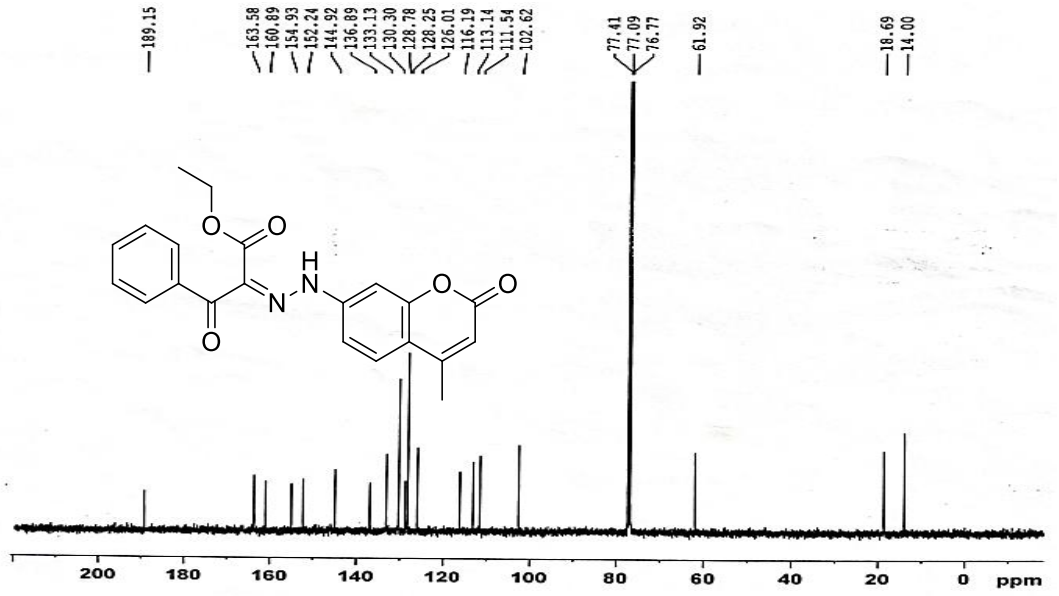

Figure- 3a.5.1 IR of (Z)-3-methyl-4-(2-(4-methyl-2-oxo-2H-chromen-7-yl)hydrazono)-1-phenyl-1H-pyrazol-5(4H)-one **(10a)**

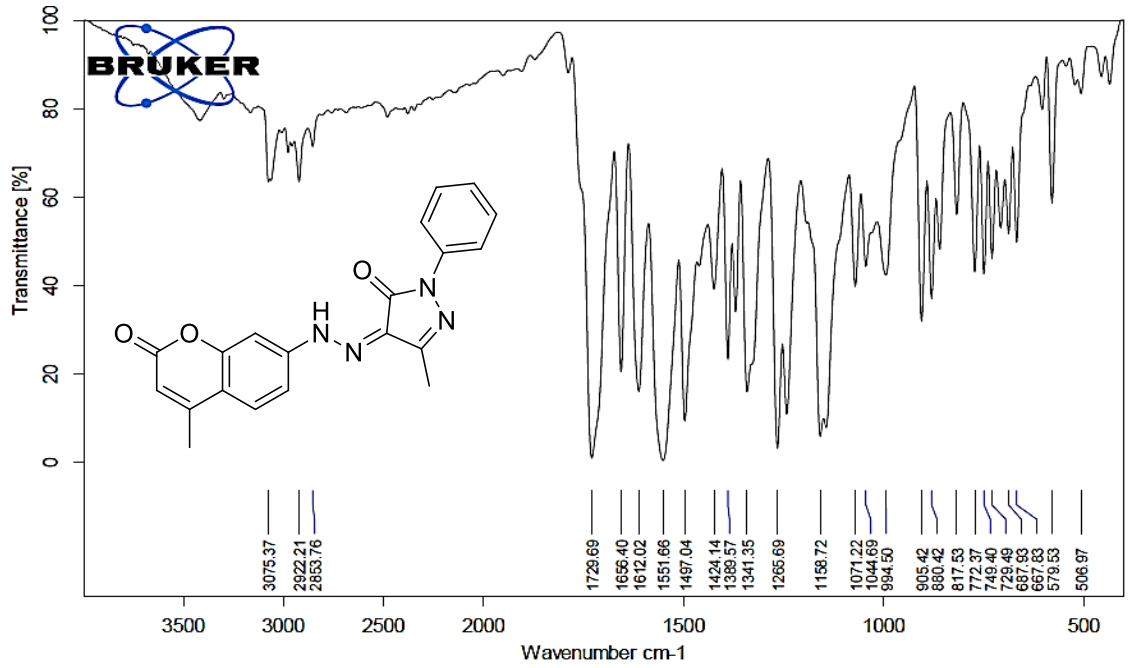

Figure- 3a.5.2 ^{1}H-NMR of (Z)-3-methyl-4-(2-(4-methyl-2-oxo-2H-chromen-7-yl)hydrazono)-1-phenyl-1H-pyrazol-5(4H)-one **(10a)**

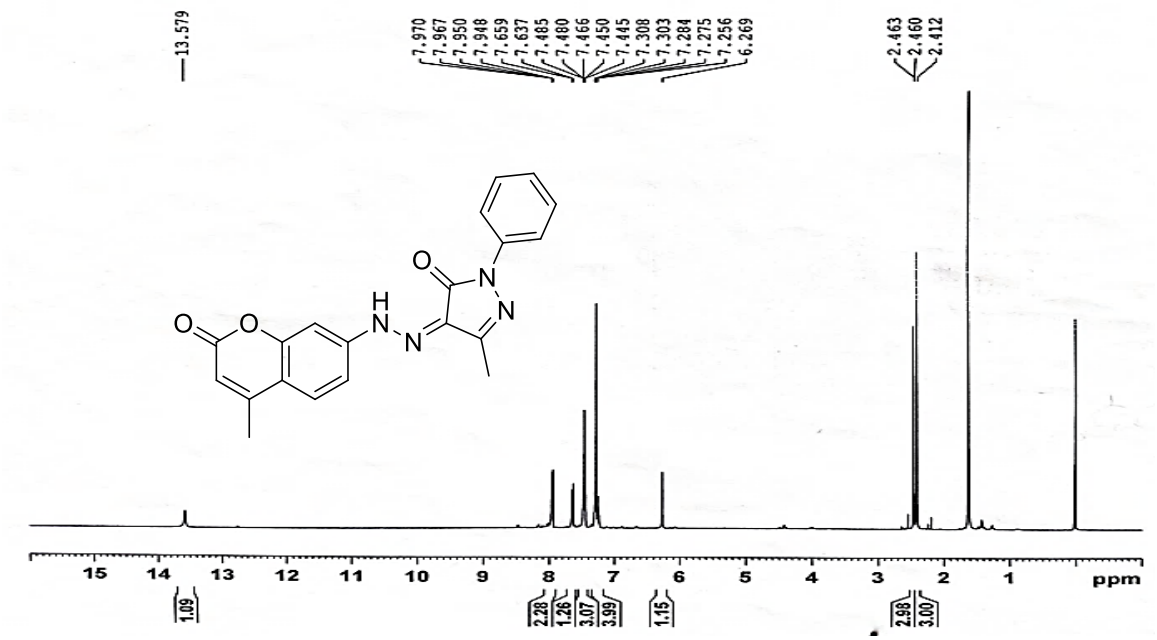

Figure- 3a.5.3 ^{13}C-NMR of (Z)-3-methyl-4-(2-(4-methyl-2-oxo-2H-chromen-7-yl)hydrazono)-1-phenyl-1H-pyrazol-5(4H)-one **(10a)**

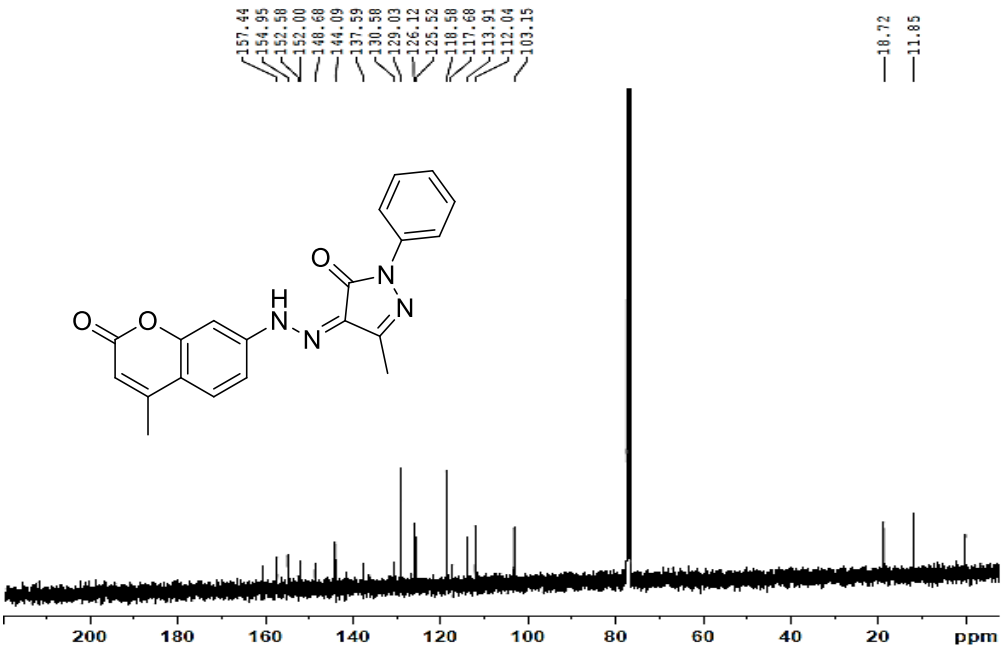

Figure- 3a.5.4 Mass of (Z)-3-methyl-4-(2-(4-methyl-2-oxo-2H-chromen-7-yl)hydrazono)-1-phenyl-1H-pyrazol-5(4H)-one **(10a)** M+H peak at 361.13

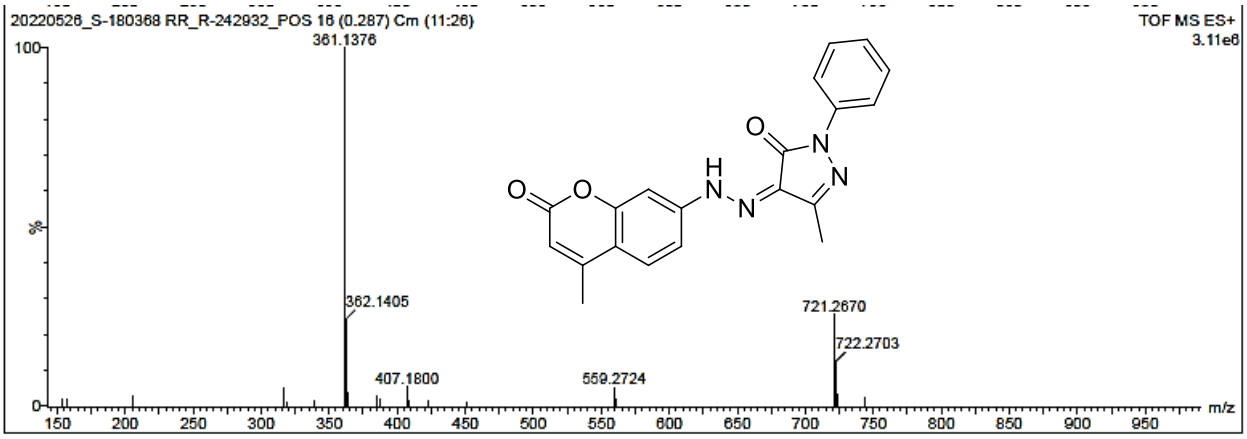

Figure- 3a.6.1 IR of (Z)-1-(4-fluorophenyl)-3-methyl-4-(2-(4-methyl-2-oxo-2H-chromen-7-yl)hydrazono)-1H-pyrazol-5(4H)-one **(10b)**

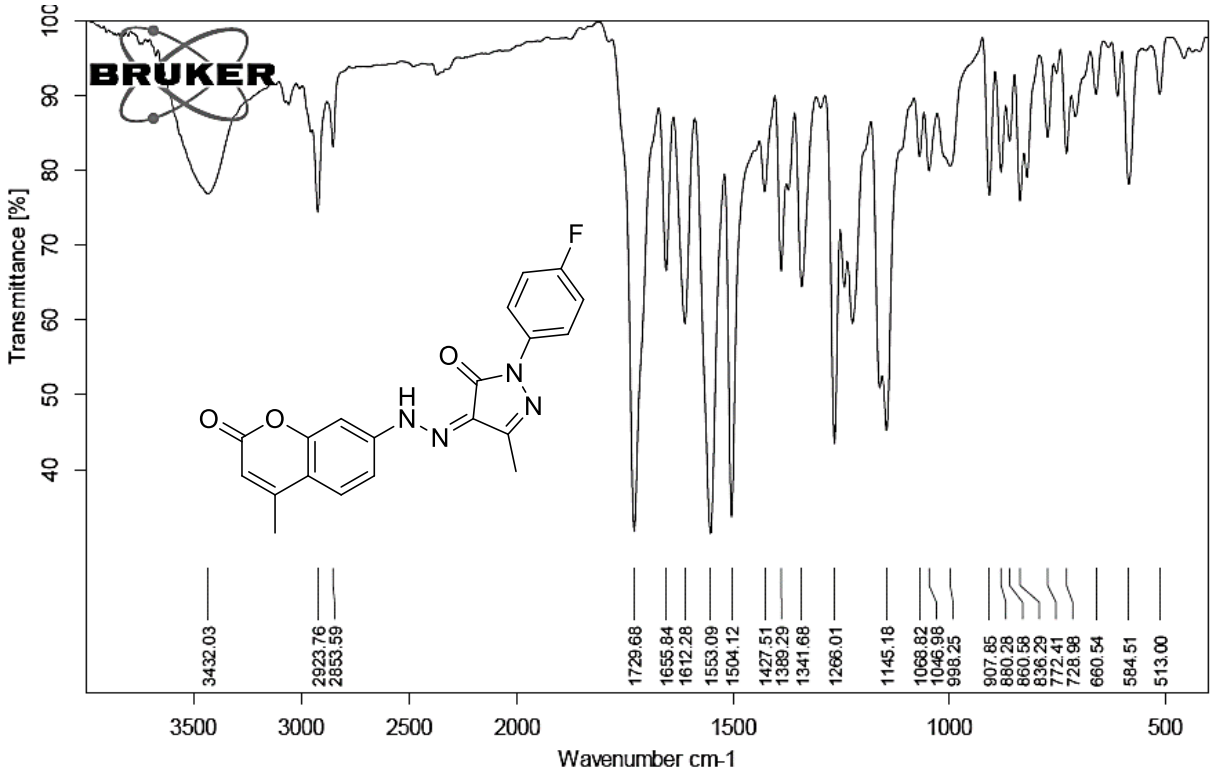

Figure- 3a.6.2 ^{1}H-NMR of (Z)-1-(4-fluorophenyl)-3-methyl-4-(2-(4-methyl-2-oxo-2H-chromen-7-yl)hydrazono)-1H-pyrazol-5(4H)-one **(10b)**

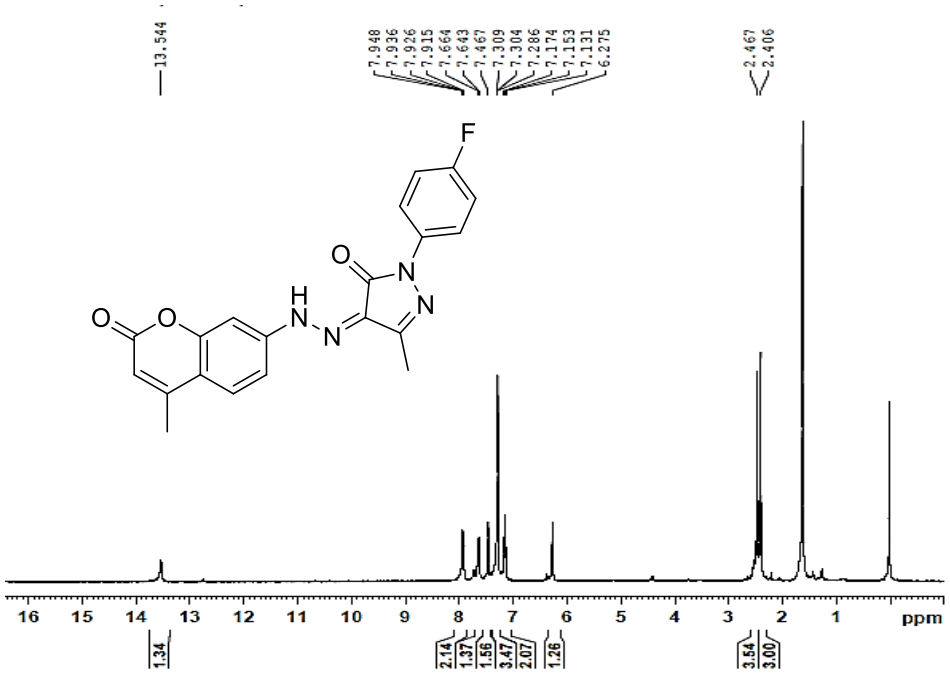

Figure- 3a.7.1 IR of (Z)-1-(4-chlorophenyl)-3-methyl-4-(2-(4-methyl-2-oxo-2H-chromen-7-yl)hydrazono)-1H-pyrazol-5(4H)-one **(10c)**

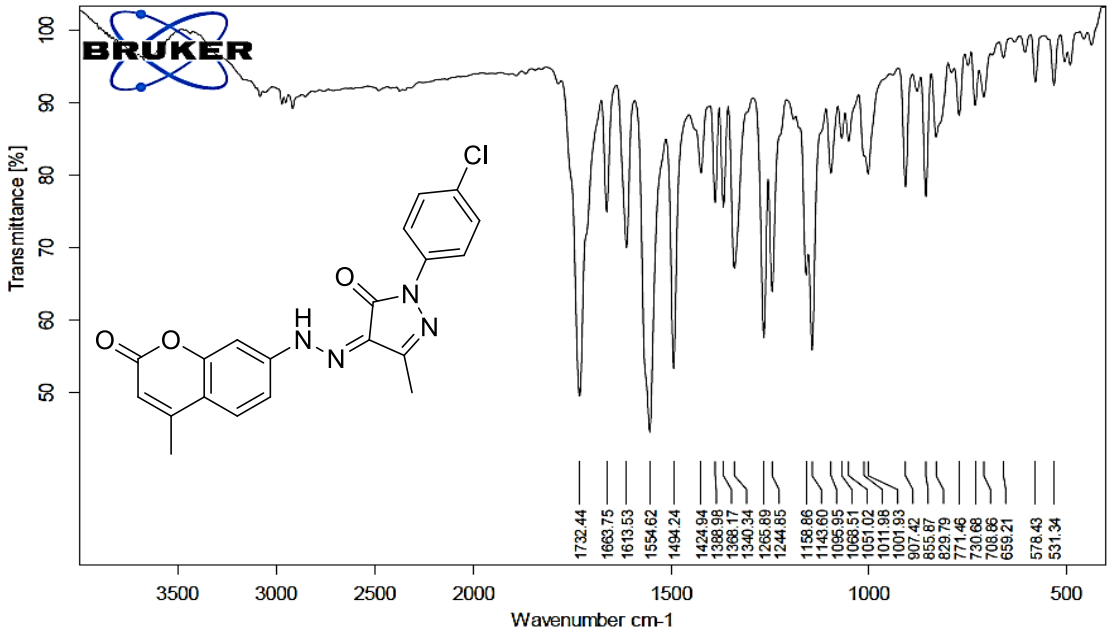

Figure- 3a.7.2 ^{1}H-NMR of (Z)-1-(4-chlorophenyl)-3-methyl-4-(2-(4-methyl-2-oxo-2H-chromen-7-yl)hydrazono)-1H-pyrazol-5(4H)-one **(10c)**

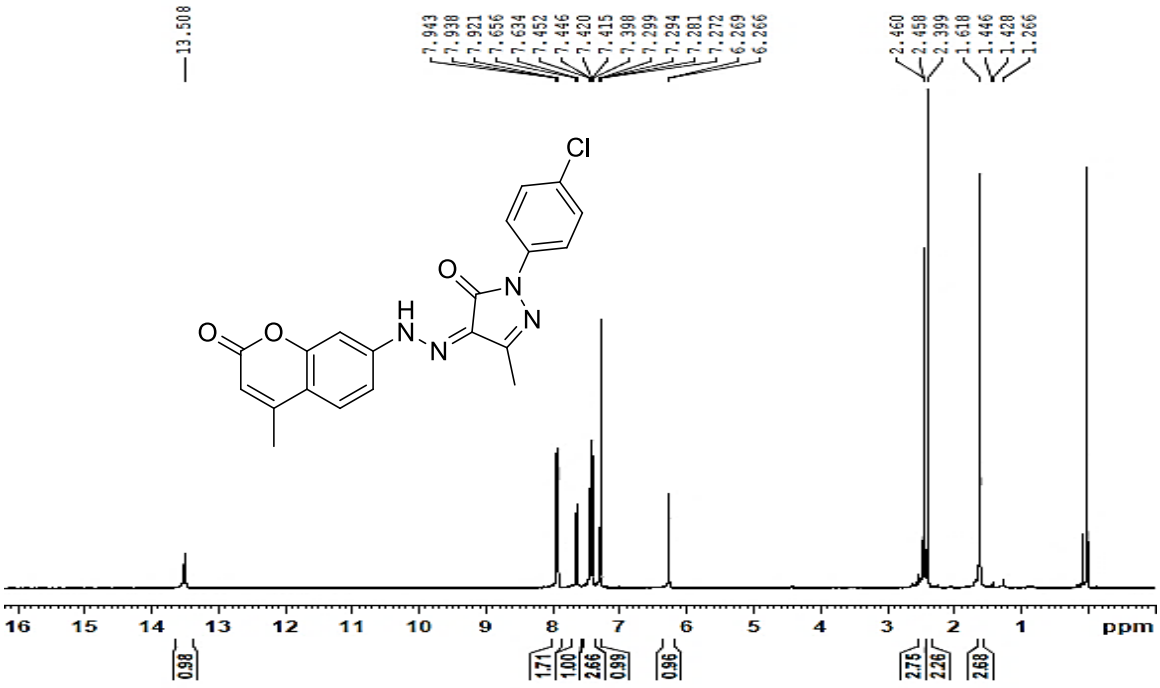

Figure- 3a.8.1 IR of (Z)-4-(2-(4-methyl-2-oxo-2H-chromen-7-yl)hydrazono)-1,3-diphenyl-1H-pyrazol-5(4H)-one **(11a)**

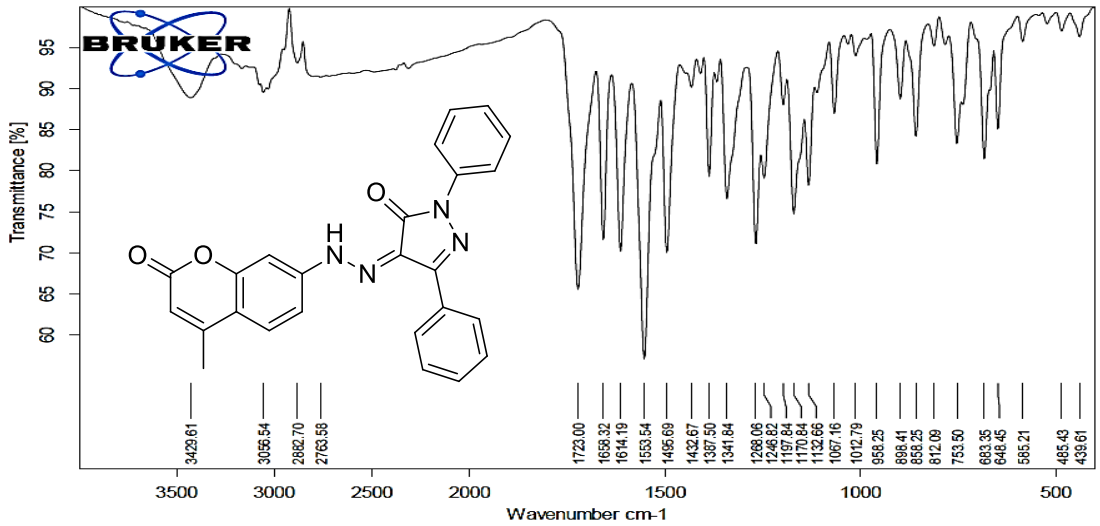

Figure- 3a.8.2 ^{1}H-NMR of (Z)-4-(2-(4-methyl-2-oxo-2H-chromen-7-yl)hydrazono)-1,3-diphenyl-1H-pyrazol-5(4H)-one **(11a)**

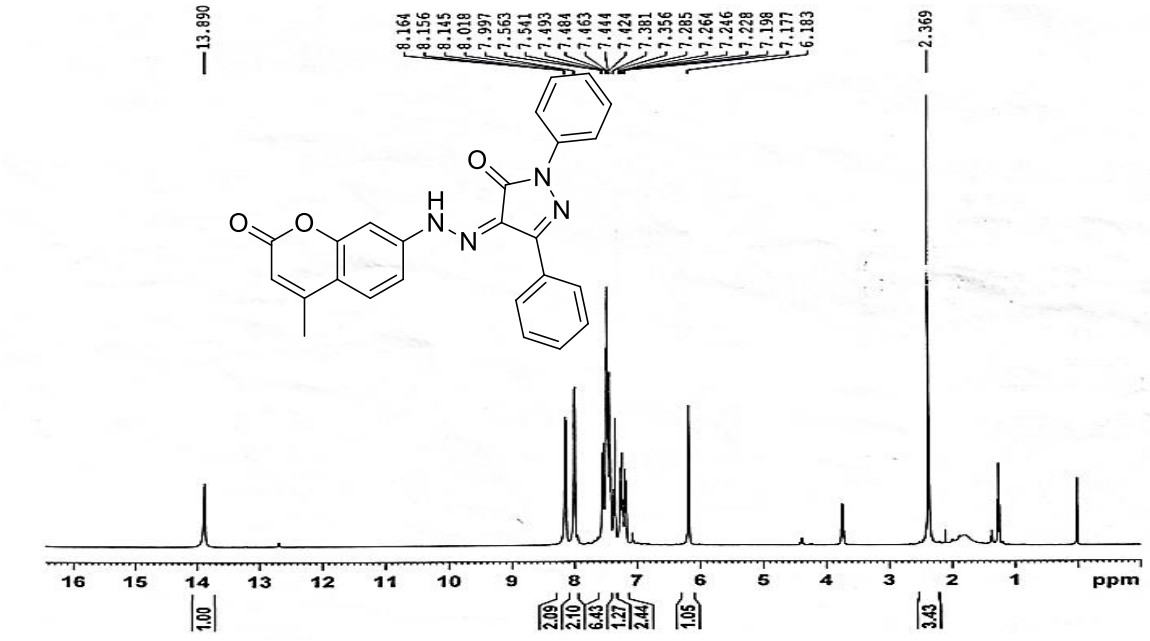

Figure- 3a.8.3 ^{13}C-NMR of (Z)-4-(2-(4-methyl-2-oxo-2H-chromen-7-yl)hydrazono)-1,3-diphenyl-1H-pyrazol-5(4H)-one **(11a)**

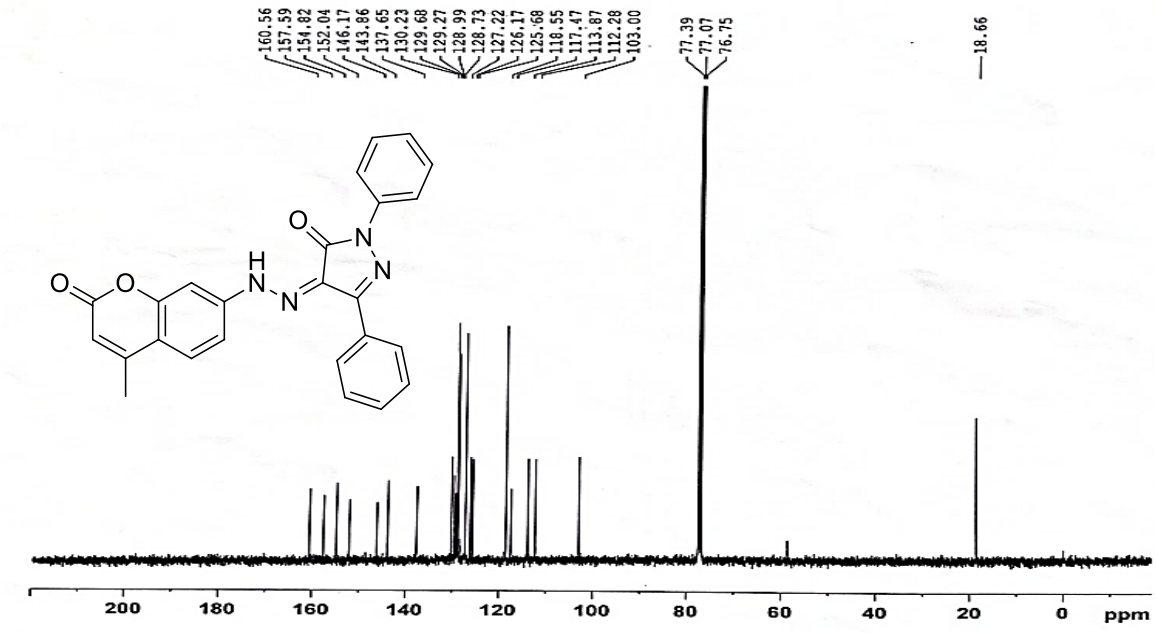

Figure- 3a.9.1 IR of (Z)-1-(4-fluorophenyl)-4-(2-(4-methyl-2-oxo-2H-chromen-7-yl)hydrazono)-3-phenyl-1H-pyrazol-5(4H)-one **(11b)**

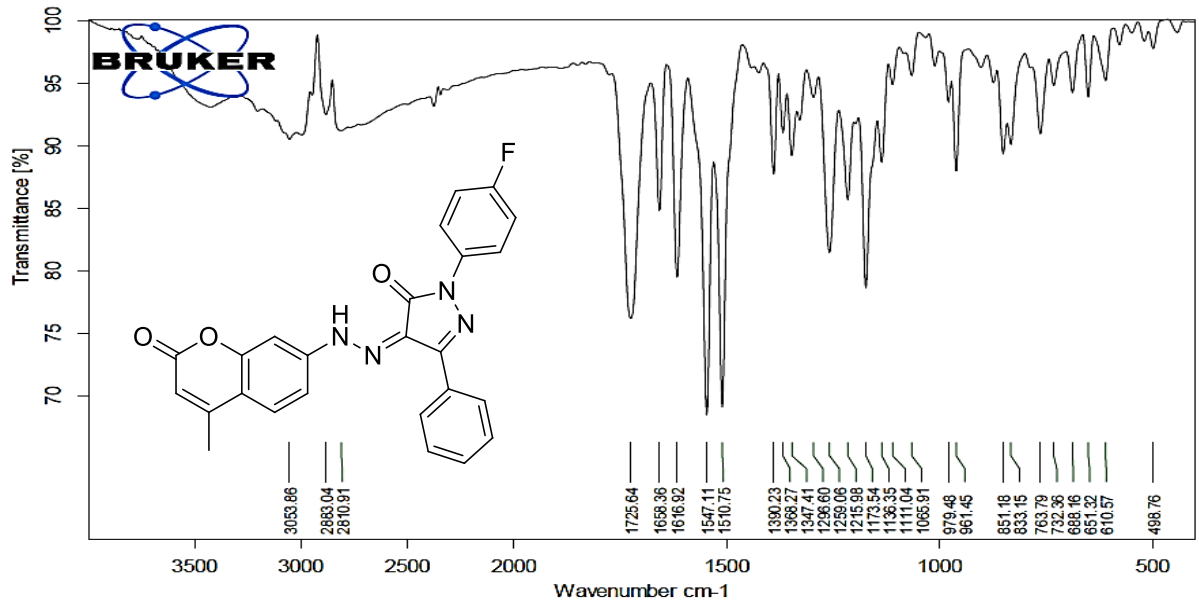

Figure- 3a.9.2 ^{1}H-NMR of (Z)-1-(4-fluorophenyl)-4-(2-(4-methyl-2-oxo-2H-chromen-7-yl)hydrazono)-3-phenyl-1H-pyrazol-5(4H)-one **(11b)**

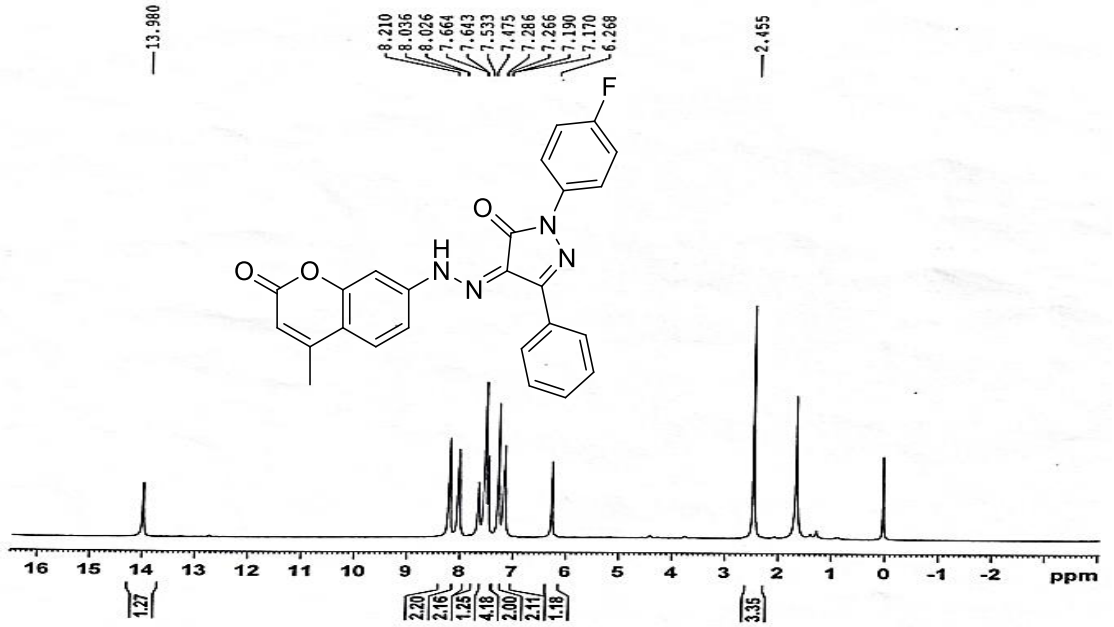

Figure- 3a.9.3 ^{13}C-NMR of (Z)-1-(4-fluorophenyl)-4-(2-(4-methyl-2-oxo-2H-chromen-7-yl)hydrazono)-3-phenyl-1H-pyrazol-5(4H)-one **(11b)**

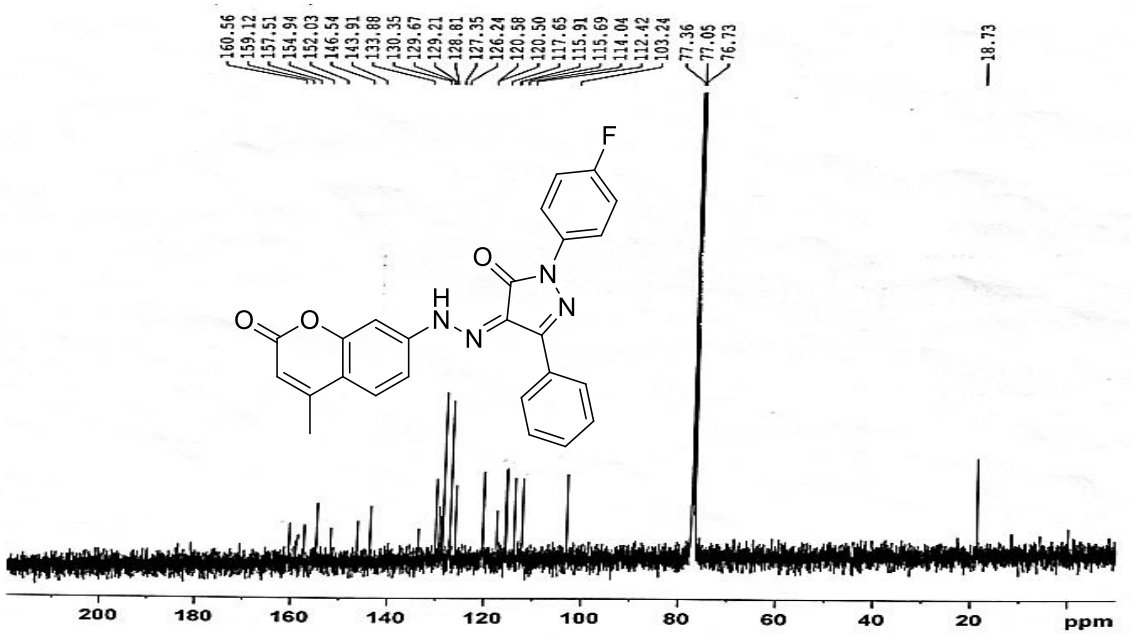

Figure- 3a.10.1 IR of (Z)-1-(4-chlorophenyl)-4-(2-(4-methyl-2-oxo-2H-chromen-7-yl)hydrazono)-3-phenyl-1H-pyrazol-5(4H)-one **(11c)**

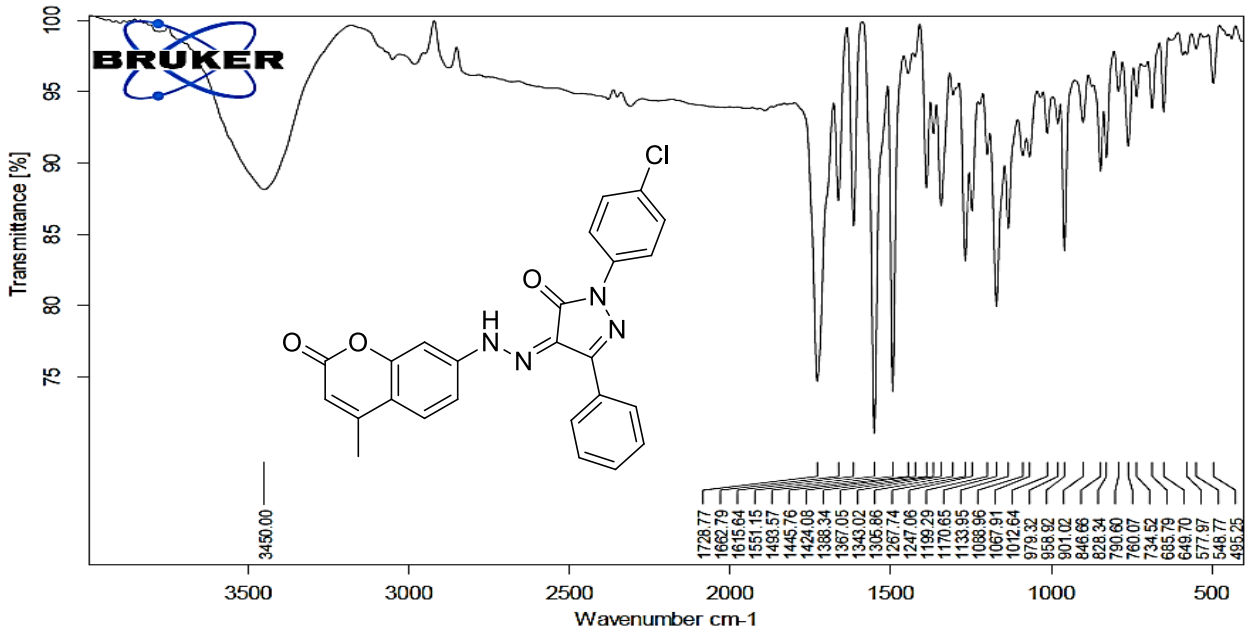

Figure- 3a.10.2 ^{1}H-NMR of (Z)-1-(4-chlorophenyl)-4-(2-(4-methyl-2-oxo-2H-chromen-7-yl)hydrazono)-3-phenyl-1H-pyrazol-5(4H)-one **(11c)**

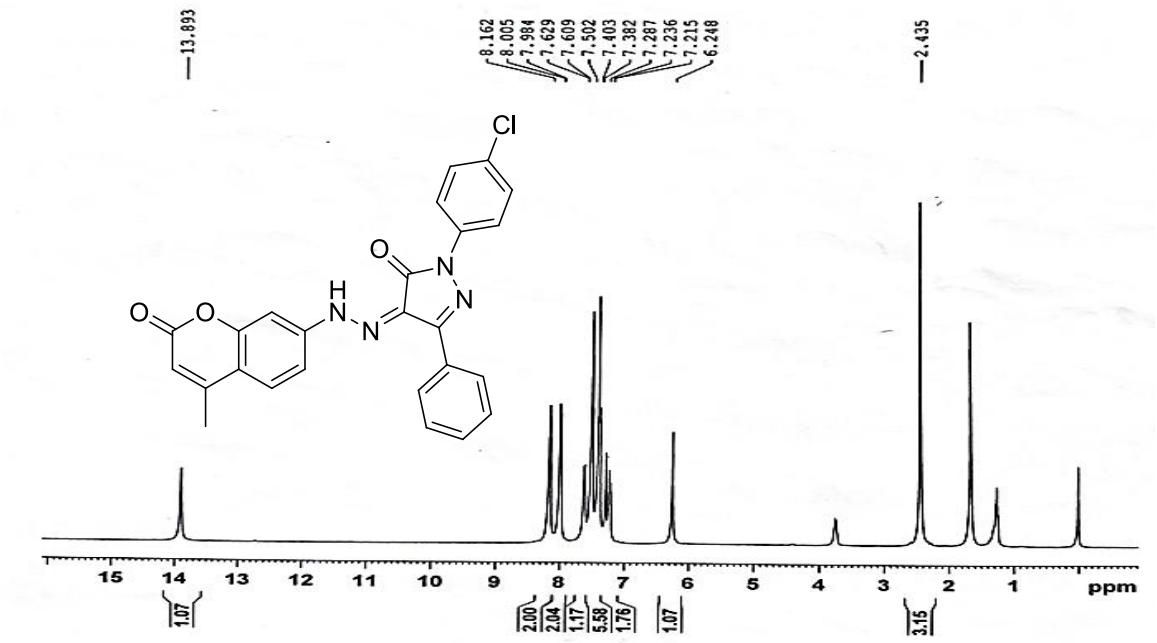

Figure- 3a.10.3 ^{13}C-NMR of (Z)-1-(4-chlorophenyl)-4-(2-(4-methyl-2-oxo-2H-chromen-7-yl)hydrazono)-3-phenyl-1H-pyrazol-5(4H)-one **(11c)**

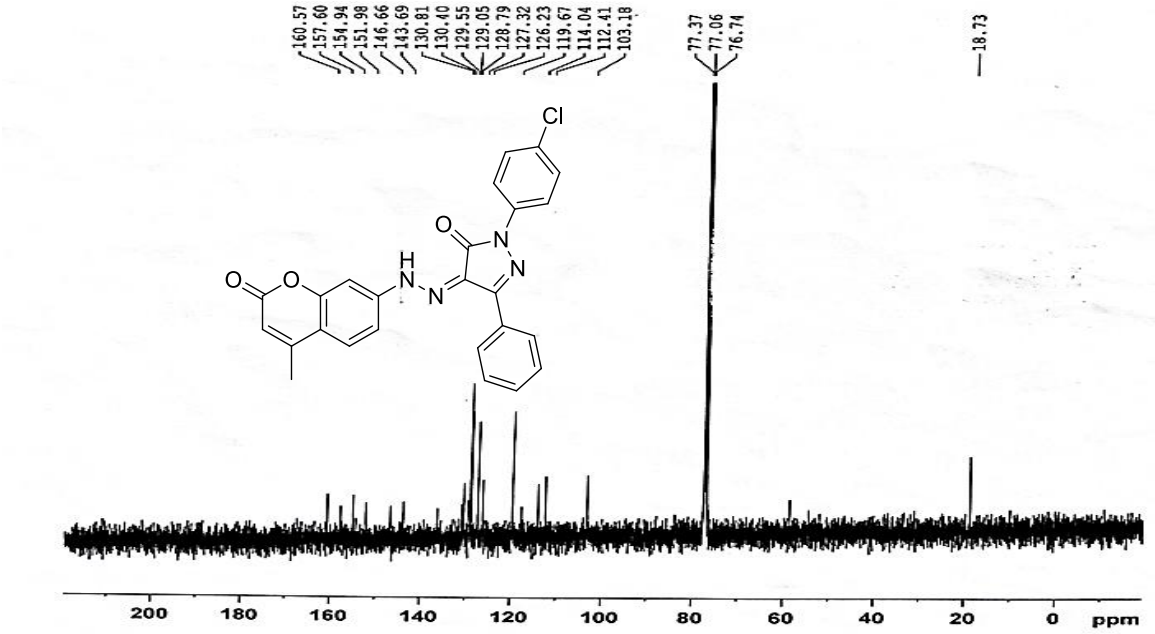

Figure- 3a.11.1 IR of (Z)-1-(2,4-dichlorophenyl)-4-(2-(4-methyl-2-oxo-2H-chromen-7-yl)hydrazono)-3-phenyl-1H-pyrazol-5(4H)-one **(11d)**

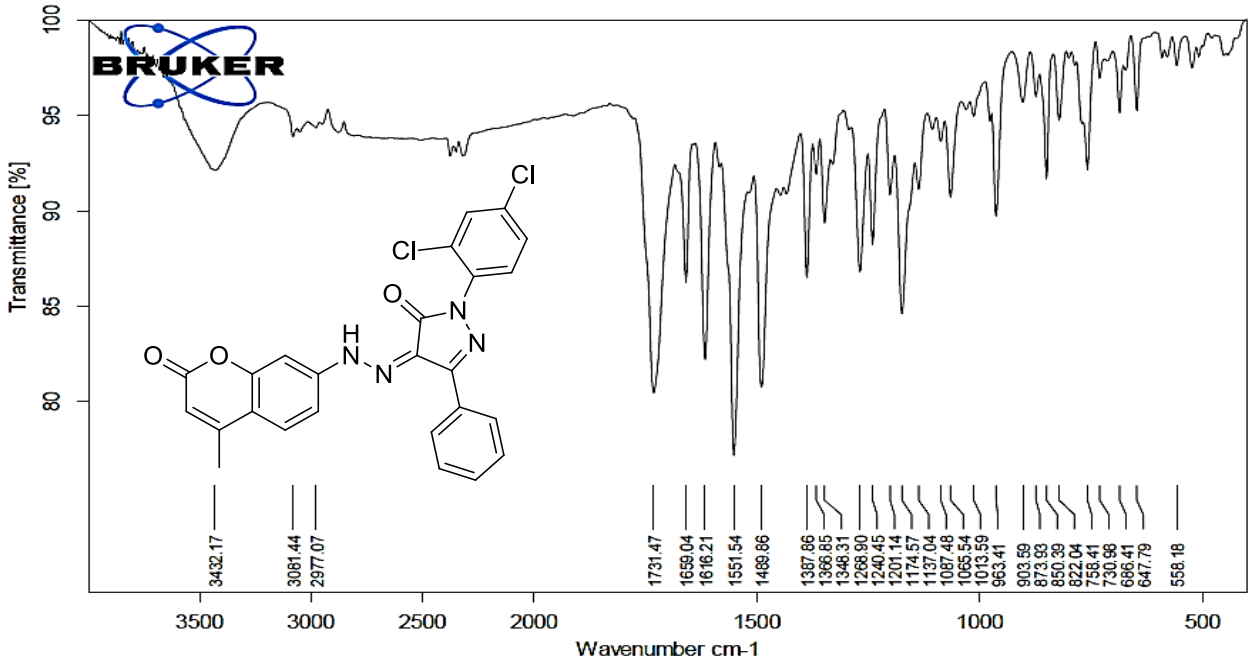

Figure- 3a.11.2 ^{1}H-NMR of (Z)-1-(2,4-dichlorophenyl)-4-(2-(4-methyl-2-oxo-2H-chromen-7-yl)hydrazono)-3-phenyl-1H-pyrazol-5(4H)-one **(11d)**

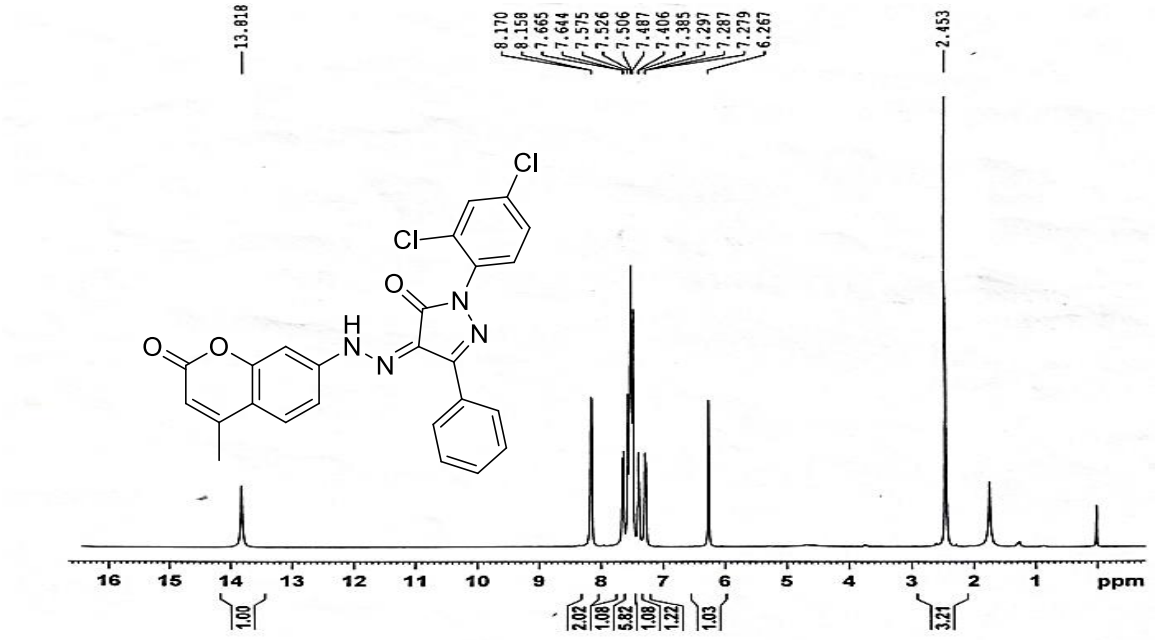

Figure- 3a.11.3 ^{13}C-NMR of (Z)-1-(2,4-dichlorophenyl)-4-(2-(4-methyl-2-oxo-2H-chromen-7-yl)hydrazono)-3-phenyl-1H-pyrazol-5(4H)-one **(11d)**

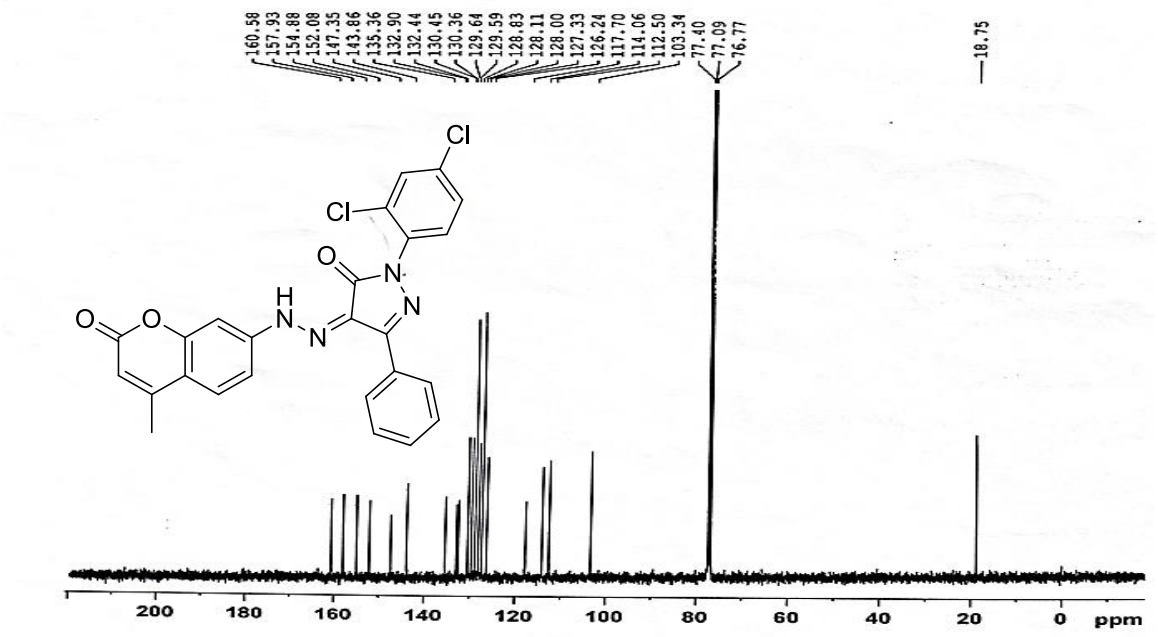

Figure- 3a.12.1 IR of (Z)-3-methyl-4-(2-(4-methyl-2-oxo-2H-chromen-7-yl)hydrazono)-1-(2-nitrobenzoyl)-1H-pyrazol-5(4H)-one **(12)**

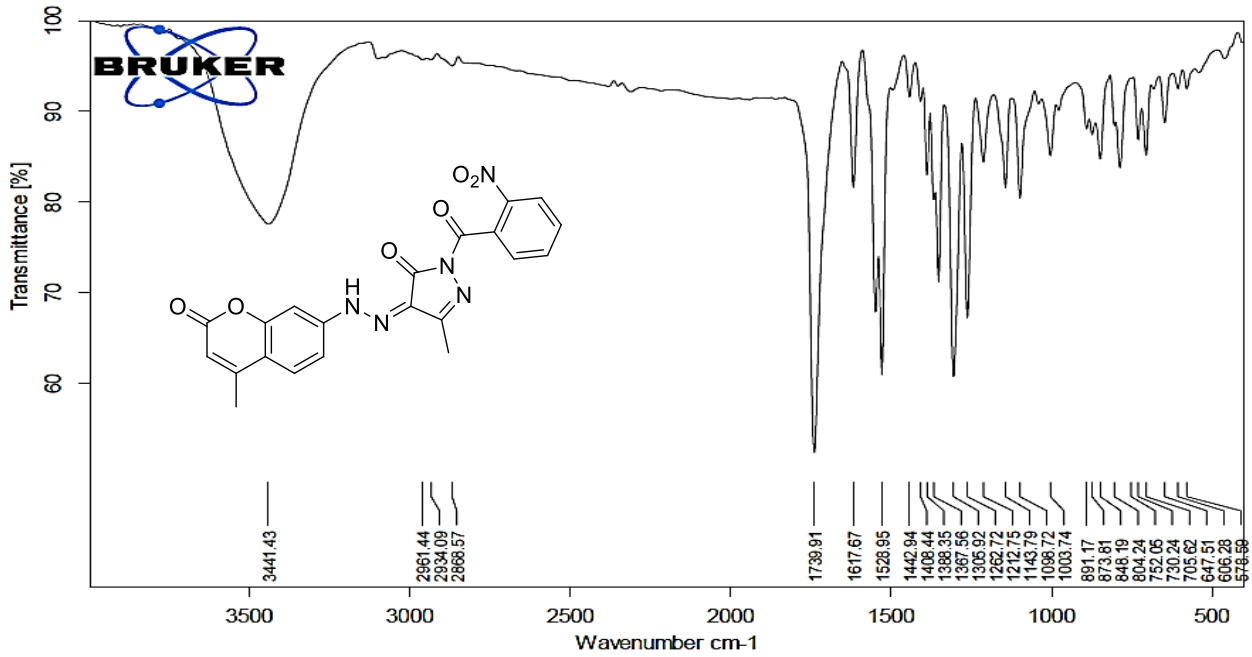

Figure- 3a.12.2 ^{1}H-NMR of (Z)-3-methyl-4-(2-(4-methyl-2-oxo-2H-chromen-7-yl)hydrazono)-1-(2-nitrobenzoyl)-1H-pyrazol-5(4H)-one **(12)**

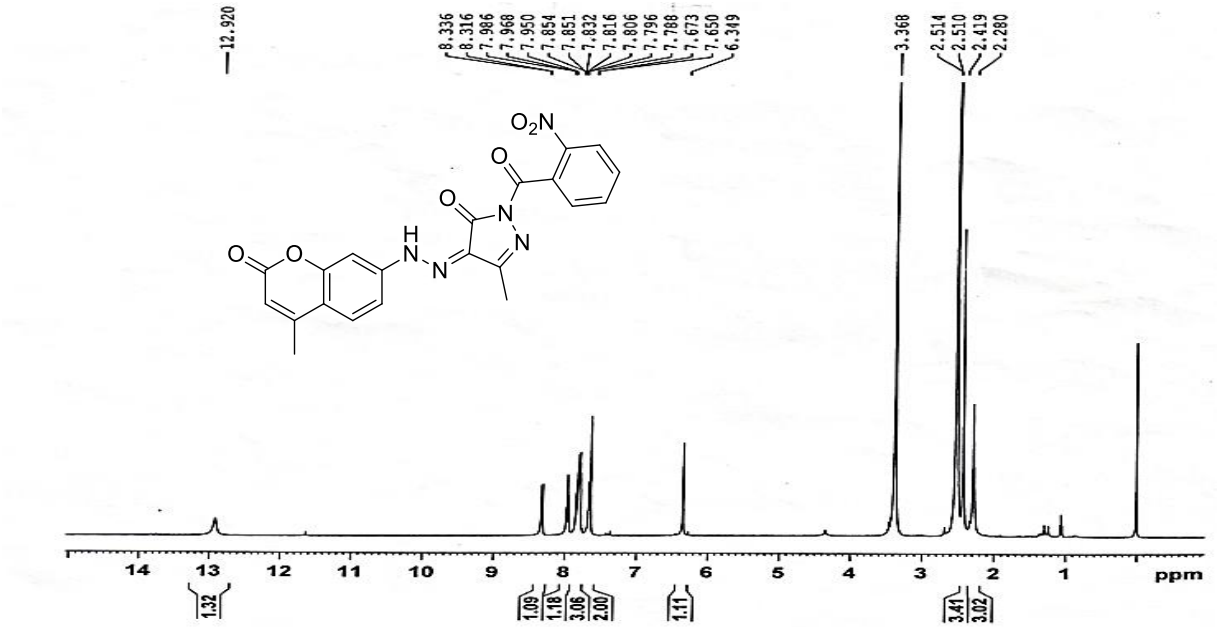

Figure- 3a.12.3 Mass of (Z)-3-methyl-4-(2-(4-methyl-2-oxo-2H-chromen-7-yl)hydrazono)-1-(2-nitrobenzoyl)-1H-pyrazol-5(4H)-one **(12)** M+H peak at 434.10

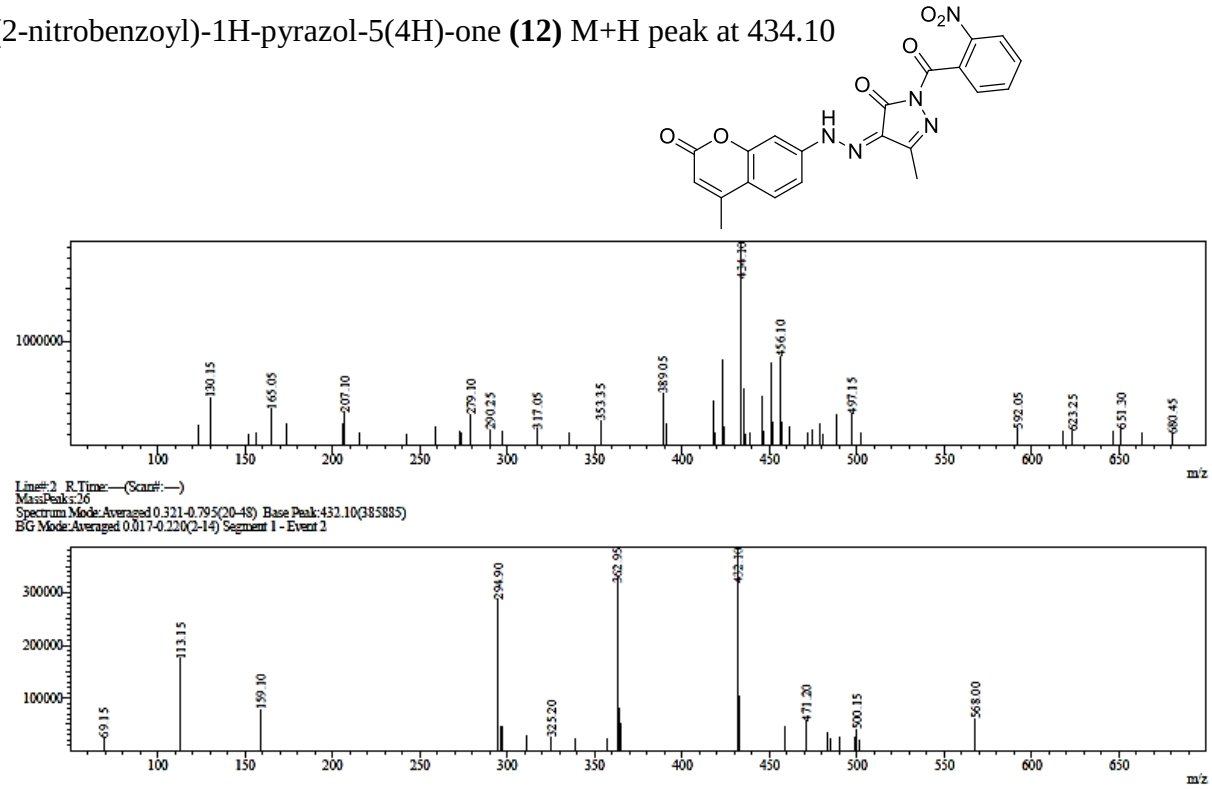

Figure- 3a.13.1 IR of (Z)-4-(2-(4-methyl-2-oxo-2H-chromen-7-yl)hydrazono)-1-(2-nitrobenzoyl)-3-phenyl-1H-pyrazol-5(4H)-one **(13)**

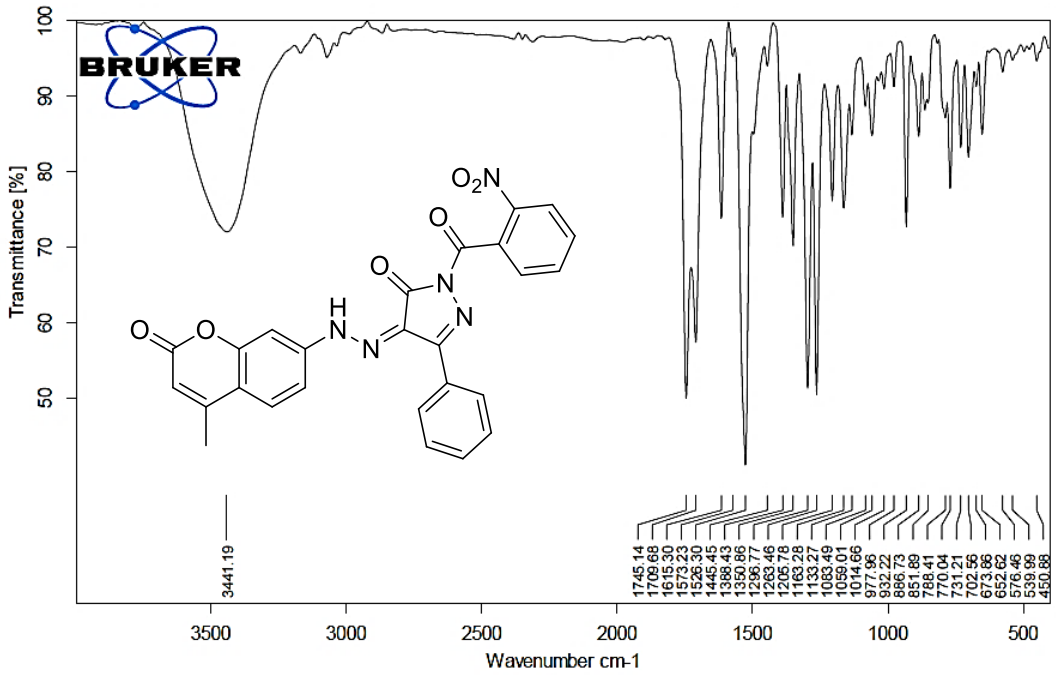

Figure- 3a.13.2 ^{1}H-NMR of (Z)-4-(2-(4-methyl-2-oxo-2H-chromen-7-yl)hydrazono)-1-(2-nitrobenzoyl)-3-phenyl-1H-pyrazol-5(4H)-one **(13)**

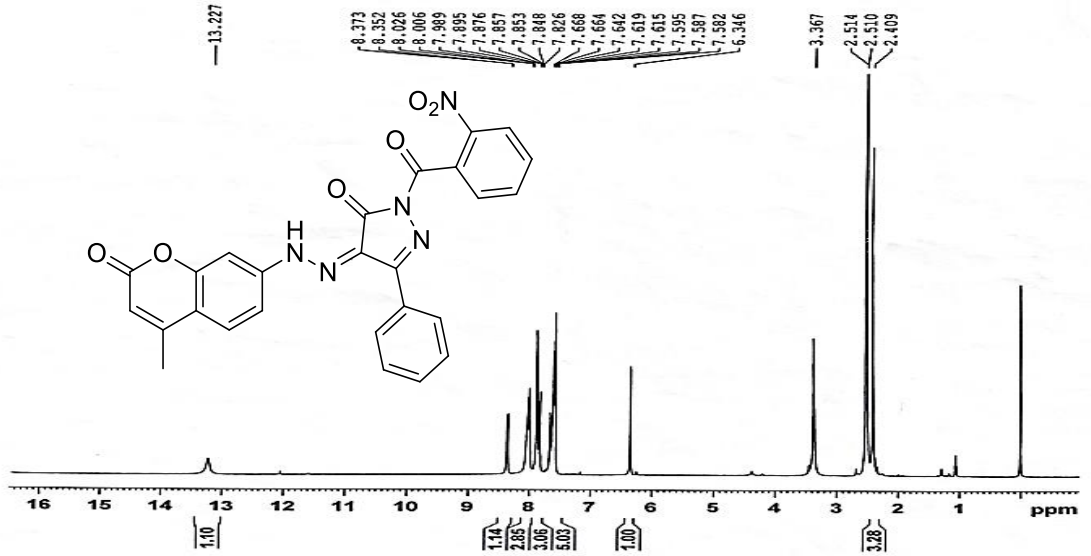

Figure- 3a.13.3 Mass of (Z)-4-(2-(4-methyl-2-oxo-2H-chromen-7-yl)hydrazono)-1-(2-nitrobenzoyl) -3-phenyl-1H-pyrazol-5(4H)-one **(13)** M+H peak at 436.15

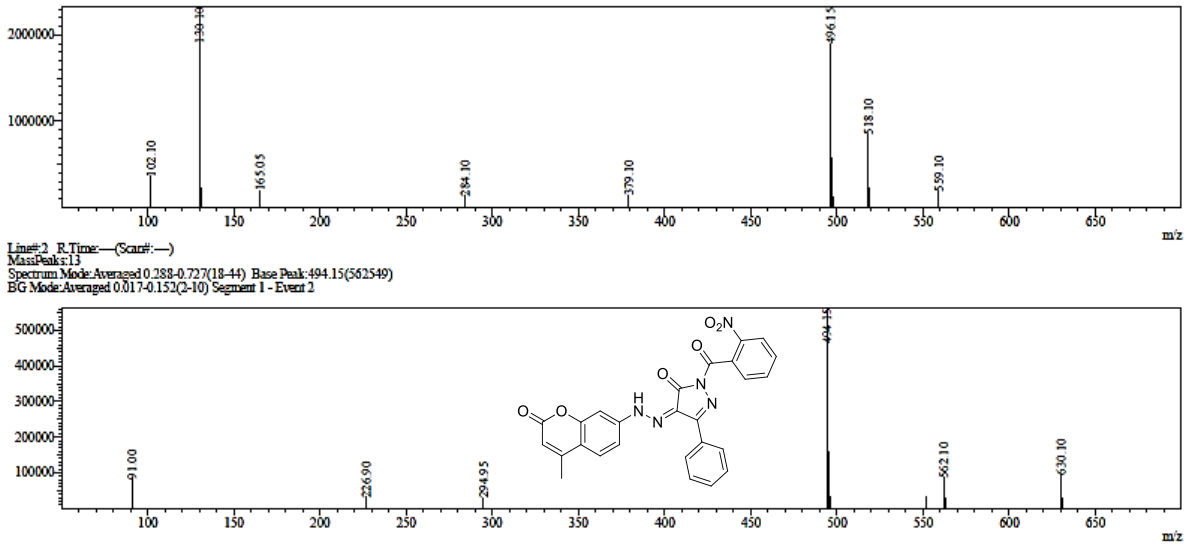

Figure- 3a.14.1 IR of (E)-ethyl 3-oxo-2-(2-(2-oxo-2H-chromen-6-yl)hydrazono)butanoate **(16)**

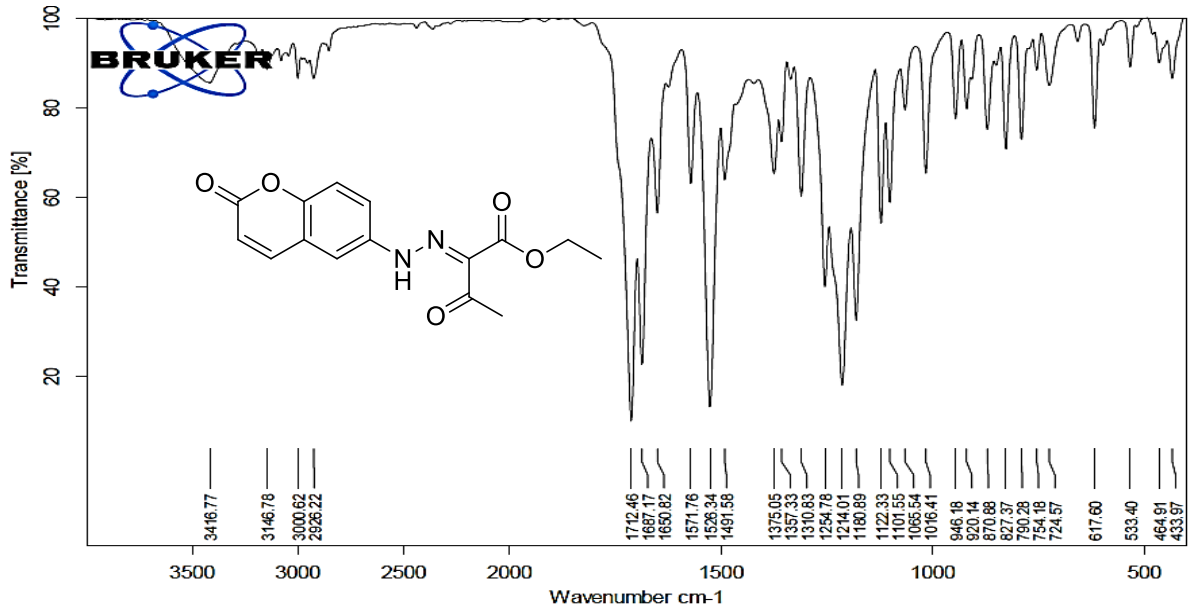

Figure- 3a.14.2 ^{1}H-NMR of (E)-ethyl 3-oxo-2-(2-(2-oxo-2H-chromen-6-yl)hydrazono) butanoate **(16)**

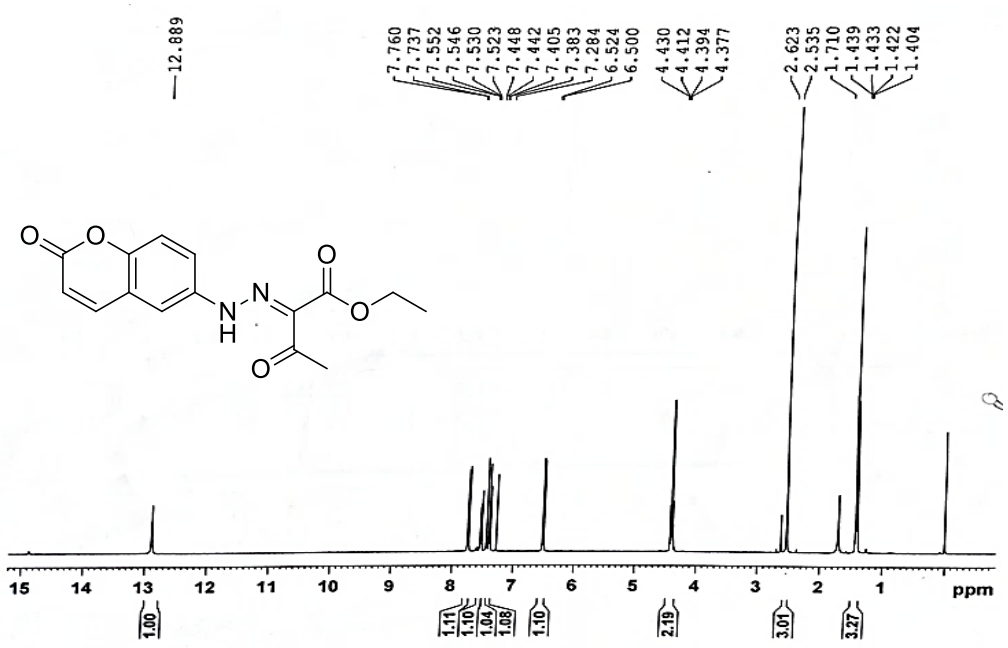

Figure- 3a.14.1 IR of (E)-ethyl 3-oxo-2-(2-(2-oxo-2H-chromen-6-yl)hydrazono)-3-phenylpropanoate **(18)**

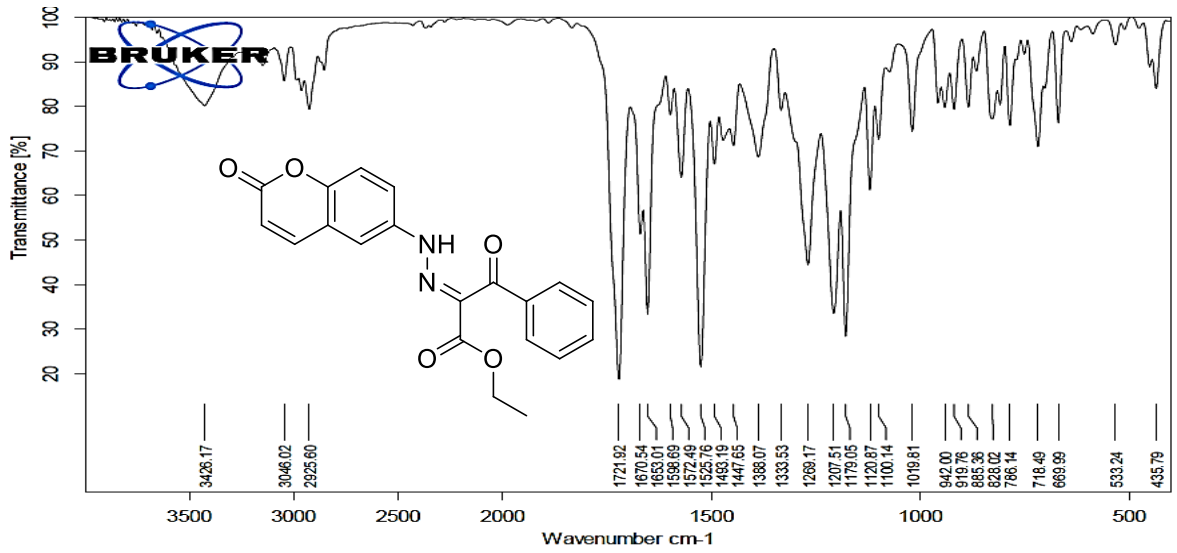

Figure- 3a.14.2 ^{1}H-NMR of (E)-ethyl 3-oxo-2-(2-(2-oxo-2H-chromen-6-yl)hydrazono)-3-phenylpropanoate **(18)**

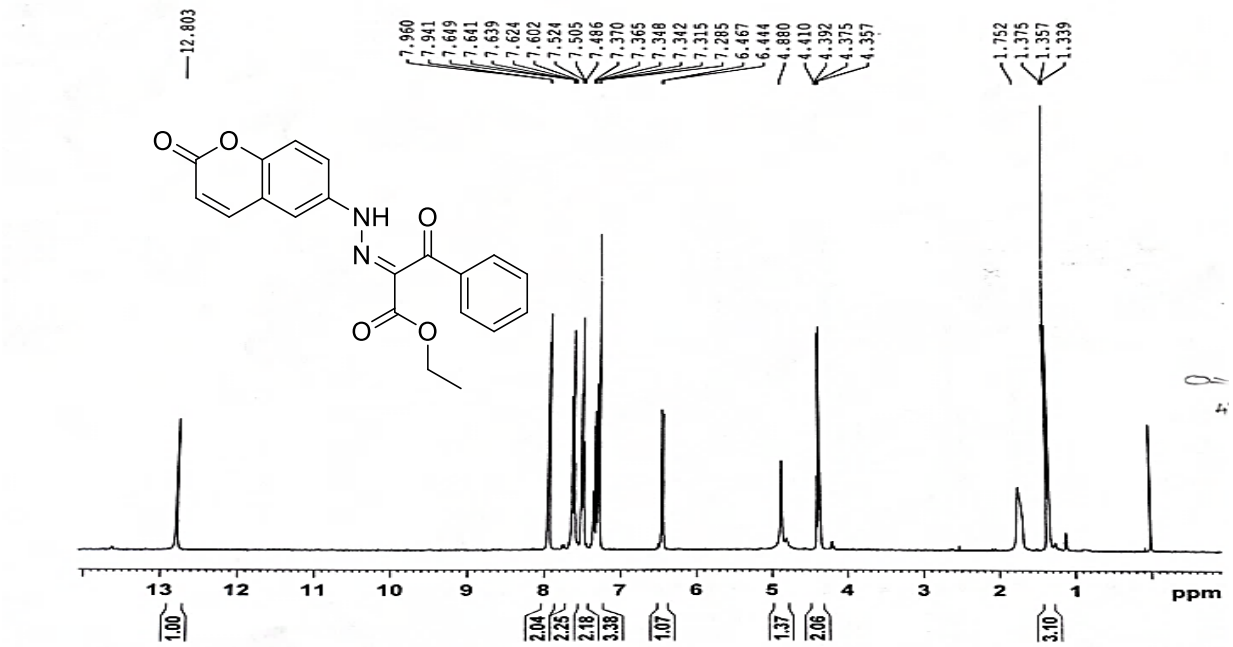

Figure- 3a.14.3 ^{13}C-NMR of (E)-ethyl 3-oxo-2-(2-(2-oxo-2H-chromen-6-yl)hydrazono)-3-phenylpropanoate **(18)**

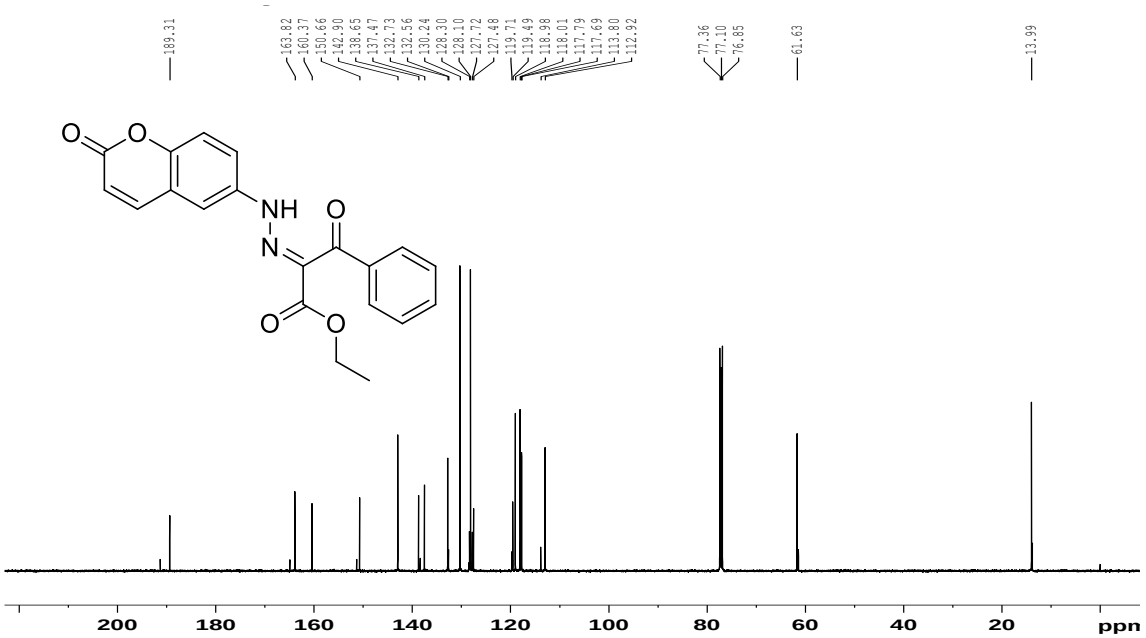

Figure- 3a.15.1 IR of (Z)-3-methyl-4-(2-(2-oxo-2H-chromen-6-yl)hydrazono)-1-phenyl-1H-pyrazol-5(4H)-one **(17a)**

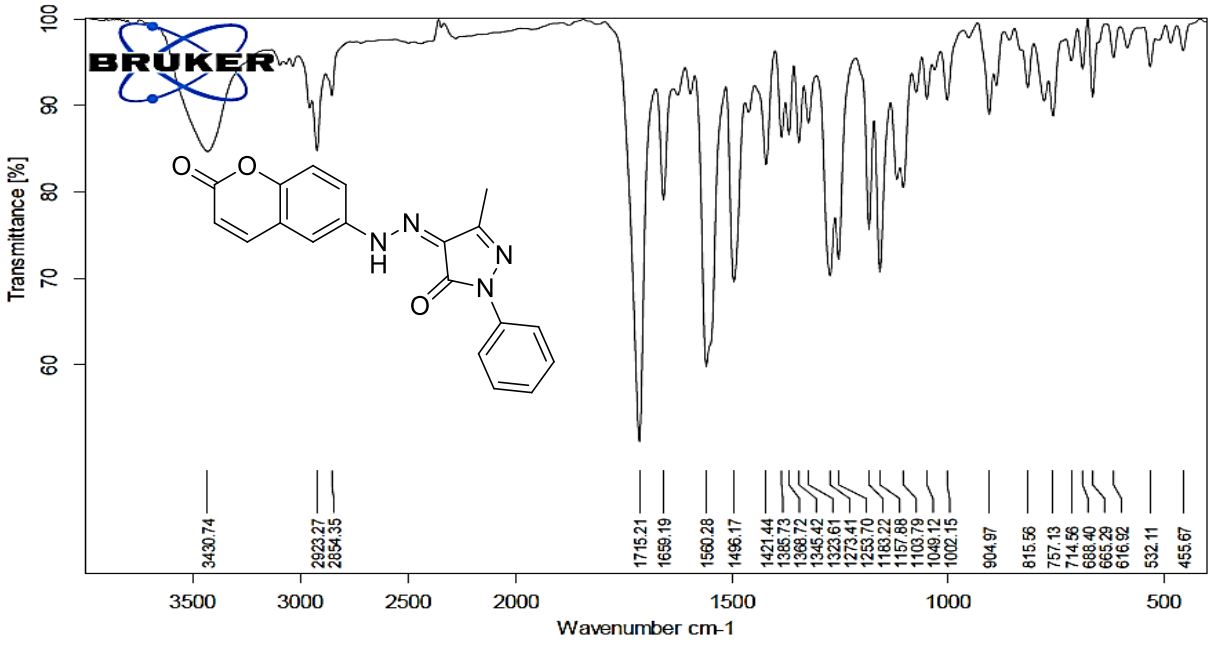

Figure- 3a.15.2 ^{1}H-NMR of (Z)-3-methyl-4-(2-(2-oxo-2H-chromen-6-yl)hydrazono)-1-phenyl-1H-pyrazol-5(4H)-one **(17a)**

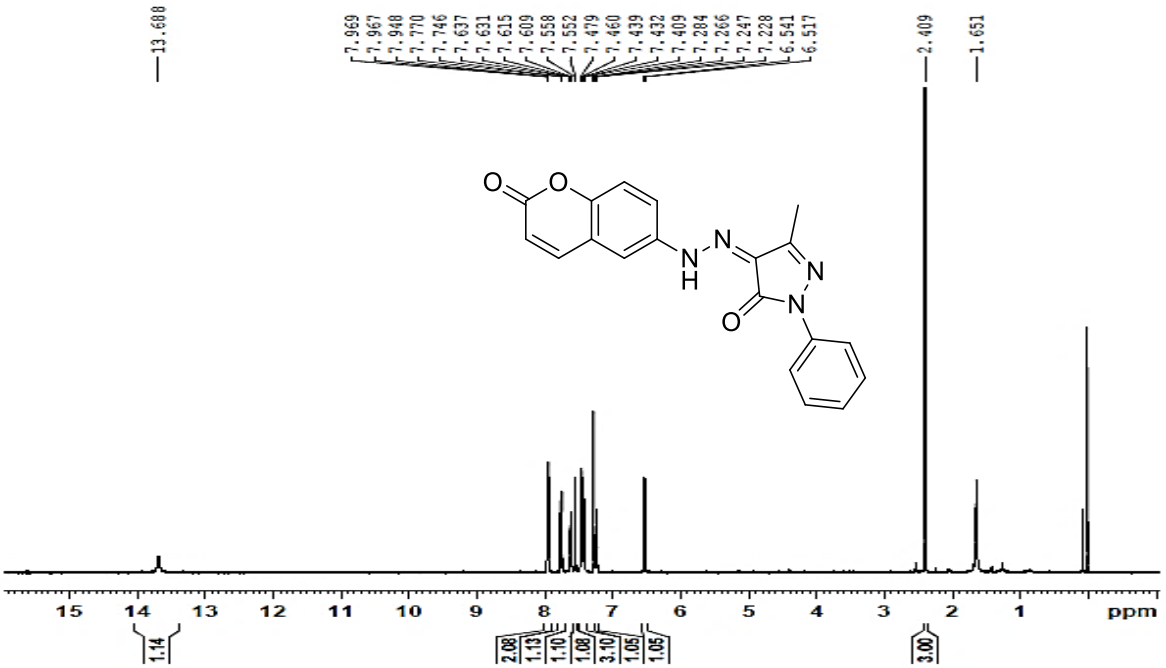

Figure- 3a.15.3 Mass of (Z)-3-methyl-4-(2-(2-oxo-2H-chromen-6-yl)hydrazono)-1-phenyl-1H-pyrazol-5(4H)-one **(17a)** M+H peak at 347.10

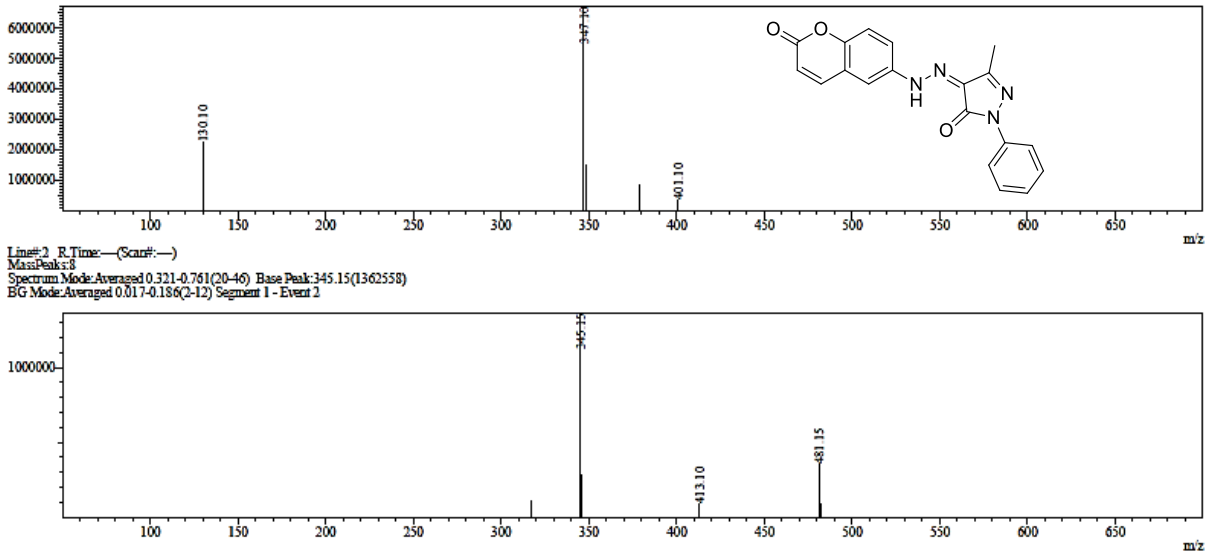

Figure- 3.16.1 IR of (Z)-1-(4-fluorophenyl)-3-methyl-4-(2-(2-oxo-2H-chromen-6-yl)hydrazono)-1H-pyrazol-5(4H)-one **(17b)**

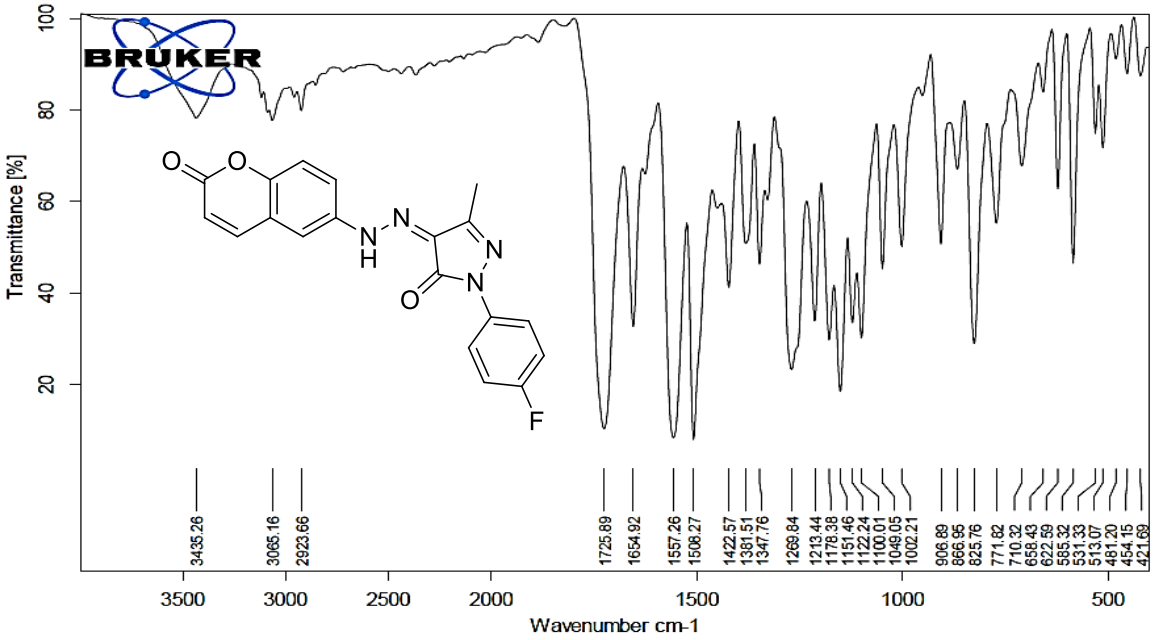

Figure- 3a.16.2 ^{1}H-NMR of (Z)-1-(4-fluorophenyl)-3-methyl-4-(2-(2-oxo-2H-chromen-6-yl)hydrazono)-1H-pyrazol-5(4H)-one **(17b)**

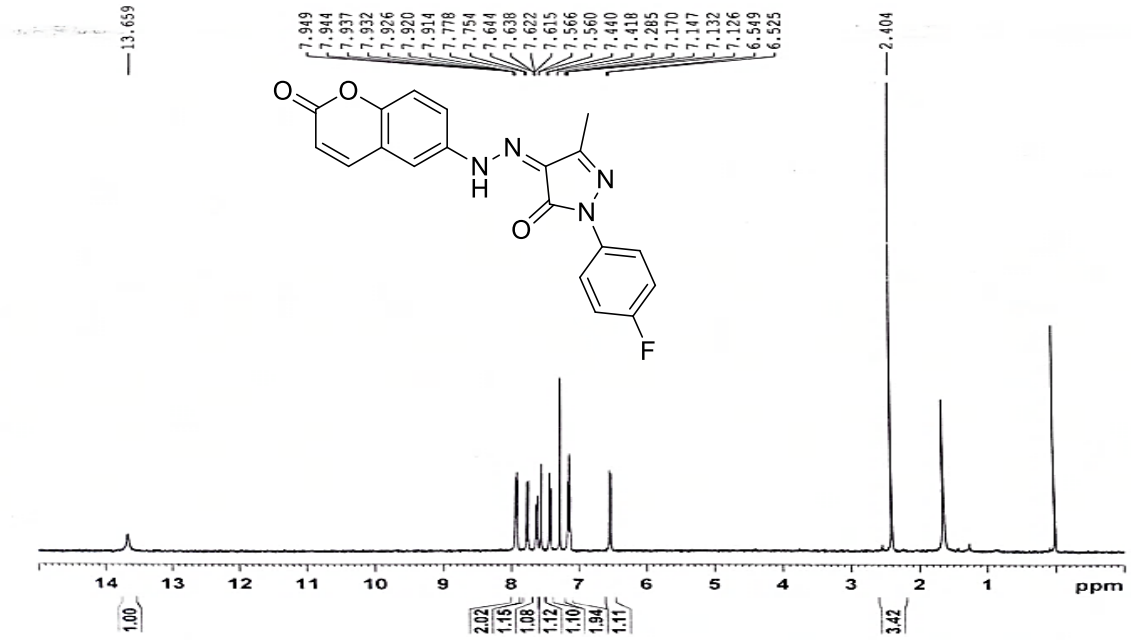

Figure- 3a.16.3 Mass of (Z)-1-(4-fluorophenyl)-3-methyl-4-(2-(2-oxo-2H-chromen-6-yl)hydrazono)-1H-pyrazol-5(4H)-one **(17b)** M+H peak at 365.10

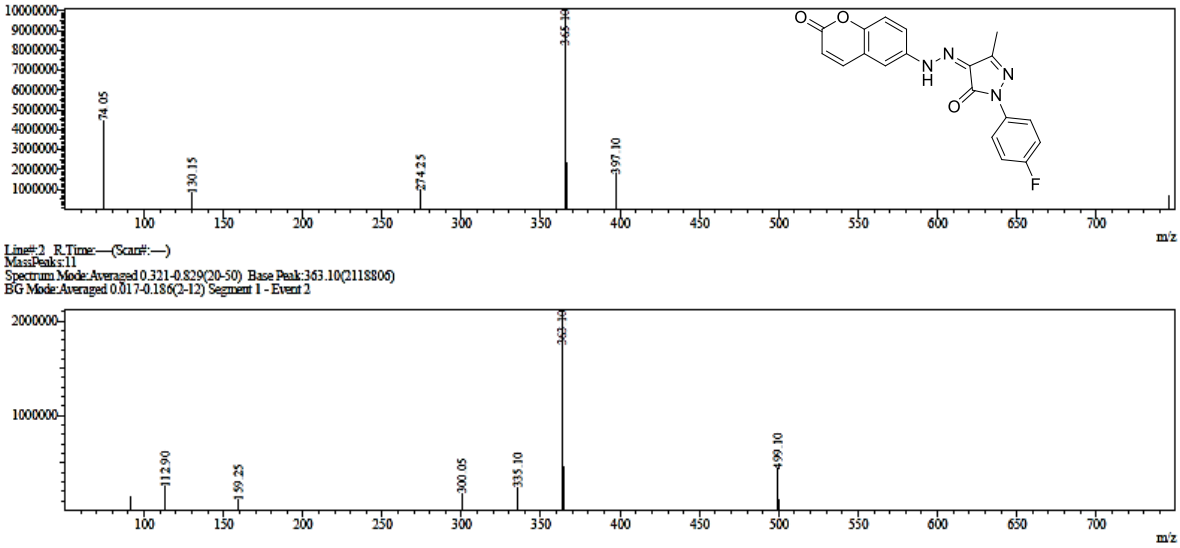

Figure- 3a.17.1 IR of (Z)-1-(4-chlorophenyl)-3-methyl-4-(2-(2-oxo-2H-chromen-6-yl)hydrazono)-1H-pyrazol-5(4H)-one **(17c)**

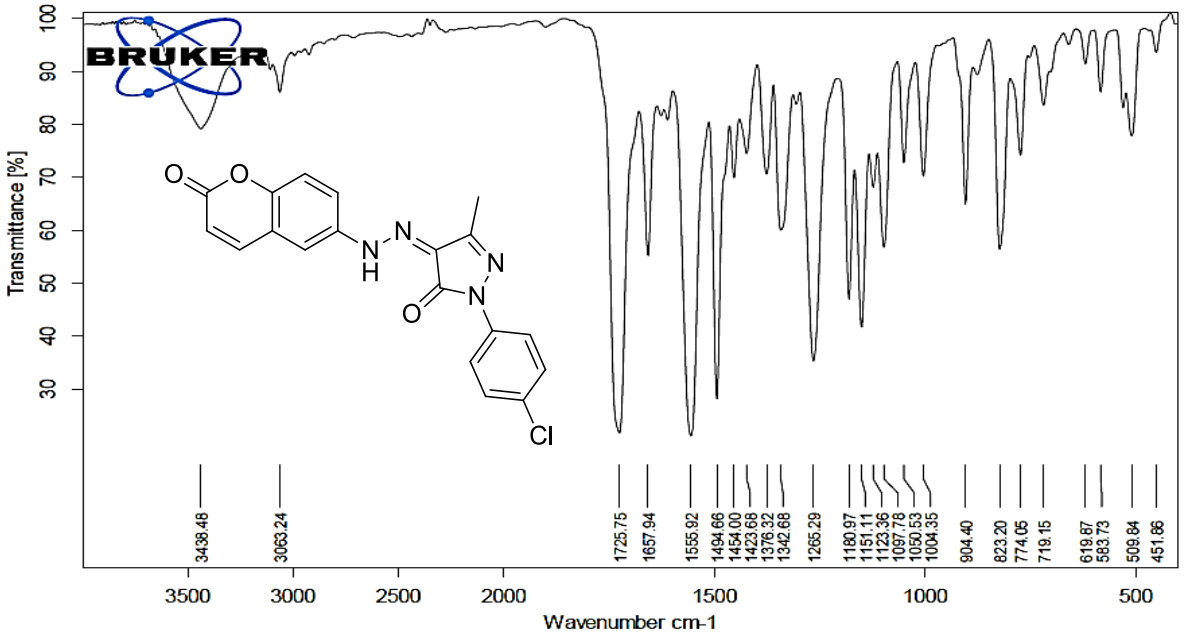

Figure- 3a.17.2 ^{1}H-NMR of (Z)-1-(4-chlorophenyl)-3-methyl-4-(2-(2-oxo-2H-chromen-6-yl)hydrazono)-1H-pyrazol-5(4H)-one **(17c)**

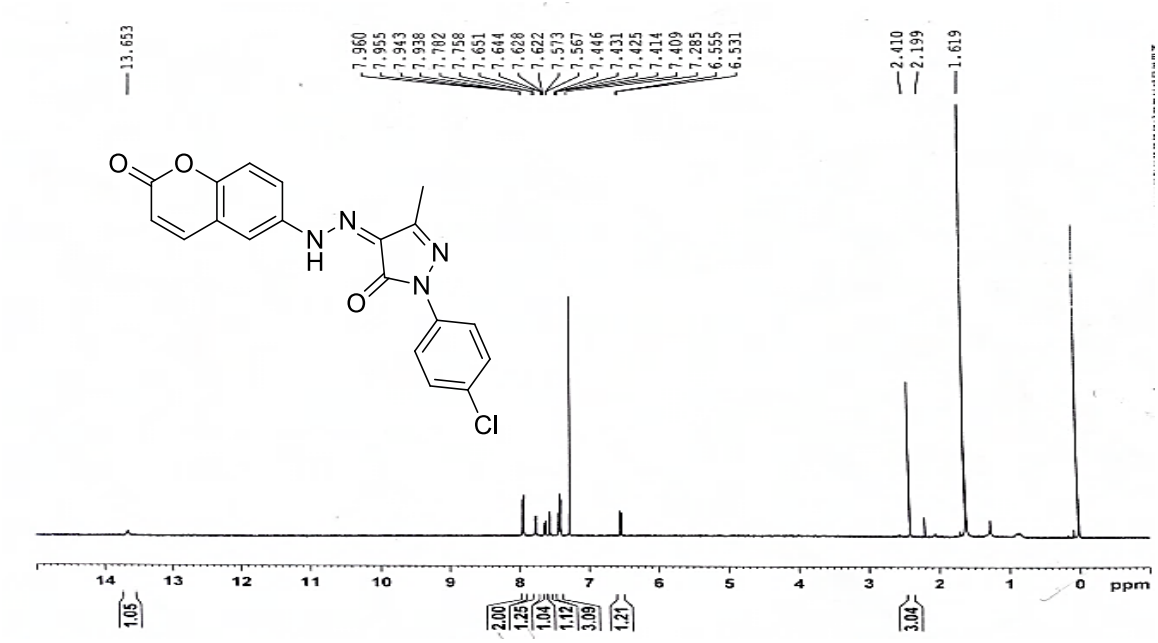

Figure- 3a.17.3 ^{13}C-NMR of (Z)-1-(4-chlorophenyl)-3-methyl-4-(2-(2-oxo-2H-chromen-6-yl)hydrazono)-1H-pyrazol-5(4H)-one **(17c)**

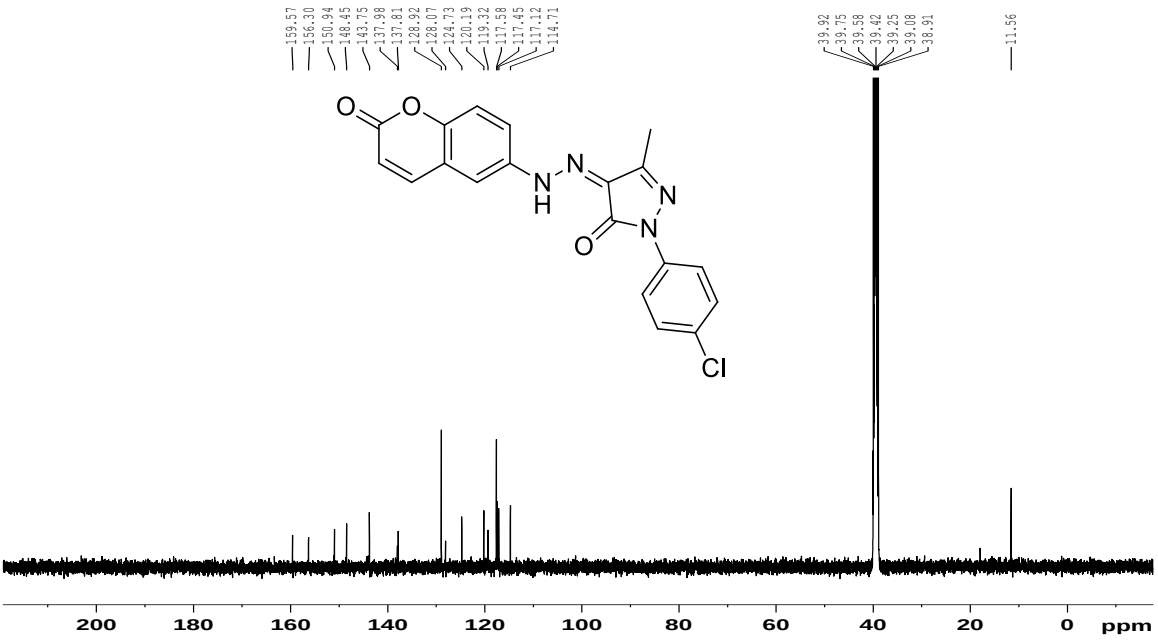

Figure- 3a.17.4 Mass of (Z)-1-(4-chlorophenyl)-3-methyl-4-(2-(2-oxo-2H-chromen-6-yl)hydrazono)-1H-pyrazol-5(4H)-one **(17c)** M+H peak at 381.09

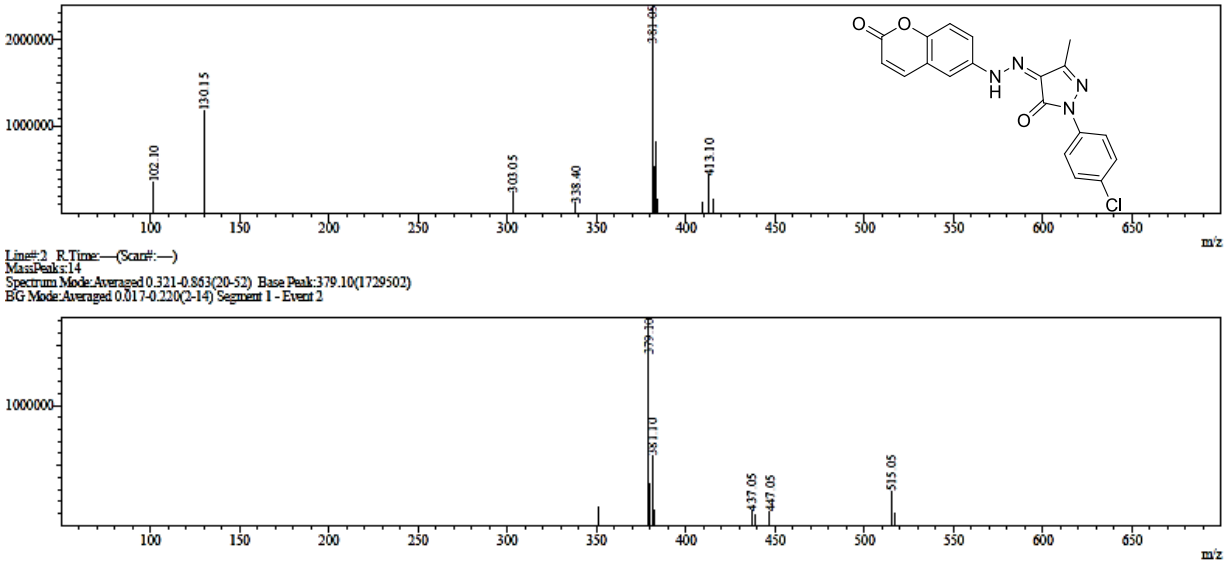

Figure- 3a.18.1 IR of (Z)-1-(2,4-dichlorophenyl)-3-methyl-4-(2-(2-oxo-2H-chromen-6-yl)hydrazono)-1H-pyrazol-5(4H)-one **(17d)**

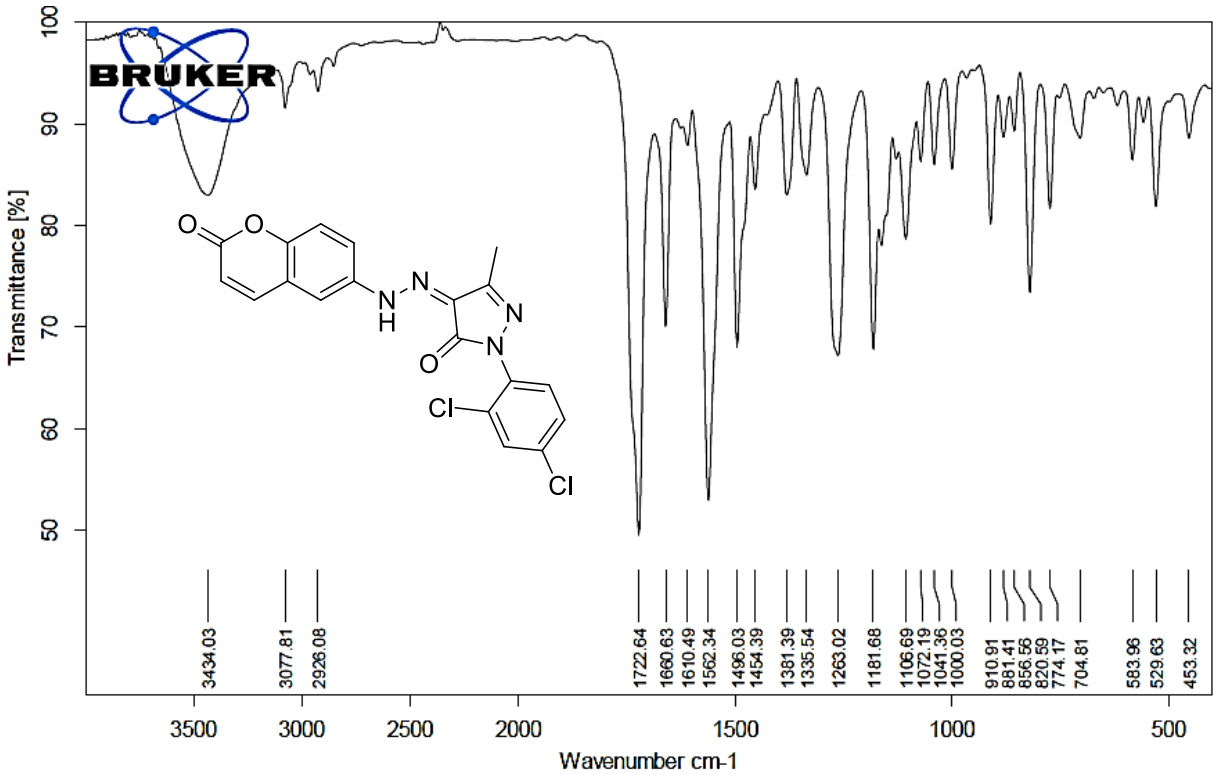

Figure- 3a.18.2 ^{1}H-NMR of (Z)-1-(2,4-dichlorophenyl)-3-methyl-4-(2-(2-oxo-2H-chromen-6-yl)hydrazono)-1H-pyrazol-5(4H)-one **(17d)**

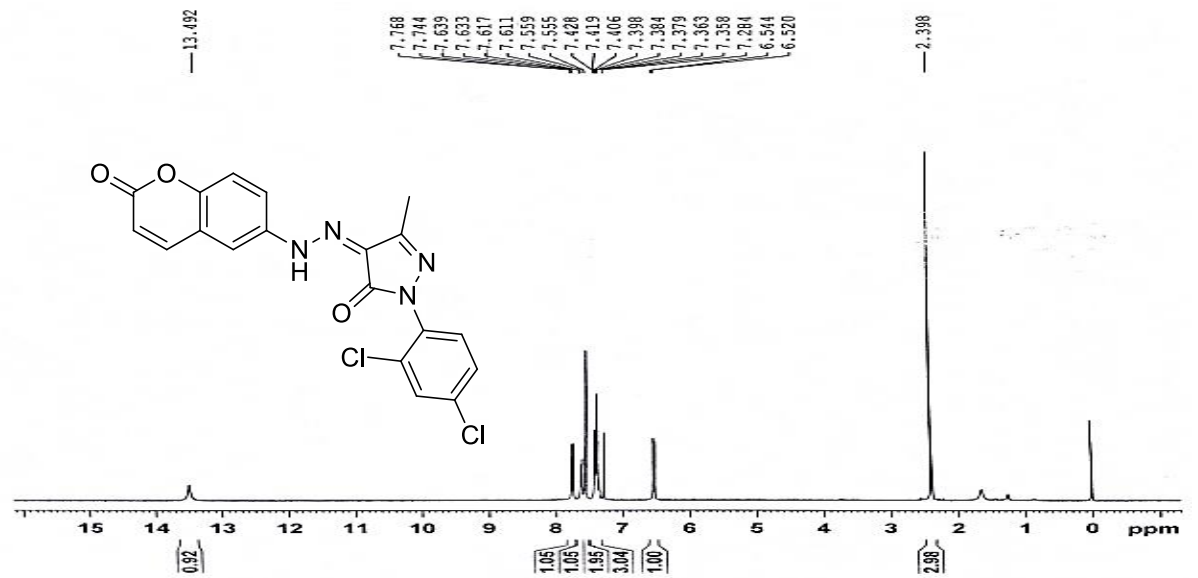

Figure- 3a.18.3 Mass of (Z)-1-(2,4-dichlorophenyl)-3-methyl-4-(2-(2-oxo-2H-chromen-6-yl)hydrazono)-1H-pyrazol-5(4H)-one **(17d)** M-H peak at 413.2

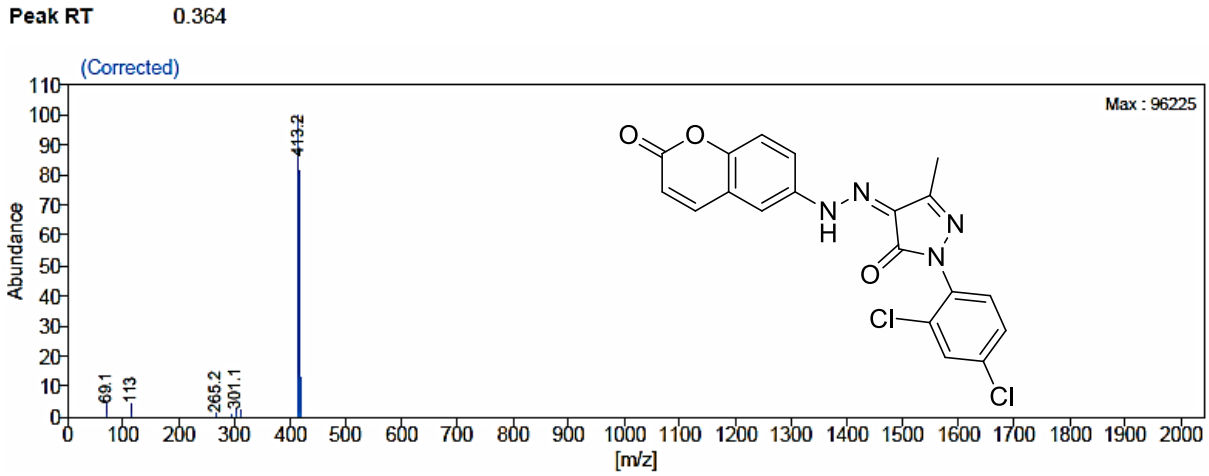

Figure- 3a.19.1 IR of (Z)-4-(2-(2-oxo-2H-chromen-6-yl)hydrazono)-1,3-diphenyl-1H-pyrazol-5(4H)-one**(19a)**

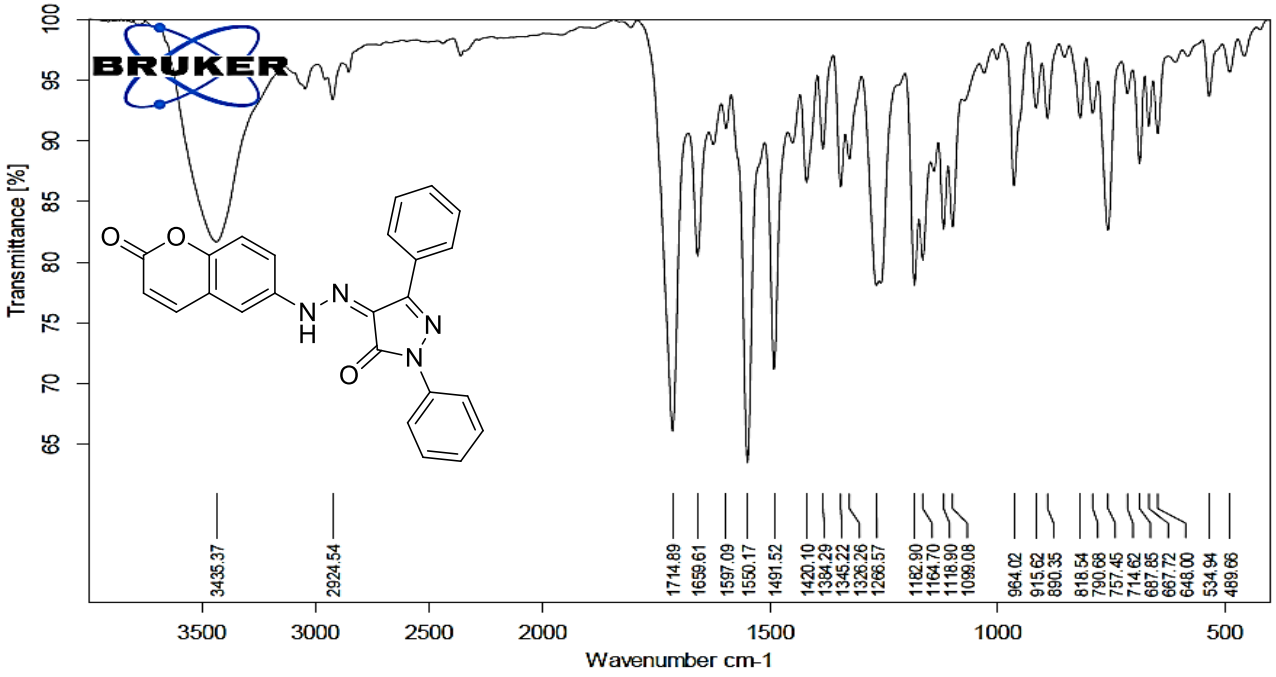

Figure- 3a.19.2 ^{1}H-NMR of (Z)-4-(2-(2-oxo-2H-chromen-6-yl)hydrazono)-1,3-diphenyl-1H-pyrazol-5(4H)-one**(19a)**

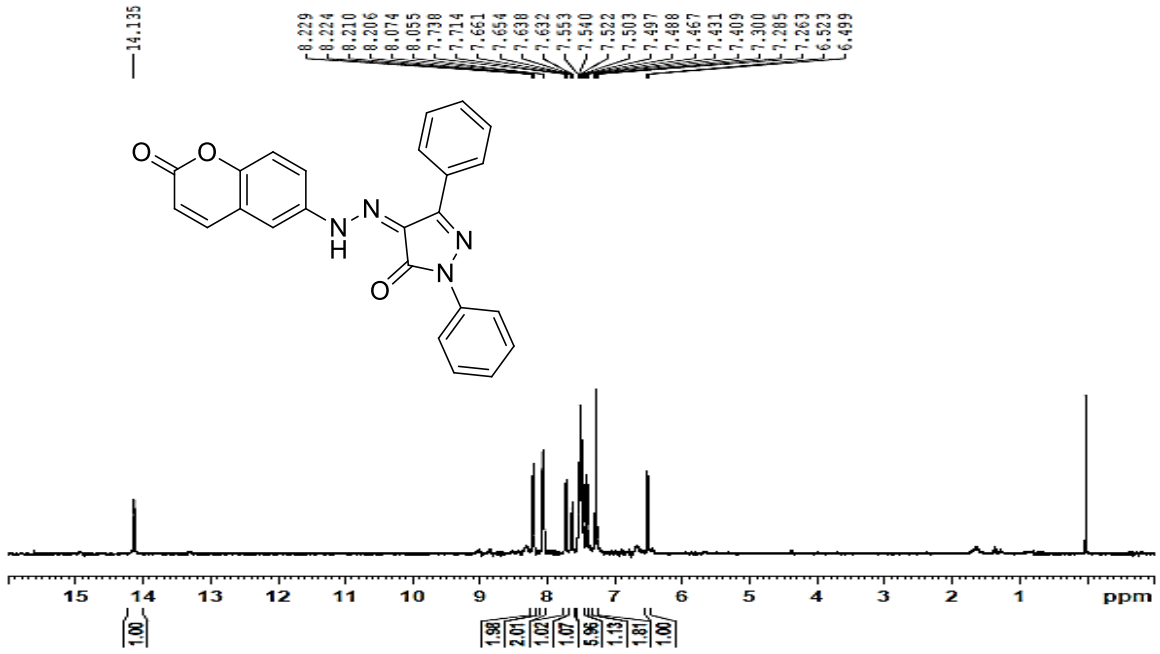

Figure- 3a.20.1 IR of (Z)-1-(4-fluorophenyl)-4-(2-(2-oxo-2H-chromen-6-yl)hydrazono)-3-phenyl-1H-pyrazol-5(4H)-one **(19b)**

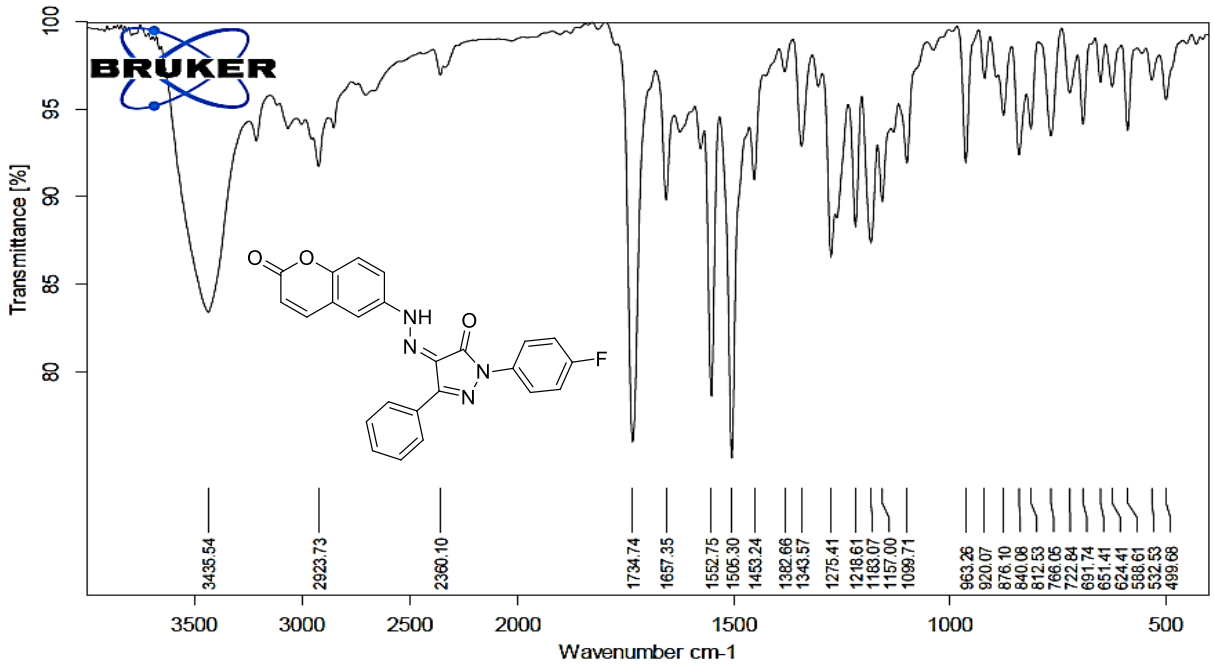

Figure- 3a.20.2 ^{1}H-NMR of (Z)-1-(4-fluorophenyl)-4-(2-(2-oxo-2H-chromen-6-yl)hydrazono)-3-phenyl-1H-pyrazol-5(4H)-one **(19b)**

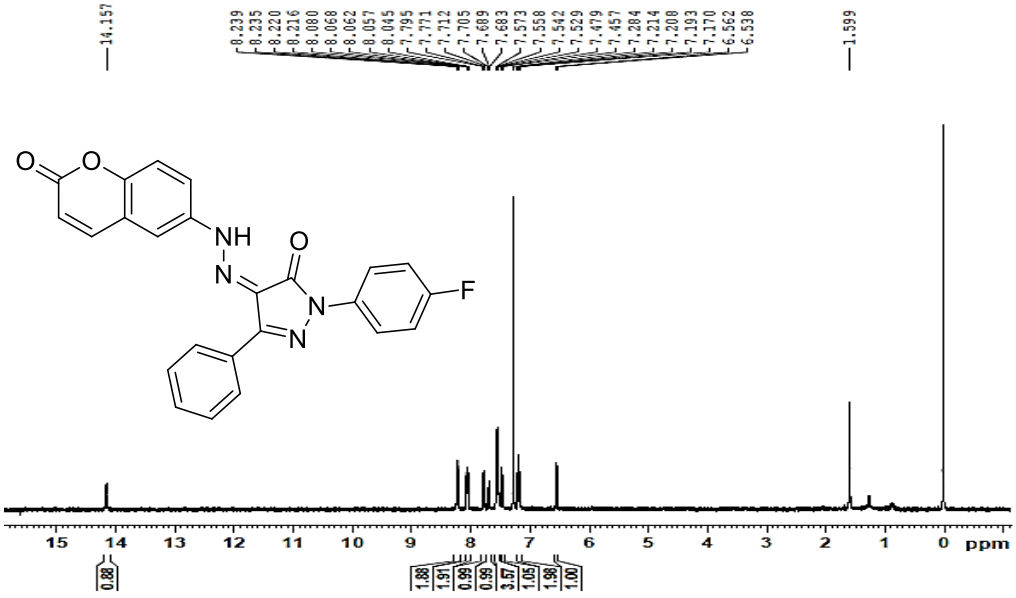

Figure- 3a.20.3 ^{13}C-NMR of (Z)-1-(4-fluorophenyl)-4-(2-(2-oxo-2H-chromen-6-yl)hydrazono)-3-phenyl-1H-pyrazol-5(4H)-one **(19b)**

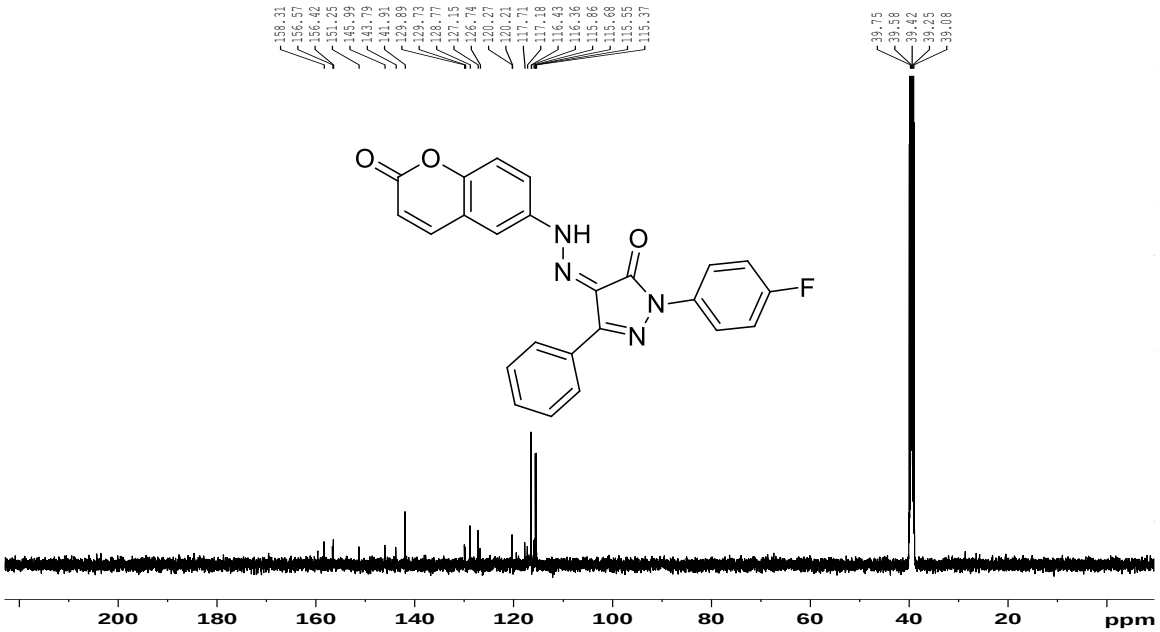

Figure- 3a.21.1 IR of (Z)-1-(4-chlorophenyl)-4-(2-(2-oxo-2H-chromen-6-yl)hydrazono)-3-phenyl-1H-pyrazol-5(4H)-one **(19c)**

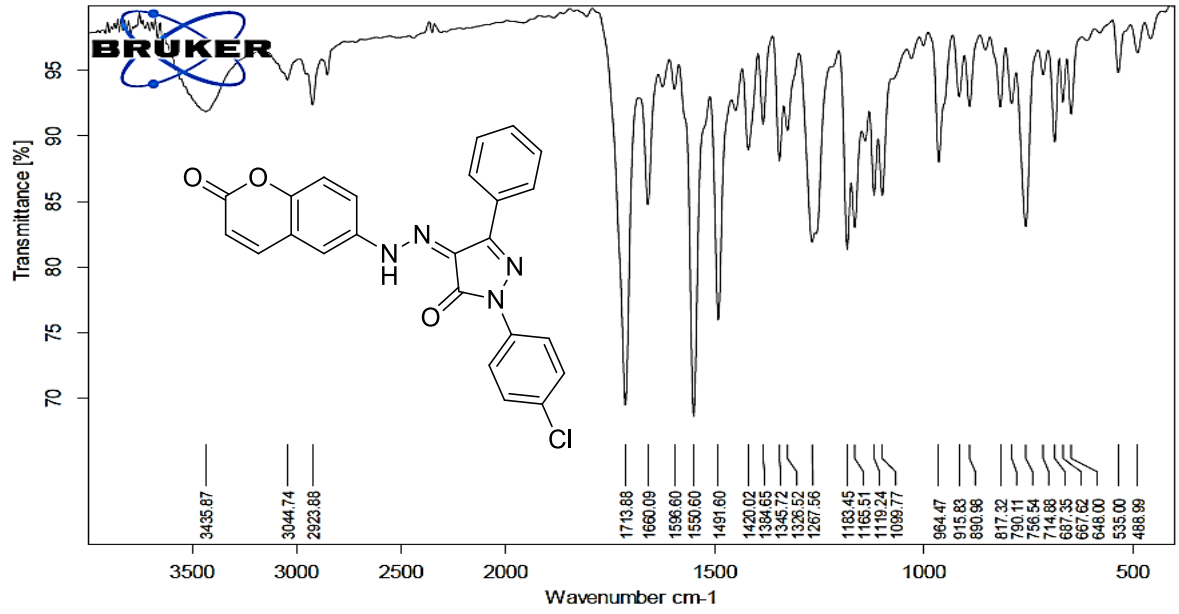

Figure- 3a.21.2 ^{1}H-NMR of (Z)-1-(4-chlorophenyl)-4-(2-(2-oxo-2H-chromen-6-yl)hydrazono)-3-phenyl-1H-pyrazol-5(4H)-one **(19c)**

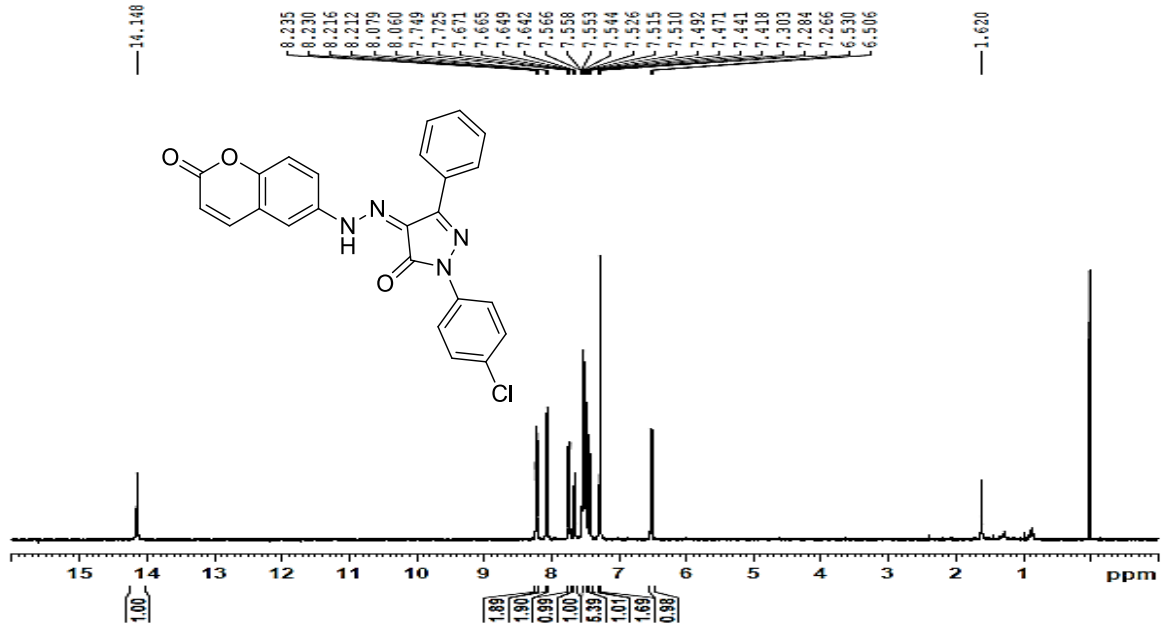

Figure- 3a.21.3 ^{13}C-NMR of (Z)-1-(4-chlorophenyl)-4-(2-(2-oxo-2H-chromen-6-yl)hydrazono)-3-phenyl-1H-pyrazol-5(4H)-one **(19c)**

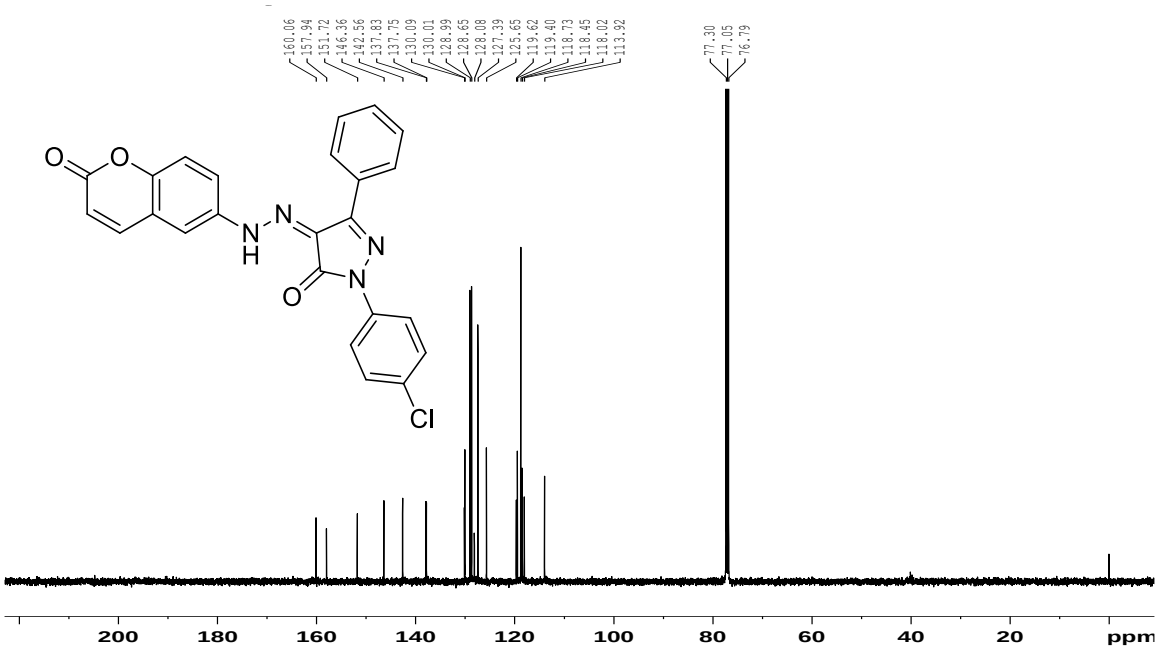

Figure- 3a.22.1 IR of (Z)-1-(2,4-dichlorophenyl)-4-(2-(2-oxo-2H-chromen-6-yl)hydrazono)-3-phenyl-1H-pyrazol-5(4H)-one **(19d)**

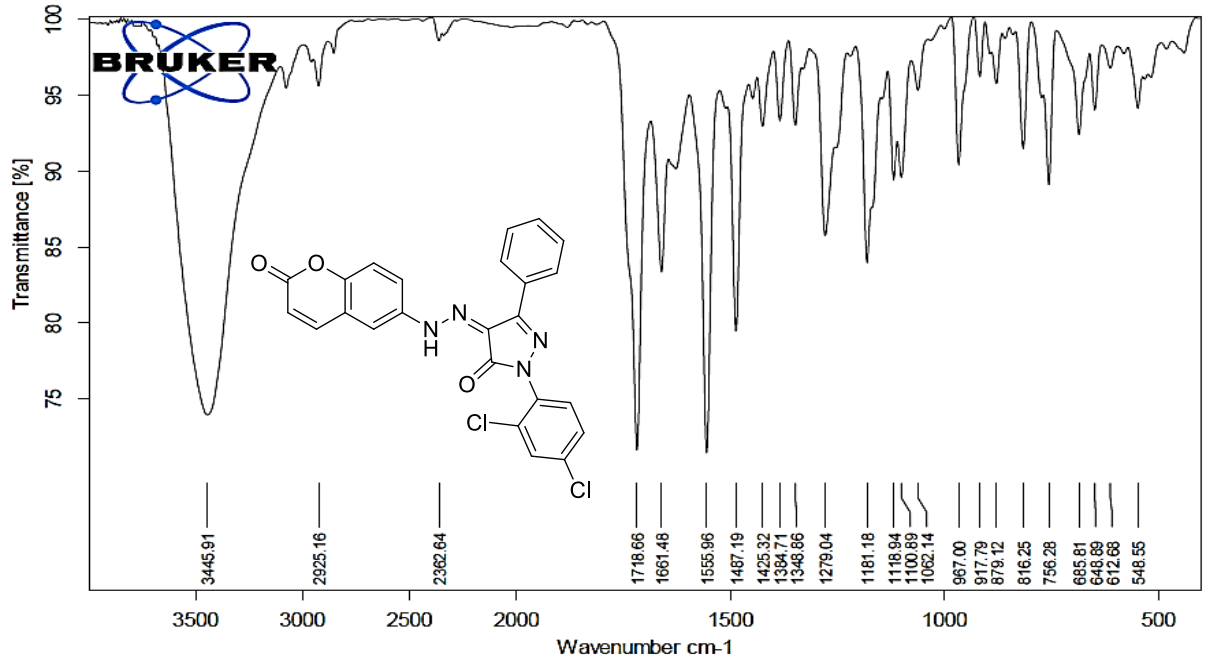

Figure- 3a.22.2 ^{1}H-NMR of (Z)-1-(2,4-dichlorophenyl)-4-(2-(2-oxo-2H-chromen-6-yl)hydrazono)-3-phenyl-1H-pyrazol-5(4H)-one **(19d)**

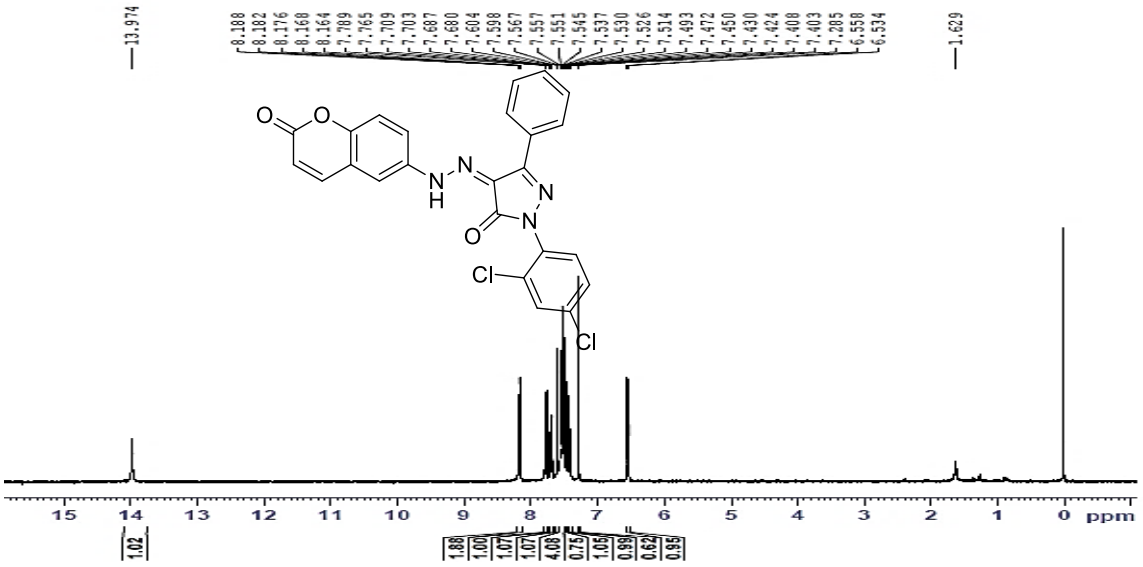

Figure- 3a.22.3 Mass (Z)-1-(2,4-dichlorophenyl)-4-(2-(2-oxo-2H-chromen-6-yl)hydrazono)-3-phenyl-1H-pyrazol-5(4H)-one **(19d)** M+H peak at 477. 09

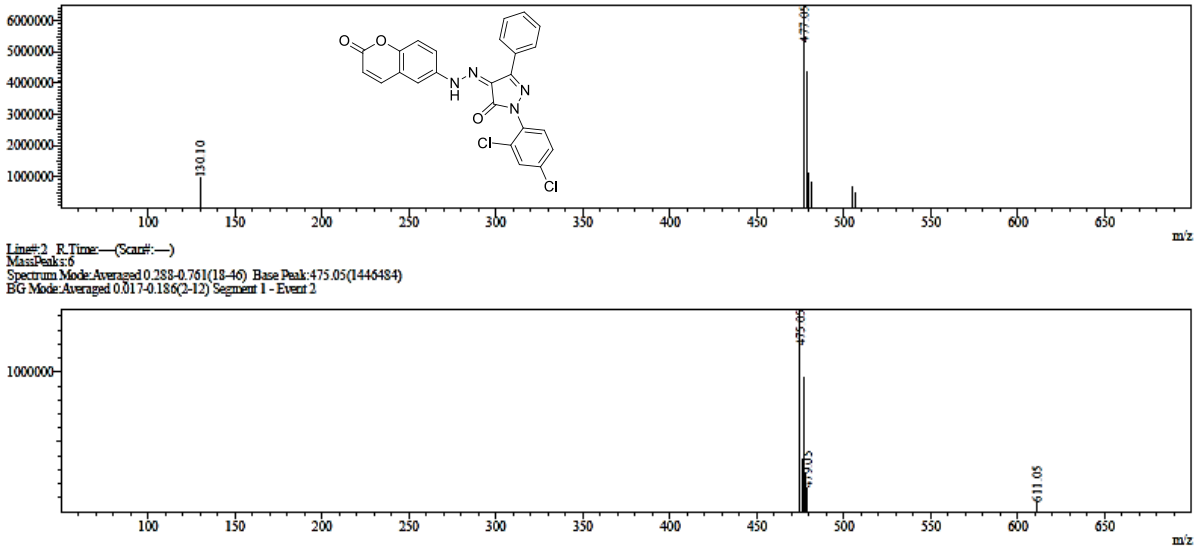

3a.2.2 Biological Evaluation

3a.2.2.1 Anticancer activity by MTT assay:

Pyrazolone derivatives of 7-amino 4-methyl coumarin **10a-c, 11a-d** on reaction with substituted hydrazines and hydrazides (for **12 and 13**) with methyl or phenyl group attached to pyrazolone ring at third position and pyrazolone derivatives of 6-aminocoumarin were studied for their anticancer activity using MTT assay against A549 (Lungs cancer cell line), MCF-7 (Breast cancer cell line) and compared the results with that of the standard drug Fluorouracil **(Table 3a.1).**

Structure activity relationship (SAR) for anticancer activity:

In methyl substituted pyrazolone derivatives **(10a-c**), compound **10a** showed poor activity against both the tested cell lines, while substitution of 4-fluoro group on aryl ring of hydrazine part in compound **10b,** resulted in improvement of activity against A549 cell line with IC_{50} value 2.32±0.06 µM and showed moderate activity against MCF-7 cell line with IC_{50} value 18.6±0.008 µM. **(Table-3a.1)** On replacing 4-fluoro with 4-chloro in compound **10c**, resulted in loss of anticancer activity against A549 cell lines and MCF-7 cell lines.

Table 3a.1: Anticancer activity against A549 (Lungs cancer cell line), MCF-7 (Breast cancer cell line) for compounds **10a-c, 11a-d, 12 and 13**

Compound	IC_{50} µM[a]	
	A549	MCF-7
10a	141.7±2.4	86.9±6.08
10b	2.32±0.06	18.6±0.08
10c	1145±17.9	624.0±12.2
11a	62.40±3.6	32.6±4.02
11b	1.26±0.005	5.9±0.074
11c	809.3±7.69	301.2±8.5
11d	167.8±3.98	206.5±10.23
12	382.0±12.1	417.5±13.2
13	2.34±0.063	10.3±0.056
Fluorouracil	11.13 ±0.083	45.04 ±1.02

[a]IC_{50} values were determined based on MTT assay using GraphPad Prism software

Replacing methyl substituent by phenyl in pyrazolone derivatives **(11a-d)** has shown improvement in anticancer activity. Compound **11a** showed poor activity but activity was found to be good as compared to methyl attached to pyrazolone in compound **10a**. Whereas 4-

fluoro analogue in compound **11b** showed very good improvement in anticancer activity with IC_{50} values 1.26±0.005µM and 5.9±0.074 µM against A549 and MCF-7 cell lines respectively. On replacing 4-fluoro with 4-chloro in compound **11c** resulted in drastic drop in activity against both tested cell lines. Addition of one more chloro as 2,4-dichloro in compound **11d** showed slight increase in activity against both tested cell line as compared to compound **11c**.

Table 3a.2: Anticancer activity against A549 (Lung cancer cell line), MCF-7 (Breast cancer cell line) for compounds **17a-d** and **19a-d**

Compound	IC_{50} µM[a]	
	A549	MCF-7
17a	1.44±0.068	9.14±0.98
17b	12.48±1.06	8.60±0.056
17c	**1.22±0.048**	65.29±1.81
17d	34.34±1.67	59.60±3.8
19a	4.11±0.048	2.21±0.014
19b	3.32±0.058	**1.66±0.015**
19c	6.10±0.050	14.00±0.011
19d	2.20±0.053	19.76±0.089
Fluorouracil	11.13 ±0.083	45.04 ±1.02

[a]IC_{50} values were determined based on MTT assay using GraphPad Prism software

On reaction with hydrazides from compound **12** (R = -CH_3) and **13** (R = -Ph), compound **12** with electron withdrawing group 2-NO_2 attached to phenyl ring showed poor anticancer activity. Interestingly, similar variation on phenyl substituted pyrazolone derivative, compound **13** showed very good anticancer activity as compared to standard drug, with IC_{50} value 2.34±0.063 µM against A549 cell line and that of 10.3±0.056 µM against MCF-7 breast cancer cell line.

In another variation we have also synthesized pyrazolone derivatives with 6-aminocoumarin by changing the position of amino group change from 7th position to 6th in compound **15** to give pyrazolone derivatives **17a-d** and **19a-d** and all synthesized compounds were also studied by MTT assay for their anticancer activity **(Table-3a.2).** In this particular series with methyl pyrazolone derivatives **17a-d** (R = -CH_3), compound **17a** showed very good activity with IC_{50} values 1.44±0.068 µM against A549 tested cell lines as compared to that of standard drug,

while remaining compounds are found to be moderately active against MCF-7 cell line with IC_{50} value 9.14±0.098 µM. Compound **17b** with 4-fluoro as a substituent on aryl ring of hydrazine showed poor activity against A549 tested cell line however activity against MCF-7 cell line remained moderate with IC_{50} value 8.6±0.56 µM. Moreover, replacing 4-fluoro with 4-chloro in compound **17c** showed very excellent activity against A549 cell line with IC_{50} value 1.22±0.048 µM and slight drop in activity against MCF-7 cell line as compared to standard drug. Interestingly, 2,4-dichloro substitution in compound **17d** resulted in loss of anticancer activity against both tested cell line.

In this series with phenyl pyrazolone derivatives **19a-d,** compound **19a** exhibited good activity against A549 cell line with IC_{50} values 4.11±0.48 µM and showed very good activity against MCF-7 cell line as compared to that of standard drug with IC_{50} values 2.21±0.014 µM. Interestingly, substitution of 4-fluoro in compound **19b** resulted in improvement of anticancer activity against both cell lines A549 and MCF-7 with IC_{50} value 3.32±0.058 µM and 1.66±0.015 µM respectively.

On replacing 4-fluoro with 4-chloro substituent in compound **19c** and 2,4-dichloro in compound **19d** resulted in loss of activity against MCF-7 cell line, while compound **19d** showed improvement in activity against A549 cell line (IC_{50} 2.20±0.053 µM) **(Table-3a.2)**.

As compared to pyrazolone derivatives of 7-amino 4-methyl coumarin, pyrazolone derivatives of 6-amino coumarin showed better anticancer activity against both tested cell lines. Compound **17c** (IC_{50} 1.22±0.048 µM against A549 cell line) and compound **19b** (IC_{50} 1.66±0.015 µM against MCF-7 cell line) were studied for cytotoxicity pathway using Ethidium bromide/acridine orange staining assay and ROS activity.

3.2.2.2 Ethidium bromide/acridine orange staining assay:

The Ethidium Bromide (EtBr) and Acridine Orange (AO) staining assay were conducted with compound **17c** and compound **19b** for the A549 cell line and MCF-7 cell line, respectively. This experimental validation is essential to elucidate the impact of compound **17c** and compound **19b** on the respective cancer cell lines. Ethidium bromide selectively stains cells that have lost membrane integrity, while the essential dye acridine orange stains both live and dead cells. In the EtBr/AO dye staining, necrotic cells exhibit red fluorescence, live cells appear green, early apoptotic cells with evident condensation also exhibit green fluorescence, and late apoptotic cells with condensation and fragmentation display an orange fluorescence. When cells were treated with IC_{50} concentrations of compound **17c** and compound **19b**, it was observed that the A549 cell line predominantly exhibited late apoptotic characteristics **(Fig-3a.23-a,b,c),** with no cells in necrosis. While in compound **19b** the majority of the MCF-7 cell

line's cells displayed early apoptotic features **(Fig- 3a.23-d,e,f),** with only a limited number in necrosis.

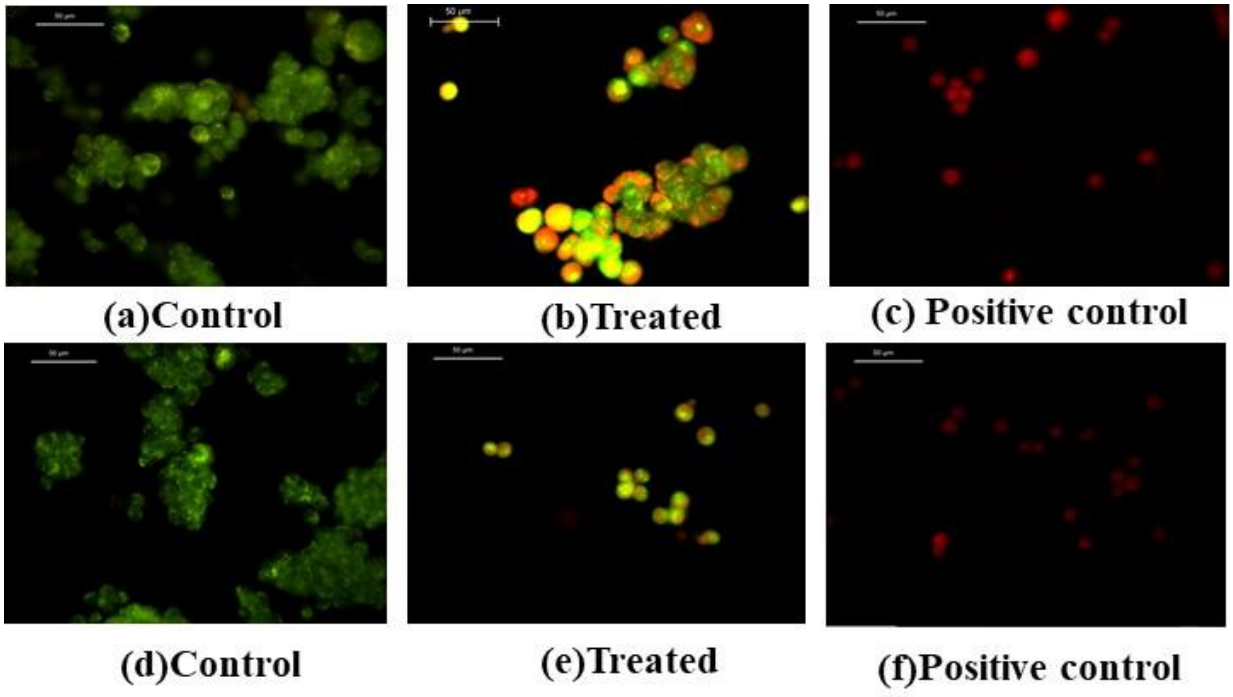

Figure- 3a.23 EtBr/AO assay: Performed with (i)A549 Lung cancer cell line for **17c (a,b,c)** images represent control, treated, positive control (ii) MCF-7 breast cancer cell line (d,e,f). For compound **19b, (d, e, f)** Images represent control, IC_{50} conc. of compound **19b** treated and positive control in MCF-7 cell line

3a.2.2.3 DCFH-DA Assay:

Most chemotherapeutics trigger an overproduction of ROS that surpasses the essential threshold required to induce cytotoxic effects in cancer cells [20]. These heightened levels of ROS are crucial for initiating apoptosis through pathways involving p53 and caspase-8, as well as Fas-associated cell death. According to Ramsey and Sharpless [21], p53, a redox-sensitive transcription factor, detects increased ROS levels and triggers apoptosis in cancer cells. As a result, this investigation focused on evaluating ROS levels in compounds **17c** and **19b** within the A549 and MCF-7 cell lines, respectively **(Figure-3a.24).** The marked elevation of ROS levels in both cell lines at the IC_{50} concentration was strongly confirmed by the results.

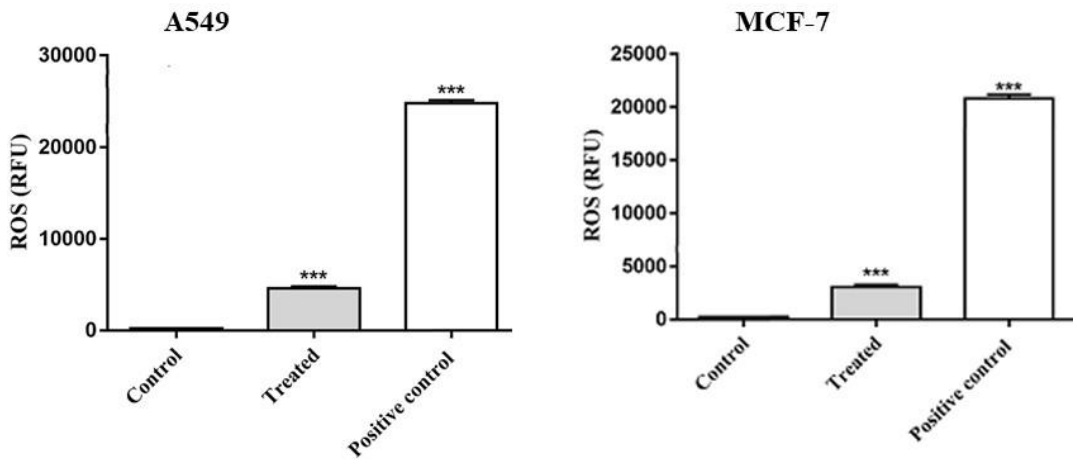

Figure- 3a.24 DCFH-DA assay to Estimate the intracellular reactive oxygen species (ROS) level by for compound **17c** in A549 and **19b** in MCF-7 respectively. (***p ≤ .001)

3a.3 DFT Study:

The geometrical structures of both active compounds **17c** and **19b** were optimized using the Gaussian 09 software B3LYP/6-31G level of theory under (d, p) basis set. Further, **Figure-3a.25** illustrates the estimated optimized structures of compounds **17c** and **19b** with a true minimum energy.

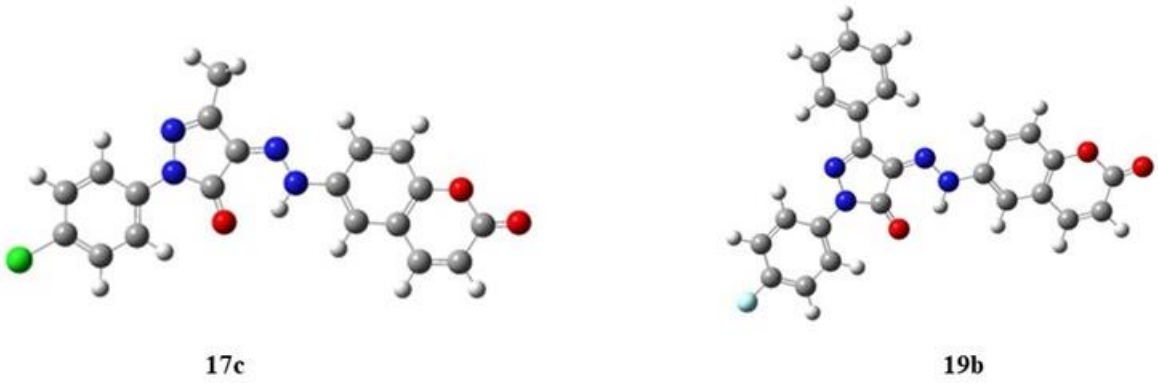

Figure- 3a.25 DFT-optimized structures of compounds **17c** and **19b**

The kinetic as well as chemical stability of both the compounds **17c** and **19b** were calculated based energy difference between highest occupied molecular orbital (HOMO) and lowest unoccupied molecular orbital (LUMO) [22]. For both compounds their frontier molecular orbitals (FMO) are shown in **Fig- 3a.26**. The negative value of E_{HOMO} and E_{LUMO} indicates the stability of compounds [23]. The energy gap (E_{HOMO} -E_{LUMO}) provides insights into to the kinetic stability and chemical reactivity of the molecules [24]. A molecule with a lower energy gap (E_{HOMO} - E_{LUMO}) signifies a high degree of intramolecular transfer of an electron from the donor to the acceptor [25]. For compounds **17c** and **19b** HOMO was predominantly localized around the pyrazolone nucleus and aromatic ring attached to pyrazolone, while the LUMO was

localized on the coumarin ring as well as on the pyrazolone. The theoretically calculated HOMO energies for compounds **17c** and **19b** have been identified to be -5.9536 and -5.7756 eV respectively and the LUMO energies for compounds **17c** and **19b** are -2.7756 and -2.8237 eV respectively. These values indicate overall high chemical stability of compound **19b** with the HOMO–LUMO energy gap 2.952 eV as compared to that of 3.178 eV for compounds **17c**.

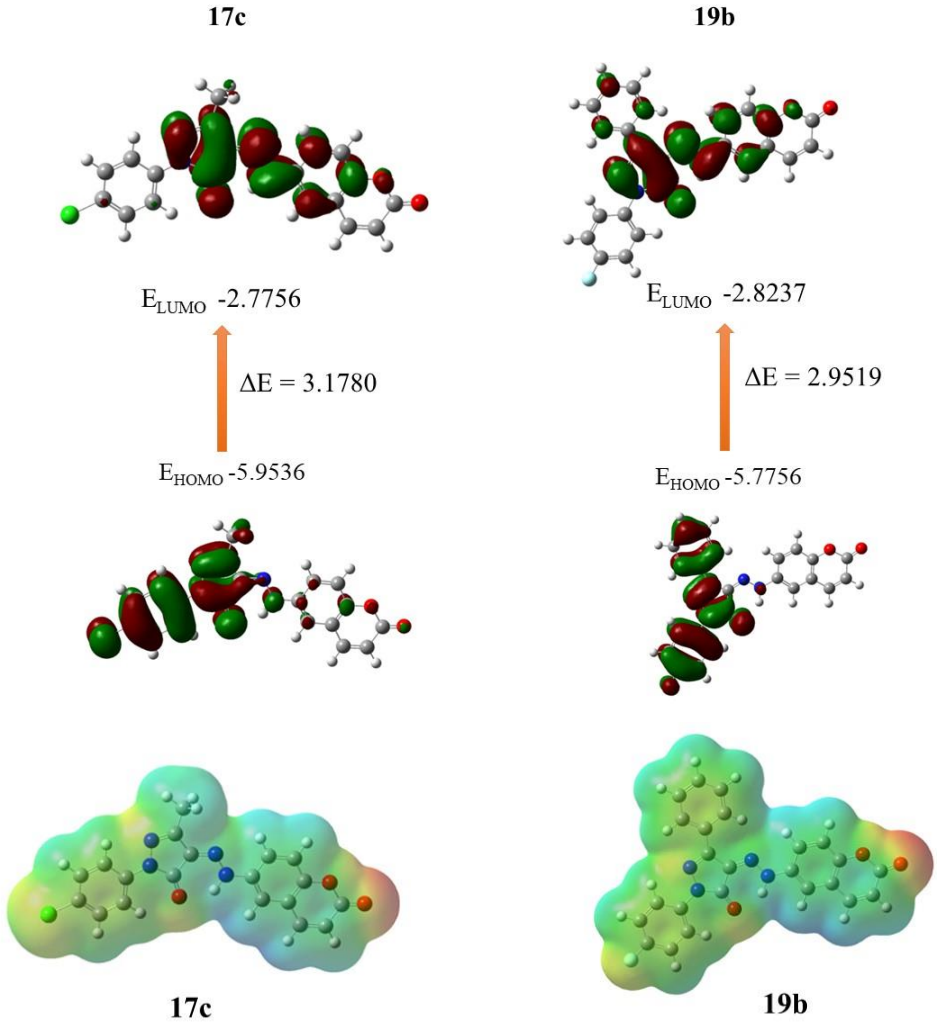

Figure- 3a.26 Frontier molecular orbital surfaces of compounds (FMO) and Molecular electrostatic potential (MEP) diagram of compounds **17c** and **19b**

Energy values of HOMO and LUMO can be utilized for the calculation of important molecular properties including ionization potential (IP), electron affinity (EA), electronegativity (χ), hardness (η), softness (*S*), electrophilicity index (*ω*) and chemical potential (μ). For both the compounds, IP and EA were calculated as IP = $-E_{HOMO}$ and EA = $-E_{LUMO}$. The compound **17c** with a higher IP value as well as a lower value of EA is found to be more stable compared compound **19b** (**Table 3a.3)** [26]. Further stability of compounds **17c** and **19b** can be correlated with Global hardness and global softness as shown in the **Table 3a.3**. Additionally, the

molecular electrostatic potential (MEP) surfaces were analyzed to gain insights into the interactions and charge distribution within the compounds. The MEP surfaces, computed using the same basis set, are depicted in **Figure 3a.26.** The MEP provides information about different reactivity sites available on the surfaces as well as sites for hydrogen bonding [27-28]. The MEP maps, obtained with the same basis sets **Figure 3a.26**, revealed negative potential sites localized on the lactone ring of coumarin and the carbonyl group of pyrazolone. These findings further support the stability of compounds **17c** and **19b**, consistent with the previous results.

Table- 3a.3: Molecular properties (in eV) of selected compounds

Parameters	Compound **17c**	Compound **19b**
E_{HOMO} (eV)	-5.9536	-5.7756
E_{LUMO} (eV)	-2.7756	-2.8237
E_{HOMO} -E_{LUMO} gap ΔE (eV)	3.178	2.952
Ionization potential (*I*) (eV)	5.9536	5.7756
Electron affinity (EA) (eV)	2.7756	2.8237
Global hardness (η)	1.589	1.4760
Global softness (*S*)	0.3146	0.3387
Electronegativity (χ)	4.3646	4.2996
Electrophilicity index (*ω*)	5.9942	6.2638
Chemical potential (μ)	-4.3646	-4.2996

3a.4 Conclusion

Two series of pyrazolone derivatives containing 7-amino 4-methylcoumarin and 6-aminocoumarin were designed, synthesized and well characterized. Compounds of both the series were studied using MTT assay for anticancer activity against A549 and MCF-7 cell line. Phenyl group attached to pyrazolone ring at 3rd position showed improvement in anticancer activity than methyl substituted pyrazolone derivatives. From all synthesized compounds, compound 1**7c** has shown excellent activity against A549 lungs cancer cell line (IC_{50} 1.22±0.048 µM), while compound **19b** has shown excellent activity against MCF-7 cell line (IC_{50} 1.66±0.015 µM). In cytotoxic studies using EtBr/AO assay, both the compounds showed apoptosis pathway for both the tested cell lines, which was further confirmed by the increased level of ROS concentration for compound **17c** and **19b** at IC_{50} value in A549 and MCF-7 cell line respectively.

3a.5 Experimental

3a.5.1 General Chemistry

All the chemicals and solvents purchased were of Reagent-grade and used after purification. TLC was carried out on silica gel F254 plates (Merck), while for column chromatographic purification Acme's silica gel (60-120 mesh) was used. All the melting points were determined using open capillary tubes. IR spectra were captured after making KBr pellet using the Perkin Elmer RX 1 spectrometer. ^{1}H-NMR and ^{13}C-NMR were recorded on Advance Bruker spectrometer (400 MHz/500 MHz) with $CDCl_3$ or DMSO-d6 as the solvent containing internal standard TMS. *J* values are given in Hz. ESI-MS was used to determine the mass spectra using a Shimadzu LCMS 2020 device. Elemental analysis was carried out on Thermo Finnigan Flash 11–12 series EA. 7-amino 4-methyl coumarin, 6-amino coumarin, and substituted pyrazolone derivatives were prepared according to literature method [29-31].

Synthesis of ethyl (3-hydroxyphenyl) carbamate (5)

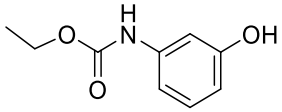

A solution of aminophenol (1.0 mmol) in ethyl acetate (20 mL) was stirred, and then ethyl chloroformate (1.0 mmol) was added slowly in the reaction mixture. This resulted in the formation of a white precipitate. The reaction mixture was stirred for a duration of 3 hours at room temperature. The amine hydrochloride precipitated out which was filtered and washed with ethyl acetate. The filtrate was subjected to concentration under reduced pressure, leading to the formation of colorless crystals of ethyl (3-hydroxyphenyl) carbamate **5**.

Yield -88% Melting Point - 94-96^{o}C.

Synthesis of ethyl (4-methyl-2-oxo-2H-chromen-7-yl)carbamate (6)

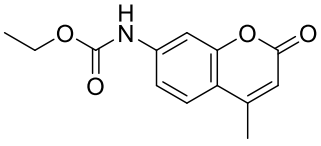

A mixture containing ethyl (3-hydroxyphenyl) carbamate **5** (1 mmol) and ethyl acetoacetate (1.2 eq) was suspended in 20 mL of 70% ethanolic H_2SO_4 which was stirred at room temperature for a period of 4-6 hours. TLC was used to monitor the product formation. After the reaction was finished, the solution was poured into ice-cold water (100 mL), leading to the formation of a brown crystalline solid. The solid was separated by filtration, washed with water, and subjected to recrystallization from ethanol to obtain compound **6**. The yield was 65%, and the melting point was recorded as 186-188°C.

Synthesis of 7-amino 4-methyl chromen-2-one (7)

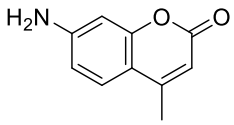

In a mixture of conc. H_2SO_4 and glacial acetic acid (1:1), Ethyl (4-methyl-2-oxo-2H-chromen-7-yl) carbamate **6** was added and refluxed for a duration of 4 hours. The completion of reaction was assessed using TLC. By checking TLC, after the reaction reached completion, the reaction mixture was allowed to cool down to room temperature, resulting in the formation of yellow precipitate. The cooled reaction mixture was poured into ice-cold water(100ml) and the neutralized the mixture by using 50% NaOH solution, yielding a white solid. The obtained solid was separated by filtration, washed with water, dried, and recrystallized from ethanol, leading to the generation of compound 7-amino 4-methyl chromen-2-one **7.** Yield - 48%, Melting Point - 218-220^oC (Lit. M.P. 222-224 ^oC).

Synthesis of 6-nitrocoumarin (14)

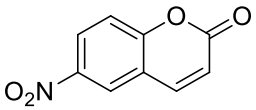

The temperature was held at 0°C while the coumarin (4g, 27.4 mmol) was dissolved in concentrated H_2SO_4 (25 mL) and 8 ml of mixed acid (HNO_3: H_2SO_4 = 1:3, v/v). Ice was poured into the mixture following an hour of stirring at room temperature. The result was a white precipitate. It was properly washed with cold water after being filtered (10mLx10). The white crude product was crystallized out using acetic acid. Yield – 95%, Melting Point-182-184^oC, (Lit.M.P. = 180-182 ^oC).

Synthesis of 6-aminocoumarin (15)

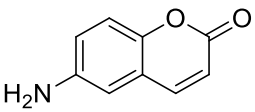

6-Nitrocoumarin (4g, 20.95 mmol) was treated with Fe powder (15g) and ammonium chloride in water (75 ml) (1.3 g, 24.3 mmol). Under stirring conditions, the mixture was maintained at 80°C in water bath for 2 hours. The precipitates produced were dark brown. It was dissolved with ethyl acetate. After removal of ethyl acetate, a silky golden precipitates were produced which were recrystallized from ethanol. M.P. 156-158°C, (Lit.M.P. =154-156 °C).

General Procedure for preparation of compounds 8, 9, 16 and 18:

7-Amino-4-methyl-coumarin **7/** 6-aminocoumarin **15** (0.01 mol) was dissolved in concentrated hydrochloric acid (7.5 ml), (15 ml) acetic acid and stirred until amine was completely dissolved then the mixture cooled (external cooling) to the temperature 0–5ºC. Sodium nitrite solution (0.01 mol) in water (10 mL) was then added dropwise with vigorous stirring during 30 min. at 0-5ºC. This solution was poured into the cooled solution of sodium acetate, ethyl acetoacetate (for Compounds **8** and **16**) / ethyl benzoyl acetate (for Compound **9** and **18**) in ethanol. After addition kept the reaction mixture at room temperature for a duration 2 hours. The reaction mixture was then poured into ice cold water, filter and recrystallized from ethanol.

(Z)-Ethyl 2-(2-(4-methyl-2-oxo-2H-chromen-7-yl)hydrazono)-3-oxobutanoate (8)

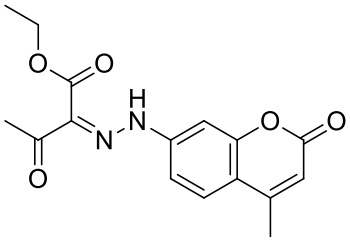

Yellow Solid, Yield: 76%; M.P: 158-160ºC; IR (KBr): 3130, 3054, 2982, 2925, 1733, 1705, 1617, 1565, 1520, 1437, 1387, 1365, 1319, 1263, 1188, 1135, 1091, 1068, 1016, 979, 943, 882, 791, 749, 606 cm^{-1}; ^{1}H-NMR (400 MHz, $CDCl_3$): δ 1.43 (t, *J* = 7.2Hz, 3H), 2.44 (s, 3H), 2.62 (s, 3H), 4.33-4.39 (q, 2H), 6.22 (s, 1H), 7.26 (dd, *J* = 2Hz and *J* = 8.8Hz, 1H), 7.42 (d, *J* = 2Hz, 1H), 7.60 (d, *J* = 8.4Hz, 1H), 14.59 (s, 1H); ^{13}C-NMR (100 MHz, $CDCl_3$): δ ppm 14.31, 18.72, 30.93, 61.39, 103.74, 112.51, 113.71, 117.25, 125.95, 127.56, 144.71, 152.19, 154.80, 160.80, 164.47, 197.60.

(Z)-Ethyl 2-(2-(4-methyl-2-oxo-2H-chromen-7-yl)hydrazono)-3-oxo-3-phenylpropanoate (9)

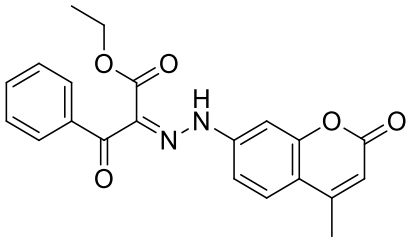

Orange solid, Yield: 85 %; M.P: 142-144 ºC; IR (KBr): 3436, 3065, 2984, 1740, 1683, 1657, 1619, 1529, 1448, 1387, 1369, 1319, 1261, 1178, 1132, 1067, 1031, 1017, 977, 904, 877, 851, 813, 779, 742, 714, 692, 670cm^{-1}; ^{1}H-NMR (400 MHz, $CDCl_3$): δ 1.37 (t, *J* = 7.2Hz, 3H), 2.40 (s, 3H), 4.37-4.42 (q, 2H), 6.18 (s, 1H), 7.07-7.10 (m, 2H), 7.49-7.55 (m, 3H), 7.62-7.65 (m, 1H), 7.95-7.97 (m, 2H), 12.70 (s, 1H); ^{13}C-NMR (100 MHz, $CDCl_3$): δ ppm 14.00, 18.69,

61.92, 102.62, 111.54, 113.14, 116.19, 126.01, 128.25, 128.78, 130.30, 133.13, 136.89, 144.92, 152.24, 154.93, 160.89, 163.58, 189.15.

(E)-Ethyl 3-oxo-2-(2-(2-oxo-2H-chromen-6-yl)hydrazono)butanoate (16)

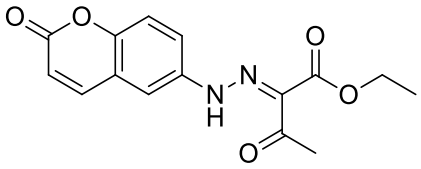

Yellow Solid, Yield: 83%; M.P: 148-150ºC; IR (KBr): 3417, 3147, 3001, 2926, 1712, 1687, 1651, 1572, 1526, 1492, 1375, 1357, 1311, 1255, 1214, 1181, 1122, 1102, 1066, 1016, 946, 920, 871, 827, 790, 754, 725, 618 cm^{-1}; ^{1}H-NMR (400 MHz, $CDCl_3$): δ 1.42 (t, *J* = 6.8 Hz, 3H), 2.54 (s, 3H), 4.42 (q, 2H), 6.51 (d, *J* = 9.6Hz, 1H), 7.39 (d, *J* = 8.8Hz, 1H), 7.44 (d, *J* =2.4Hz, 1H), 7.54 (dd, *J* = 2.4Hz and *J* = 8.8Hz, 1H), 7.75 (d, *J* = 9.2Hz, 1H), 12.89 (s, 1H).

(E)-Ethyl 3-oxo-2-(2-(2-oxo-2H-chromen-6-yl)hydrazono)-3-phenylpropanoate (18)

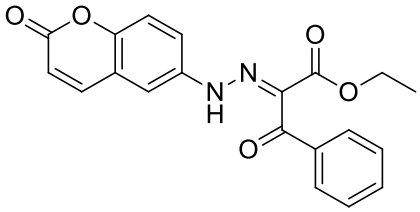

Yellow Solid, Yield: 86%; M.P: 142-144ºC; IR (KBr): 3426, 3046, 2926, 1722, 1671, 1653, 1599, 1572, 1526, 1493, 1448, 1388, 1334, 1269, 1208, 1179, 1121, 1100, 1020, 942, 920, 885, 828, 786, 718, 670 cm^{-1}; ^{1}H-NMR (400 MHz, $CDCl_3$): δ 1.36 (t, *J* = 7.2Hz, 3H), 4.40 (q, 2H), 6.45 (d, *J* = 9.2Hz, 1H), 7.31-7.37 (m, 3H), 7.51 (t, *J* = 7.6Hz, 2H), 7.62 (t, *J* = 8.8Hz, 2H), 7.64 (dd, *J* = 2.4Hz, 8.8Hz, 1H), 7.95 (d, *J* = 7.6Hz, 2H), 12.80 (s, 1H); ^{13}C-NMR (100 MHz, $CDCl_3$): δ ppm 13.99, 61.63, 112.92, 117.69, 118.01, 119.49, 119.71, 127.72, 128.10, 130.24, 132.73, 137.47, 138.65, 142.90, 150.66, 160.37, 163.82, 189.31.

General procedure for compounds 10a-c, 11a-d, 12,13,17a-d and 19a-d:

Compounds **8/9/16/18** and different substituted hydrazines/hydrazids were added in absolute ethanol (20 mL), and the reaction mixture was then refluxed for 18–20 hours. 2-3 drops of acetic acid were added to catalyze the reaction. It was then concentrated to half its original volume and reaction mixture allowed to cool down at ambient temperature. The solid separated out was filtered, washed with ethanol and dried to give compounds target pyrazolone derivatives**10a-c,11a-d, 12,13, 17a-d** and **19a-d.** Recrystallized from ethanol.

Characterization data

(Z)-3-Methyl-4-(2-(4-methyl-2-oxo-2H-chromen-7-yl)hydrazono)-1-phenyl-1H-pyrazol-5(4H)-one (10a)

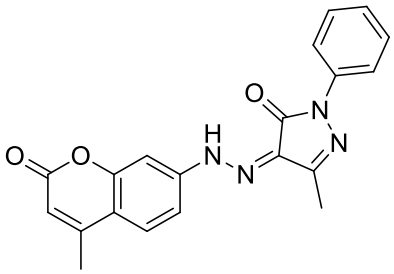

Yellow Solid, Yield: 79%; M.P: Above 270ºC; IR (KBr): 3075, 2922, 2854, 1730, 1656, 1612, 1552, 1497, 1424, 1390, 1341, 1266, 1159, 1071, 1045, 995, 905, 880, 818,772, 749, 729, 688, 668 cm^{-1}; ^{1}H-NMR (400 MHz, $CDCl_3$): δ 2.41 (S, 3H), 2.46 (s, 3H), 6.27 (s, 1H), 7.26-7.31 (m, 2H), 7.45-7.49 (m, 3H), 7.64 (d, *J* = 8.8Hz, 1H), 7.95-7.97 (m, 2H), 13.58 (s, 1H); ^{13}C-NMR (100 MHz, $CDCl_3$): δ ppm 11.85, 18.72, 103.15, 112.04, 113.91, 117.68, 118.58, 125.52, 126.12, 129.03, 130.58, 137.59, 144.09, 148.68, 152.00, 152.58, 154.95, 157.44; Anal. calc. for $C_{20}H_{16}N_4O_3$ C,66.66; H,4.48; N,15.55; found: C,66.64; H,4.44; N,15.59; ESI-MS: 361.13$[M+H]^+$.

(Z)-1-(4-Fluorophenyl)-3-methyl-4-(2-(4-methyl-2-oxo-2H-chromen-7-yl)hydrazono)-1H-pyrazol-5(4H)-one (10b)

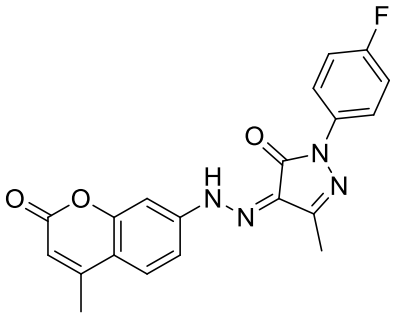

Yellow Solid; Yield=76%; M.P: Above 270ºC; IR (KBr): 3432, 2924, 2854, 1730, 1656, 1612, 1553, 1504, 1428, 1389, 1342, 1266, 1145, 1069, 1047, 998, 908,880, 861, 836,772,729, 661, 585 $cm^{-1;}$ ^{1}H-NMR (400MHz, $CDCl_3$): δ 2.41(s, 3H), 2.47 (s, 3H), 6.28 (s, 1H), 7.13-7.17 (m, 2H), 7.30-7.31(m, 1H) 7.47 (s, 1H), 7.65 (d, *J* = 8.4Hz, 1H) 7.92-7.95 (m, 2H) 13.54 (s, 1H); Anal. Calc. for $C_{20}H_{15}FN_4O_3$ C,63.49; H, 4.00; N,14.81; found: C,63.53; H,3.95; N,14.83; ESI-MS: 378.36[M+].

(Z)-1-(4-Chlorophenyl)-3-methyl-4-(2-(4-methyl-2-oxo-2H-chromen-7-yl)hydrazono)-1H-pyrazol-5(4H)-one (10c)

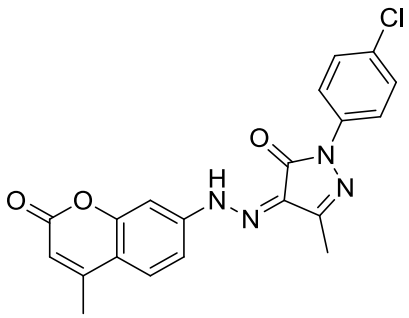

Orange Solid, Yield: 78 %; M.P: Above 270ºC; IR(KBr): 3054, 2980, 2925, 1732, 1664, 1614, 1555, 1494, 1425, 1389, 1368, 1340, 1266, 1245, 1159, 1144, 1096, 1069, 1051, 1012, 1002, 907, 856, 830, 771, 731, 709, 659 cm^{-1}**;** ^{1}H-NMR (400 MHz, $CDCl_3$): δ 2.40 (s, 3H), 2.46 (s, 3H), 6.27 (s, 1H), 7.27-7.30 (m, 1H),7.40-7.45 (m, 3H), 7.64 (d, *J* = 8.8Hz, 1H), 7.92 -7.94 (m, 2H), 13.51 (s, 1H); Anal. calc. for $C_{20}H_{15}ClN_4O_3$ C, 60.84; H, 3.83; N, 14.19; found: C,60.89; H,3.78; N,14.16; ESI-MS: 394.34 [M+].

(Z)-4-(2-(4-Methyl-2-oxo-2H-chromen-7-yl)hydrazono)-1,3-diphenyl-1H-pyrazol-5(4H)-one (11a)

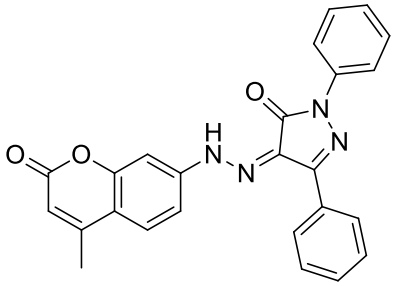

Yellow Solid; Yield: 76%; M.P: Above 270ºC; IR(KBr):, 3430, 3057, 2883, 2764, 1723, 1658, 1614, 1554, 1496, 1433, 1388, 1342, 1268, 1247, 1198, 1171, 1133, 1067, 1013, 958, 898, 858, 812, 754, 683, 648 cm^{-1}; ^{1}H-NMR (400 MHz, $CDCl_3$): δ 2.37 (s, 3H), 6.18 (s, 1H), 7.18 (d, *J* = 8.4Hz, 2H), 7.23-7.29 (m, 1H), 7.36-7.56 (m, 6H), 8.00 (d, *J* = 8.4Hz, 2H), 8.15-8.16 (m, 2H), 13.90 (s, 1H); ^{13}C-NMR (100 MHz, $CDCl_3$): δ ppm 18.66, 103.00, 112.28, 113.87, 117.47, 118.55, 125.68, 126.17, 127.22, 128.73, 128.99, 129.27, 129.68, 130.23, 137.65, 143.86, 146.17, 152.04, 154.82, 157.59, 160.56; Anal. calc. for $C_{25}H_{18}N_4O_3$; C, 71.08; H, 4.29; N, 13.26; found: C, 71.10; H, 4.33; N, 13.23; ESI-MS: 422.09[M+].

(Z)-1-(4-Fluorophenyl)-4-(2-(4-methyl-2-oxo-2H-chromen-7-yl)hydrazono)-3-phenyl-1H-pyrazol-5(4H)-one (11b)

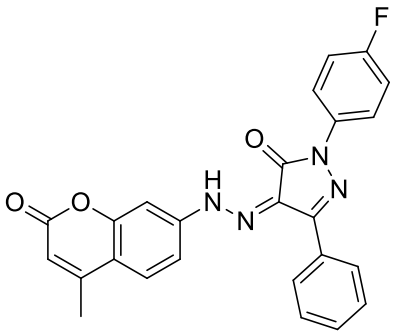

Yellow Solid; Yield: 72%; M.P: Above 270ºC; IR(KBr): 3054, 2883, 2811, 1726, 1658, 1617, 1547, 1511, 1390, 1368, 1347, 1297, 1259, 1216, 1174, 1136, 1111, 1066, 979, 961, 851, 833, 764, 732, 688, 651cm^{-1}; ^{1}H-NMR (400 MHz, $CDCl_3$): δ 2.46 (s, 3H), 6.27 (s, 1H), 7.18 (d, *J* = 8.0Hz, 2H), 7.27 (d, *J* = 8.0Hz, 1H), 7.48-7.53 (m, 4H), 7.65 (d, *J* = 8.4Hz, 1H), 8.03-8.04 (m, 2H), 8.21 (s, 2H), 13.98 (s, 1H); ^{13}C-NMR (100 MHz, $CDCl_3$): δ ppm 18.73, 103.24, 112.42, 114.04, 115.69, 115.91, 117.65, 120.58, 126.24, 127.35, 128.81, 129.21, 129.67, 130.35, 133.88, 143.91, 146.54, 152.03, 154.94, 157.51, 160.56; $C_{25}H_{17}FN_4O_3$; Anal. calc. for C, 68.18; H,3.89; N,12.72; found: C,68.23; H,3.85; N, 12.71; ESI-MS: 441.13$[M+H]^+$.

(Z)-1-(4-Chlorophenyl)-4-(2-(4-methyl-2-oxo-2H-chromen-7-yl)hydrazono)-3-phenyl-1H-pyrazol-5(4H)-one (11c)

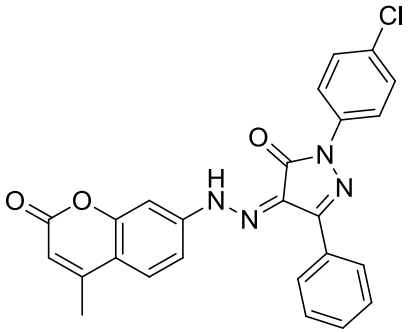

Yellow Solid; Yield: 89%; M.P: Above 270ºC; IR(KBr): 3436, 2993, 2881, 2784, 1729, 1663, 1615, 1552, 1494, 1422, 1388, 1342, 1269, 1248, 1200, 1171, 1135, 1089, 959, 901, 846, 771, 686, 650 cm^{-1}; ^{1}H-NMR (400 MHz, $CDCl_3$): δ 2.44 (s, 3H), 6.25 (s, 1H), 7.22 (d, *J* = 8.4Hz, 1H), 7.38-7.50 (m, 6H), 7.62 (d, *J* =8.0Hz, 1H), 7.99 (d, *J* =8.4Hz, 2H), 8.16 (s, 2H), 13.9 (s, 1H); ^{13}C-NMR (100 MHz, $CDCl_3$): δ ppm 18.73, 103.18, 112.41, 114.04, 117.70, 119.67, 126.23, , 127.32, 128.79, 129.05, 129.55, 130.40, 130.81, 136.21, 143.69, 146.66, 151.98, 154.94, 157.60, 160.57; Anal. calc. for $C_{25}H_{17}ClN_4O_3$; C,65.72; H,3.75; N, 12.26; found: C, 65.73; H, 3.70; N,12.23; ESI-MS: 457.11$[M+H]^+$.

(Z)-1-(2,4-Dichlorophenyl)-4-(2-(4-methyl-2-oxo-2H-chromen-7-yl)hydrazono)-3-phenyl-1H-pyrazol-5(4H)-one (11d)

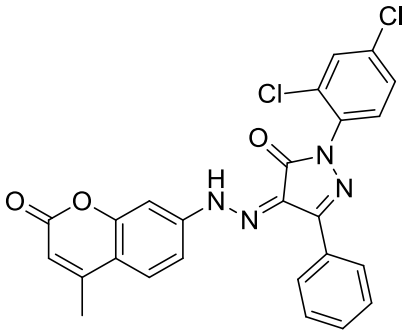

Yellow Solid; Yield: 78%; M.P: Above 270ºC; IR(KBr): 3442, 3081, 3052, 2883, 2813, 1732, 1659, 1616, 1551, 1491, 1430, 1388, 1348, 1270, 1240, 1201, 1175, 1088, 1065, 1012, 963, 904, 851, 822, 758, 730, 686, 648 cm^{-1}; ^{1}H-NMR (400 MHz, $CDCl_3$): δ 2.45 (s, 3H), 6.27 (s, 1H), 7.28-7.30 (m, 1H), 7.39 (d, *J* =8.4Hz, 1H), 7.49-7.58 (m, 6H), 7.65 (d, *J* = 8.4Hz, 1H), 8.16 (s, 2H) 13.8 (s, 1H); ^{13}C-NMR (100 MHz, $CDCl_3$): δ ppm 18.75, 103.34, 112.50, 114.06, 117.70, 126.24, , 127.33, 128.00, 128.11, 128.83, 129.59, 129.64, 130.36, 130.45, 132.44, 132.90, 135.36, 143.86, 147.35, 152.08, 154.88, 157.93, 160.58; $C_{25}H_{16}Cl_2N_4O_3$; Anal. calc. for C,61.11; H,3.28; N,11.40; found: C,61.08; H,3.30; N,11.42; ESI-MS: 490.02 [M+].

(Z)-3-Methyl-4-(2-(4-methyl-2-oxo-2H-chromen-7-yl)hydrazono)-1-(2-nitrobenzoyl)-1H-pyrazol-5(4H)-one (12)

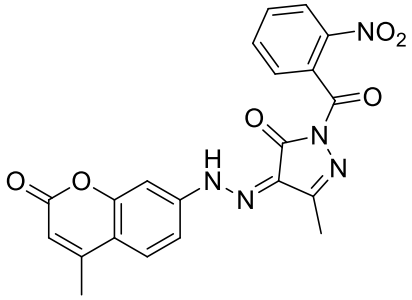

Orange solid, Yield: 85%; M.P: Above 270ºC; IR (KBr): 3441, 2961, 2934, 2868, 1740, 1616, 1531, 1354, 1304, 1262, 1214, 1214, 1146, 1098, 1002, 880, 849, 788, 728 cm^{-1}; ^{1}H-NMR (400 MHz, DMSO-d_6): δ 2.42 (s, 3H), 2.51 (s, 3H), 6.35 (s, 1H), 7.65-7.67 (m, 2H), 7.79-7.85 (m, 3H), 7.95-7.99 (m, 1H), 8.32 (d, J = 8Hz, 1H), 13.00 (s 1H); Anal. calc. for $C_{21}H_{15}N_5O_6$; C, 58.20; H,3.49; N, 16.16; found: C,58.25; H,3.51; N,16.14; ESI-MS: 434.25$[M+H]^+$.

(Z)-4-(2-(4-Methyl-2-oxo-2H-chromen-7-yl)hydrazono)-1-(2-nitrobenzoyl)-3-phenyl-1H-pyrazol-5(4H)-one (13)

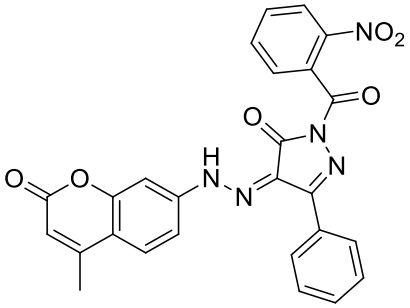

Brown Solid; Yield: 70%; M.P: Above 270ºC; IR(KBr): 3441, 3071, 2881, 1745, 1710, 1615, 1526, 1388, 1351, 1297, 1264, 1206, 1164, 1060, 978, 932, 887, 863, 771, 731, 703, 653cm^{-1}; ^{1}H-NMR (400 MHz, DMSO-d_6): δ 2.41 (s, 3H), 6.35 (s, 1H), 7.58-7.67 (m, 5H), 7.83-7.90 (m, 3H), 7.99-8.03 (m, 3H), 8.36 (d, J = 8.4Hz, 1H), 13.22 (s, 1H); Anal. calc. for $C_{26}H_{17}N_5O_6$; C,63.03; H,3.46; N,14.14; found: C,63.08; H, 3.50; N,14.13; ESI-MS: 496.15 [M+H]$^+$.

(Z)-3-Methyl-4-(2-(2-oxo-2H-chromen-6-yl)hydrazono)-1-phenyl-1H-pyrazol-5(4H)-one (17a)

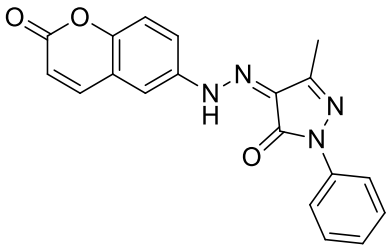

Yellow Solid, Yield: 75%; M.P: Above 270ºC; IR (KBr): 3431, 2923, 2854, 1715, 1659, 1560, 1496, 1421, 1386, 1369, 1345, 1324, 1273, 1254, 1183, 1158, 1104, 1049, 1002, 905, 816, 757, 715, 688 cm^{-1}; ^{1}H-NMR (400 MHz, $CDCl_3$): δ 2.41 (S, 3H), 6.53 (d, *J* = 9.6Hz, 1H), 7.25 (t, *J* = 7.6Hz, 1H), 7.41-7.48 (m, 3H), 7.55 (d, *J* = 2.4Hz, 1H), 7.63 (dd, *J* = 2.4Hz and 8.8Hz, 1H), 7.75 (d, *J* = 9.6Hz, 1H), 7.95-7.97 (m, 2H), 13.69 (s, 1H); Anal. calc. for $C_{19}H_{14}N_4O_3$; C, 65.89; H, 4.07; N, 16.18; found: C,65.92; H,4.01; N,16.14; ESI-MS: 347.10 [M+H]$^+$.

(Z)-1-(4-Fluorophenyl)-3-methyl-4-(2-(2-oxo-2H-chromen-6-yl)hydrazono)-1H-pyrazol-5(4H)-one (17b)

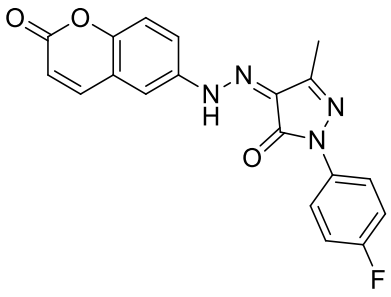

Yellow Solid, Yield: 70 %; M.P: Above 270ºC; IR (KBr): 3435, 3065, 2924, 1726, 1655, 1557, 1508, 1423, 1382, 1348, 1270, 1213, 1178, 1151, 1122, 1100, 1049, 1002, 907, 867, 826, 772,

710, 658cm^{-1}; 1H-NMR (400 MHz, $CDCl_3$): δ 2.40 (S, 3H), 6.53 (d, *J* = 9.6Hz, 1H), 7.13(d, *J* = 2.4Hz, 1H), 7.16 (d, *J* = 9.2Hz, 1H), 7.43 (d, *J* = 8.8Hz, 1H), 7.56 (d, *J* = 2.4Hz, 1H), 7.63 (dd, *J* = 2.4Hz & 8.8Hz, 1H), 7.76 (d, *J* = 9.6Hz, 1H), 7.91-7.95 (m, 2H), 13.66 (s, 1H); Anal. calc.for $C_{19}H_{13}FN_4O_3$; C, 62.64; H, 3.60; N, 15.38; found: C,62.59; H,3.58; N,15.41; ESI-MS: 365.10 $[M+H]^+$.

(Z)-1-(4-Chlorophenyl)-3-methyl-4-(2-(2-oxo-2H-chromen-6-yl)hydrazono)-1H-pyrazol-5(4H)-one (17c)

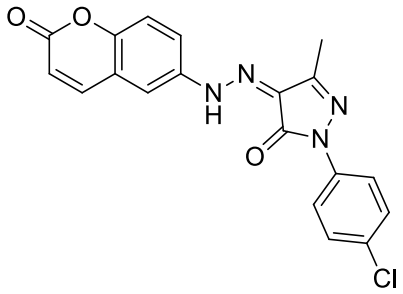

Yellow Solid, Yield: 70 %; M.P: Above 270ºC; IR (KBr): 3438, 3063, 1726, 1658, 1556, 1495, 1454, 1424, 1376, 1343, 1265, 1181, 1151, 1123, 1098, 1051, 1004, 904, 823, 774, 719, 620 cm^{-1}; ^{1}H-NMR (400 MHz, $CDCl_3$): δ 2.41 (S, 3H), 6.54 (d, *J* = 9.6Hz, 1H), 7.41-7.45 (m, 3H), 7.57 (d, *J* = 2.4Hz, 1H), 7.64 (dd, *J* = 2.4Hz and 8.8Hz, 1H), 7.77 (d, *J* = 9.6Hz, 1H), 7.94-7.96 (m, 2H), 13.65 (s, 1H); ^{13}C-NMR (100 MHz, DMSO-d_6): δ ppm 11.56, 114.71, 117.12, 117.45, 117.58, 119.32, 120.19, 124.73, 128.07, 128.93, 137.81, 137.98, 143.75, 148.45, 150.94, 156.30, 159.57; Anal. calc. for $C_{19}H_{13}ClN_4O_3$ C, 59.93; H, 3.44; N, 14.71; found: C,59.96; H,3.47; N,14.69; ESI-MS: 381.05 $[M+H]^+$.

(Z)-1-(2,4-Dichlorophenyl)-3-methyl-4-(2-(2-oxo-2H-chromen-6-yl)hydrazono)-1H-pyrazol-5(4H)-one (17d)

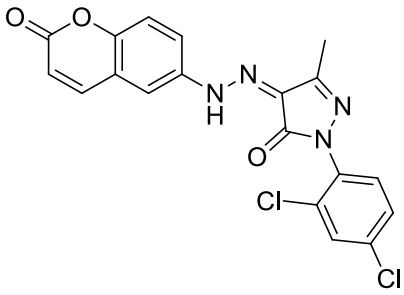

Yellow Solid, Yield: 70 %; M.P: Above 270ºC; IR (KBr): 3434, 3078, 2926, 1723, 1661, 1610, 1562, 1496, 1454, 1381, 1336, 1263, 1182, 1107, 1072, 1041, 1000, 911, 881, 857, 821, 774, 705 cm^{-1}; ^{1}H-NMR (400 MHz, $CDCl_3$): δ 2.40 (S, 3H), 6.53 (d, *J* = 9.6Hz, 1H), 7.36-7.43 (m, 3H), 7.55-7.56 (m, 2H), 7.63 (dd, *J* = 2.4Hz and 8.8Hz, 1H), 7.75 (d, *J* = 9.6Hz, 1H), 13.49 (s,

1H); Anal. calc. for $C_{19}H_{12}Cl_2N_4O_3$; C,54.96; H,2.91; N,13.49; found: C,54.92; H,2.95; N,13.52; 414.03; ESI-MS: 413.2 $[M-H]^+$.

(Z)-4-(2-(2-Oxo-2H-chromen-6-yl)hydrazono)-1,3-diphenyl-1H-pyrazol-5(4H)-one(19a)

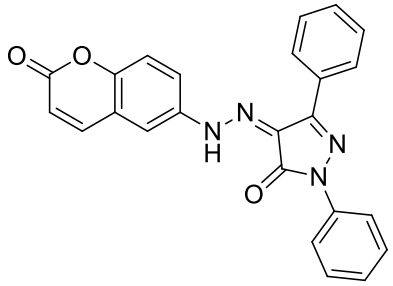

Yellow Solid, Yield: 70 %; M.P: Above 270ºC; IR (KBr): 3435, 2925, 1715, 1660, 1597, 1550, 1492, 1420, 1384, 1345, 1326, 1267, 1183, 1165, 1119, 1099, 964, 916, 890, 819, 791, 757, 715, 688 cm^{-1}; ^{1}H-NMR (400 MHz, $CDCl_3$): δ 6.50 (d, *J* = 9.6Hz, 1H), 7.26-7.30 (m, 1H), 7.42 (d, *J* = 8.8Hz, 1H), 7.47-7.55 (m, 6H), 7.65 (dd, *J* = 2.4Hz, 8.8Hz, 1H), 7.72 (d, *J* = 9.6Hz, 1H), 8.06 (d, *J* = 7.6Hz, 2H), 8.21-8.23 (m, 2H), 14.14 (s, 1H); Anal. calc. for $C_{24}H_{16}N_4O_3C$, 70.58; H, 3.95; N, 13.72; found: C,70.61; H,3.93; N,13.70; ESI-MS: 408.09 [M+].

(Z)-1-(4-Fluorophenyl)-4-(2-(2-oxo-2H-chromen-6-yl)hydrazono)-3-phenyl-1H-pyrazol-5(4H)-one (19b)

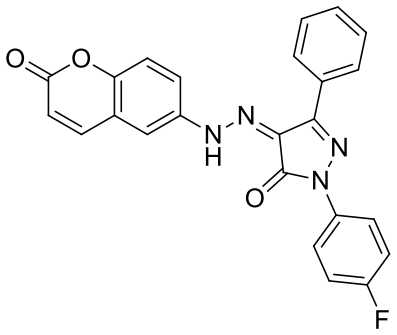

Yellow Solid, Yield: 70 %; M.P: Above 270ºC; IR (KBr): 3436, 2924, 1735, 1657, 1553, 1505, 1453, 1383, 1344, 1275, 1219, 1183, 1157, 1100, 963, 920, 876, 840, 813, 766, 723, 692, 651 cm^{-1}; ^{1}H-NMR (400 MHz, $CDCl_3$): 6.55 (d, *J* = 9.6Hz, 1H), 7.19 (t, *J* = 9.2Hz, 2H), 7.46 (d, *J* = 8.8Hz, 1H), 7.53-7.57 (m - 4H), 7.70 (dd, *J* = 2.6Hz & 8.4Hz, 1H), 7.78 (d, *J* = 9.6Hz, 1H), 8.05-8.08 (m, 2H), 8.22-8.24 (m, 2H), 14.16 (s, 1H); ^{13}C-NMR (100 MHz, DMSO-d_6): δ ppm 115.37, 115.55, 115.68, 115.86, 116.36, 116.43, 117.18, 117.71, 120.27, 126.74, 127.15, 128.77, 129.73, 129.89, 141.91, 143.79, 145.99, 151.25, 156.57, 158.31; Anal. calc. for $C_{24}H_{15}FN_4O_3$; C, 67.60; H, 3.55; N, 13.14; found: C,67.57; H,3.58; N,13.18; ESI-MS: 427.21 $[M+H]^+$.

(Z)-1-(4-Chlorophenyl)-4-(2-(2-oxo-2H-chromen-6-yl)hydrazono)-3-phenyl-1H-pyrazol-5(4H)-one (19c)

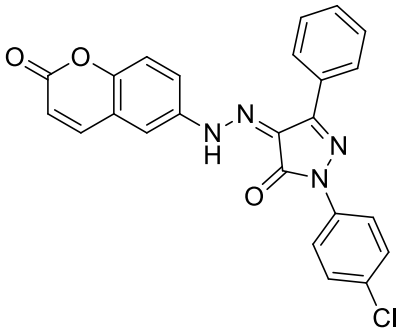

Yellow Solid, Yield: 70 %; M.P: Above 270ºC; IR (KBr): 3436, 3045, 2924, 1714, 1660, 1597, 1551, 1492, 1420, 1385, 1346, 1327, 1268, 1183, 1166, 1119, 1100, 964, 916, 891, 817, 790, 757, 715, 687, 668 cm^{-1}; ^{1}H-NMR (400 MHz, $CDCl_3$): 6.52 (d, *J* = 9.6Hz, 1H), 7.30 (t, *J* = 7.6Hz, 1H), 7.43 (d, *J* = 9.2Hz, 1H), 7.47-7.57 (m, 5H), 7.66 (dd, *J* = 2.4Hz and *J* = 8.8Hz, 1H), 7.73 (d, *J* = 9.6Hz, 1H), 8.07 (d, *J* = 7.6Hz, 2H), 8.23 (dd, *J* = 2.4Hz, 7.4Hz, 2H), 14.15 (s, 1H); ^{13}C-NMR (100 MHz, $CDCl_3$): δ ppm 113.92, 118.02, 118.45, 118.73, 119.40, 119.62, 125.65, 127.39, 128.08, 128.08, 128.65, 128.99, 130.01, 130.09, 137.75, 137.83, 142.56, 146.36, 151.72, 157.94, 160.06; Anal. calc. for $C_{24}H_{15}ClN_4O_3$; C, 65.09; H, 3.41; N, 12.65; found: C,65.14; H,3.39; N,12.61; ESI-MS: 442.86 [M+].

(Z)-1-(2,4-Dichlorophenyl)-4-(2-(2-oxo-2H-chromen-6-yl)hydrazono)-3-phenyl-1H-pyrazol-5(4H)-one (19d)

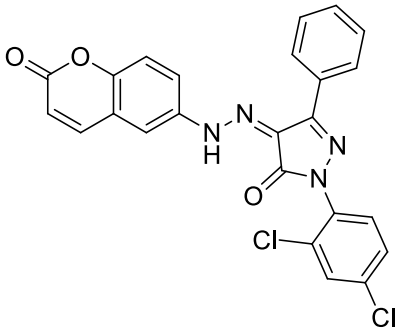

Yellow Solid, Yield: 70 %; M.P: Above 270ºC; IR (KBr): 3446, 2925, 1719, 1661, 1556, 1487, 1425, 1385, 1349, 1279, 1181, 1119, 1101, 1062, 967, 918, 879, 816, 756, 686 cm^{-1}; ^{1}H-NMR (400 MHz, $CDCl_3$): 6.54 (d, *J* = 9.6Hz, 1H), 7.42 (dd, *J* = 2.4Hz & 8.8Hz, 1H), 7.46 (d, *J* = 8.8Hz, 1H), 7.50 (d, *J* = 8.4Hz, 1H), 7.53-7.57 (m, 4H), 7.60 (d, *J* = 2.4Hz, 1H), 7.70 (dd, *J* =

2.4Hz and 8.8Hz, 1H), 7.77 (d, *J* = 9.6Hz, 1H), 8.16-8.18 (m, 2H), 13.97 (s, 1H); Anal. calc. for $C_{24}H_{14}Cl_2N_4O_3$ C, 60.39; H, 2.96; N, 11.74; found: C,60.43; H,3.01; N,11.72; ESI-MS: 477.05 [M+].

3a.6 Biological activity screening

3a.6.1 MTT assay:

According to procedure, the MTT [3-(4,5-dimethylthiazol-2-yl)-2,5-diphenyltetrazolium bromide] test was used to determine the half minimum inhibitory concentration. In DMEM medium supplemented with 10% FBS, cells were plated in a 96-well plate (1 x 104 cells/well) and allowed to incubate overnight. Each substance was added in concentrations of 0.5, 1, 10, 25, 50, 75, and 100 M micromolar. before being kept further 48 hours' incubation. After adding 20 µl of MTT solution (5 mg/mL in PBS), the plate underwent a further 4-hour incubation. 100 µl of acidified isopropanol was used to dissolved the blue formazan. after the supernatant solution was removed. At 570 nm (Metertech 960), the microplate reader was used to measure the absorbance. control group yields 100% for cell viability (%). Graph Pad Prism was used to calculate the IC_{50} values.

Cell viability (%) = (average absorbance of treated groups/average absorbance of control group) × 100%. IC_{50} values were calculated using Graph Pad Prism. Each experiment was performed in triplicates.

3a.6.2. Ethidium bromide/acridine orange staining assay:

Using the EtBr/AO staining approach, morphological alterations brought on by apoptosis and necrosis were seen. For 48 hours, the IC_{50} concentrations of compounds **17c** and **19b** were applied to the appropriate cells. The positive control utilized was Triton-X 100. Following treatment, cells were stained in a 1:1 mixture of EtBr and AO solution (100 g/ml). The ratio of cells to stain was kept constant at 1:25 µl. Using a Leica DM 2500 fluorescent microscope equipped with a Leica EZ camera, 10 µl of cell suspension was placed on a tiny slide.

3a.6.3 DCFH-DA assay:

DCFH-DA staining was employed to measure the intracellular ROS levels subsequent to treating both cell lines (A549 and MCF-7) with derivative **17c** and **19b**. To perform ROS quantification using Fluorimetry, cells at a density of $5x10^5$ cells/well were cultured in 6-well plates and allowed to adhere overnight. On the following day, the cells were treated to the IC_{50} concentration of compounds **17c** and **19b** and then incubated for 48 hours. After the incubation period, the procedure was carried out according to the previously outlined protocol in the work by Umar et al [32].

3a.6.4 Computational method:

All calculations for the examined derivatives were finished using a Pentium IV machine and Gaussian 09 software. The method selected for the calculations was DFT/B3LYP method at 6-31 G (d, p) basis set. A geometrical optimization process was done for both molecules without enforcing any molecular symmetry constraints to develop a geometrical structure of the lowest energy. All the optimized structures were stable as the imaginary frequency was not present. Gauss View has been used to show the structures of the optimized geometries. Furthermore, the frequency process was carried out for the optimized structures using the same basis set and level of theory to calculate various parameters. All structures in the optimization processes were demonstrated by the frequency calculations to be stationary points, but none were demonstrated by the vibrational analyses.

3a.7 References

[1] Cancer fact sheet, World Health Organisation (**2022**) Feb 2022.

[2] WHO, Global Breast Cancer Initiative Implementation Framework: Assessing, Strengthening and Scaling up of Services for the Early Detection and Management of Breast Cancer, **2023**.

[3] D.K. Lang, R. Kaur, R. Arora, B. Saini, S. Arora, *Anticancer. Agents Med. Chem*., **2020**, *20*, 2150.

[4] S. Pearce, *Drug Discov. World*, **2017**, *18*, 66.

[5] C. Kharbanda, M.S. Alam, H. Hamid, K. Javed, S. Bano, A. Dhulap, Y. Ali, S. Nazreen, S. Haider, *Bioorg. Med. Chem.*, **2014**, *22*, 5804.

[6] S. Viveka, Dinesha, P. Shama, G.K. Nagaraja, S. Ballav, S. Kerkar, *Eur. J. Med. Chem*., **2015**, *101*, 442.

[7] Z. Zhao, X. Dai, C. Li, X. Wang, J. Tian, Y. Feng, J. Xie, C. Ma, Z. Nie, P. Fan, M. Qian, X. He, S. Wu, Y. Zhang, X. Zheng, *Eur. J. Med. Chem.*, **2020**, *186*, 111893.

[8] C. M. Sayes, A. M. Gobin, K. D. Ausman, J. Mendez, J. L. West, V. L. Colvin, *Biomaterials*, **2005**, *26*, 7587.

[9] L. Zhang, Z. Xu, *Eur. J. Med. Chem.*, **2019**, *181*, 111587.

[10] T. Al-Warhi, A. Sabt, E.B. Elkaeed, W.M. Eldehna, *Bioorg. Chem.*, **2020**, *103*, 104163.

[11] T.K. Mohamed, R.Z. Batran, S.A. Elseginy, M.M. Ali, A.E. Mahmoud, *Bioorg. Chem.*, **2019**, *85*, 253.

[12] G. Saidachary, K. Veera Prasad, D. Divya, A. Singh, U. Ramesh, B. Sridhar, B. China Raju, *Eur. J. Med. Chem.*, **2014**, *76*, 460.

[13] R. Kenchappa, Y.D. Bodke, A. Chandrashekar, M. Aruna Sindhe, S.K. Peethambar, *Arab. J. Chem.*, **2017**, *10*, S3895.

[14] K.K. Sivakumar, A. Rajasekaran, P. Senthilkumar, P.P. Wattamwar, *Bioorg. Med. Chem. Lett.*, **2014**, *24*, 2940.

[15] C.G. Naik, G.M. Malik, H.M. Parekh, *South African J. Chem.*, **2019**, *72*, 248.

[16] R.C. Kulkarni, J.M. Madar, S.L. Shastri, F. Shaikh, N.S. Naik, R.B. Chougale, L.A. Shastri, S.D. Joshi, S.R. Dixit, V.A. Sunagar, *Chem. Data Collect.*, **2018**, *17-18*, 497.

[17] R. Soni, S.S. Soman, *Bioorg. Chem.*, **2018**, *79*, 277.

[18] S.D. Durgapal, R. Soni, S. Umar, B. Suresh, S.S. Soman, *ChemistrySelect.*, **2017**, *2*, 147.

[19] J. V. Patil, S. Umar, R. Soni, S.S. Soman, S. Balakrishnan, *Synth. Commun.*, **2023**, *53*, 217.

[20] H. Yang, R.M. Villani, H. Wang, M.J. Simpson, M.S. Roberts, M. Tang, X. Liang, *J. Exp. Clin. Cancer Res.*, **2018**, *37*, 1.

[21] M.R. Ramsey, N.E. Sharpless, *Nat. Cell Biol.*, **2006**, *8*, 1213.

[22] T. Yanai, D.P. Tew, N.C. Handy, *Chem. Phys. Lett.*, **2004**, *393*, 51.

[23] M. Govindarajan, M. Karabacak, A. Suvitha, S. Periandy, *Spectrochim. Acta - Part A Mol. Biomol. Spectrosc.*, **2012**, *89*, 137.

[24] M. Odabaşoğlu, Ç. Albayrak, B. Koşar, O. Büyükgüngör, *Spectrochim. Acta - Part A Mol. Biomol. Spectrosc.*, **2012**, *92*, 357.

[25] M.N. Arshad, A. Bibi, T. Mahmood, A.M. Asiri, K. Ayub, *Molecules*, **2015**, *20*, 5851–5874.

[26] A.S. Girgis, A.F. Mabied, J. Stawinski, L. Hegazy, R.F. George, H. Farag, E.S.M. Shalaby, I.S.A. Farag, *New J. Chem.*, **2015**, *39*, 8017.

[27] G. Bouchain, S. Leit, S. Frechette, A. E. Khalil, R. Lavoie, O. Moradei, S. H. Woo, M. Fournel, P. T. Yan, A. Kalita, M. C. Trachy-Bourget, C. Beaulieu, Z. Li, M. F. Robert, A. R. MacLeod, J. M. Besterman, D. J. Delorme, *Med. Chem.,* **2003**, *46,* 820.

[28] N. Kerru, L. Gummidi, S.V.H.S. Bhaskaruni, S.N. Maddila, P. Singh, S.B. Jonnalagadda, *Sci. Rep.*, **2019**, *9*, 1.

[29] S.N. Kanchana, V. Burra, L.K. Ravindra Nath, *Orient. J. Chem.*, **2014**, *30*, 1349.

[30] A.P. Rajput, S.S. Rajput, *Int. J. Pharm. Pharm. Sci.*, **2011**, *3*, 346.

[31] T. Aysha, M. Zain, M. Arief, Y. Youssef, *Heliyon*, **2019**, *5*, e02358.

[32] S. Umar, R. Soni, S.D.Durgapal,S. Soman, S.Balakrishnan, *J. Biochem. Mol. Toxicol.*, **2020**, *34*, e22553.